CAPA

Ana Rafaela Gomes Soares Oliveira

MiRNAs and risk gene interactions in Alzheimer's disease: from mechanisms to therapeutics

Dissertação de Mestrado em Biologia Celular e Molecular, orientada pela Doutora Ana Luísa Colaço Cardoso (Centro de Neurociências e Biologia Celular, Universidade de Coimbra) e pela Professora Doutora Maria Amália da Silva Jurado (Departamento de Ciências da Vida, Universidade de Coimbra) e apresentada ao Departamento de Ciências da Vida da Universidade de Coimbra

Julho de 2016

Ana Rafaela Gomes Soares Oliveira

MiRNAs and risk gene interactions in Alzheimer's disease: from mechanisms to therapeutics

Dissertação apresentada à Universidade de Coimbra para cumprimento dos requisitos necessários à obtenção do grau de Mestre em Biologia Celular e Molecular, realizada sob orientação da Doutora Ana Luísa Colaço Cardoso (Centro de Neurociências e Biologia Celular, Universidade de Coimbra) e pela Professora Doutora Maria Amália da Silva Jurado (Departamento de Ciências da Vida, Universidade de Coimbra)

Julho de 2016

UNIVERSIDADE DE COIMBRA

Cover note: miRNAs are expressed in the brain and play key roles in neuronal activities. Consequently, alterations in miRNA expression in the brain may contribute to neurodegenerative diseases, including Alzheimer's disease.

Image adapted from:

http://img13.deviantart.net/94e9/i/2009/318/7/2/alzheimer__s_disease_by_the_infinite_opi.jpg and

https://upload.wikimedia.org/wikipedia/commons/thumb/a/a7/MiRNA.svg/2181px-MiRNA.svg.png

This work was performed in the Center for Neuroscience and Cell Biology, University of Coimbra, Portugal, in the group of Vectors and Gene Therapy under the supervision of Dr. Ana Luísa Colaço Cardoso and Prof. Dr. Maria Amália da Silva Jurado (internal supervisor).

Ana Rafaela Oliveira was a student of the Master Degree in Cellular and Molecular Biology coordinated by the Department of Life Sciences of the University of Coimbra. The execution of this work was supported by FCT and FEDER/COMPETE (PTDC/BIM-MEC/0651/2012 and PEst-C/SAU/LA0001/2013-2014).

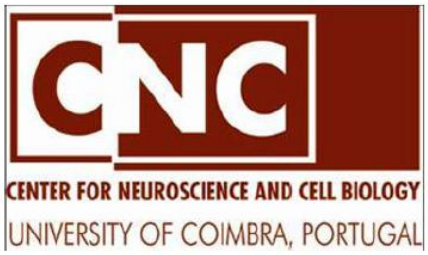

AGRADECIMENTOS

Como não podia deixar de ser quero deixar um agradecimento muito especial à minha orientadora, Doutora Ana Luísa Cardoso. Obrigado por teres acreditado em mim, obrigado por teres 'lutado' para que a minha entrada no grupo fosse possível, obrigado por teres estado sempre presente em todos os momentos, obrigado por me ajudares a crescer enquanto cientista e obrigada pela tua compreensão, pelo apoio e pela força num dos momentos mais complicados da minha vida. Por tudo isto, foste, sem qualquer dúvida, a melhor orientadora que podia ter escolhido. Mil obrigados não chegam!

Quero também agradecer à Doutora Conceição e à Doutora Amália Jurado por me terem dado a oportunidade de trabalhar neste grupo. Muito obrigado pelo voto de confiança!

Um enorme obrigado também à Joana Guedes. Joaninha, obrigado por me teres feito pensar muitas vezes, por me teres chamado à razão outras quantas e por me ouvires quando eu colapsava por achar que não tinha resultados. Obrigada!

Agradeço também aos elementos do grupo de Vectores e Terapia Génica, por me terem acompanhado nesta fase.

Quero deixar também um obrigado a todas aquelas pessoas que contribuíram diretamente para o meu projeto: à Joana Fernandes, à Sara Silva, ao Calil, ao Pedro Cunha, ao João Cruzeiro, ao Marco Ferreira, à Filipa Brito, à Joana Guedes e à Ana Luísa (mais uma vez). Um obrigado também à Sara Oliveira pela ajuda com as imagens da dissertação (e por me ter aturado nos 2 anos que morou comigo). Um agradecimento muito especial à Gladys pela ajuda nas clonagens. Devo dizer que para mim foste, e vais ser sempre, a mãe das clonagens. É bom saber que existem pessoas como tu, sempre dispostas a ajudar os outros.

E claro que não me podia esquecer dos meus pilares dos últimos 2 anos, as minhas princesas lindas. Andreia, Beatriz, Carina, Inês Gomes, Joana, Laetitia, Madalena, Marta, Rafa 2 e Raquel, obrigada por terem aparecido na minha vida. Obrigado por deprimirem comigo quando mais precisei e obrigado por se rirem na minha cara quando deprimia sozinha. Sem vocês tenho a certeza que estes 2 últimos anos não iam fazer tanto sentido. Obrigada por me mostrarem que os amigos a sério existem mesmo e que estão presentes nos bons e maus momentos, como se diz por aí. E por falar em amigos a sério é aqui que tu entras, Ju. Muito obrigada por mesmo longe estares sempre perto (igualmente para vocês,

Filipa e Rita). E a ti, Inês Santos, um agradecimento especial por me aturares há tantos anos e me fazeres sair de casa mesmo quando a vontade é mínima. A todas, um mega obrigado pela vossa amizade.

Quero agradecer aos meus pais, e também ao meu irmão, pelo voto de confiança que me dão todos os dias, por me deixarem sempre à vontade nas minhas decisões e por me apoiarem em tudo (ou vá, quase tudo). Sem o vosso apoio não estaria, certamente, a escrever estes agradecimentos. Sei que se tudo me falhar, vocês vão estar sempre lá.

Por último quero agradecer à Alicia que, apesar dos seus 3 aninhos, me mostra todos os dias o quão forte podemos ser e que apesar de todas as dificuldades no fim vai correr tudo bem. És uma Rainha, pequenota!

A todos estes, e àqueles que não mencionei mas que sabem o quão foram e são importantes, mil obrigadas por me ajudarem a concretizar mais um projeto.

TABLE OF CONTENTS

ABBREVIATIONS

A

ABCA7 – ATP-Binding Cassette Transporter A7

AD – Alzheimer's disease

ADAM – a disintegrin and metalloproteinase

ADAS-Cog – Alzheimer's Disease Assessment Scale-Cognitive

ADGC – Alzheimer Disease Genetics Consortium

AGO - Argonaute

AICD – Amyloid precursor protein intracellular domain

AmphII – Amphiphysin 2

ANTH – AP180 N-terminal Homolog

AP2 – Adaptor Protein 2

APOE – Apolipoprotein E

APP – Amyloid Precursor Protein

Arg 1 – Arginase 1

Aβ – Aβ-amyloid peptide

B

BACE1 – β-secretase

BAR domain – Bin-Amphiphysin-Rvs domain

BBB – Blood Brain Barrier

BDMs – Blood-Derived Monocytes

BIN1 – Bridging Integrator 1

C

CASS4 – Cas Scaffolding Protein Family Member 4

CCL2 – Chemokine (C-C motif) ligand 2

CCR2 – C-C chemokine receptor type 2

CD14 – Cluster of Differentiation 14

CD2AP - CD2-Associated Protein

CD45 – Cluster of Differentiation 45

CDK5 – Cyclin-dependent Kinase 5

cDNA – Complementary DNA

CDR – Clinical Dementia Rating

CELF1 - CUGBP, Elav-like Family Member 1.

CFH – Complement Factor H

CLAP – Clathrin and AP2 adaptor complex binding domain

CLU – Clusterin

CNS – Central Nervous System

CR1 – Complement Receptor 1 (3b/4b)

CSF – Cerebral Spinal Fluid

CTFα – C-terminal fragment alpha

CTFβ – C-terminal fragment beta

CX3CL1 – Chemokine (C-X3-C motif) ligand 1 / fractalkine

CX3CR1 – CX3C Chemokine Receptor 1

CXCL9 – C-X-C chemokine ligand type 9

D

DGCR8 – DiGeorge syndrome chromosomal [or critical] region 8

DLS – Delivery Liposomal System

DOGS – Dioctadecylamidoglycylspermidine

DOPE – 1,2-dioleoyl-sn-glycero-3-phosphoethanolamine

DRS- Direct RNA Sequencing

DSG2 - Desmoglein 2

DSM-IV-TR – Diagnostic and Statistical Manual of Mental Disorders – fourth edition

E

EGFP – Enhanced Green Fluorescent Protein

EMP **–** Erythromyeloid Precursor

EOAD – Early-Onset Alzheimer's Disease

ER –Endoplasmic Reticulum

F

FAD – Familial AD

FBS – Fetal Bovine Serum

FDA – USA Food and Drug Administration

FERMT2 – Fermitin Family Member 2

FITC – Fluorescein isothiocyanate

FRMD4A – FERM domain containing 4A

G

GDS – Geriatric Depression Scale

GFP – Green Fluorescent Protein

GM-CSF – Granulocyte Macrophage Colony-Stimulating Factor

GSK3β – Glycogen Synthase Kinase 3-beta

GWAS – Genome-Wide Association Studies

H

HEXB – Hexosaminidase B

HPRT – hypoxanthine Phosphoribosyl- Transferase

I

IFN-γ – Interferon gamma

IL-10 – Interleukin-10

IL-13 – Interleukin-13

IL-1β – Interleukin-1β

IL-34 – Interleukin-34

IL-4 – Interleukin-4

IL-6 - Interleukin-6

iMGs – Microglia-like Cells

INPP5D – Inositol Polyphosphate-5-Phosphatase

IRAK1 – IL-1 receptor associated kinase

J

JAK – Janus Kinase

JNK – Jun N-terminal Kinase

L

LC 3 – Microtubule-associated protein light chain 3

LOAD – Late-Onset Alzheimer's Disease

LPS – Lipopolysaccharide

Ly6C – Lymphocyte Antigen 6C

M

MACS – Magnetic activated Cell Sorting

MAPT – Microtubule-associated protein tau

MCI – Mild Cognitive Impairment

M-CSF – Macrophage Colony-Stimulating Factor

MDMs – Monocytes-Derived Macrophages

MEF2C – Myocyte Enhancer Factor 2C

MiRNAs – MicroRNAs

MMSE – Mini-Mental State Examination

MoCA – Montreal Cognitive Assessment

MRE – miRNA response element

MRI – Magnetic Resonance Imaging

mRNA – Messenger RNA

MS4A – Membrane-Spanning four-domains, subfamily A

N

NF-κB – Nuclear Factor-κB

NFTs – Neurofibrillary Tangles

NINCDS-ADRDA – National Institute of Neurological and Communicative Disorders and Stroke-Alzheimer's Disease and Related Disorders

NMDA – N-methyl-D-aspartate receptor

NME8 - NME/NM23 Family Member 8

NO – Nitric Oxide

NSAIDs – Non-steroidal anti-inflammatory drugs

P

P2RY12 – Purinergic Receptor P2Y, G-protein coupled, 12

PBMCs – Peripheral Blood Mononuclear Cells

PBS – Phosphate-buffered saline

pDNA – plasmid DNA

PE – Phycoerythrin

Pen – Penicillin

PET – Positron Emission Tomography

PFA – Paraformaldehyde

PICALM – Phosphatidyl Inositol Clathrin Assembly Lymphoid Myeloid

PLD3 – Phospholipase D Family, Member 3

pMiRs – plasmids with a miRNA sequence

Pol II – RNA Polymerase II

PPARs – Peroxisome Proliferator Activated Receptors

PPARs – Peroxisome Proliferator Activated Receptors

PPs – Protein Phosphatases

PRRs- Pattern Recognition Receptors

PRRs- Pattern Recognition Receptors

PS1 – Presenilin-1

PS2 – Presenilin-2

p-tau – Hyperphosphorylated tau

PTK2B - Protein Tyrosine Kinase 2 Beta

Q

qRT-PCR – quantitative real-time polymerase chain reaction

R

RISC – RNA-inducing silencing complex

ROS – Reactive Oxygen Species

RT – Room Temperature

S

sAPPα – Soluble N-terminal fragment of APP alpha (non-amyloidogenic pathway)

sAPPβ – Soluble N-terminal fragment of APP beta (amyloidogenic pathway)

SD – Standard Deviation

SH3 – Src homology 3

siRNAs – Small interfering RNA

SLC24A4-RIN3 – Solute Carrier Family 24 (Sodium/ Potassium/Calcium Exchanger), Member 4/Ras and Rab Interactor 3

SNAREs – Soluble NSF Attachment Receptors

SNORD110 – Small Nucleolar RNA, C/D box 110

SNORD44 – Small Nucleolar RNA, C/D box 44

SNPs – Single Nucleotide Polymorphisms

SOCS-1 – Suppressor of Cytokine Signaling 1

SORL1 – Sortilin-Related Receptor L 1

STAT – Signal Transducer and Activator of Transcription

sTREM2 – Soluble TREM2

Strep – Streptomycin

T

TGF-β – Transforming Growth Factor-β

TLRs – Toll-like Receptors

TNF-α – Tumor Necrosis Factor-α

TNRC6 – Trinucleotide repeat-containing gene 6 protein

TREM2 – Triggering receptor expressed on myeloid cells 2

U

UTR – Untranslated region

W

WHO – World Health Organization

Z

ZCWPW1 - Zinc Finger, CW Type with PWWP Domain

Abstract

Alzheimer's disease (AD) is the most common form of dementia, whose definitive clinical diagnosis is only possible after death. Until recently, this disease has been characterized by two major pathological hallmarks: the extraneuronal deposition of the β-amyloid peptide (Aβ) and the presence of intraneuronal aggregates of hyperphosphorylated tau (NFTs). Currently, neuroinflammation is also considered an important hallmark of AD, since experimental, genetic and epidemiological data have revealed a crucial role for the activation of the innate immune system during disease onset and progression. The recent identification of several new AD risk genes, by genome-wide association studies (GWAS), found to play a role in immune system responses, provided additional evidence that immune cell dysfunction contributes to aggravate neuronal and tissue loss. To date, the therapeutic strategies used to fight or at least delay the progression of this disease are limited and unsuccessful, in part due to its late diagnosis and to the appearance of clinical symptoms only in a later stage of the disease. Importantly, at the present, several miRNAs were found to be deregulated, both locally and systemically, in AD pathology, which brings forward the possibility of at least part of LOAD cases being linked to miRNA deregulation.

In this context, the main goals of this work included the clarification of the newly identified AD risk genes contribution to the molecular pathways underlying AD pathogenesis, by evaluating the expression of these genes under different experimental variables, including age, immune cell activation state and disease status. Moreover, we also aimed to better understand the importance and therapeutic potential of miRNA modulation strategies, directed towards mononuclear phagocytes, in the clearance mechanisms associated with this disease. Taking into consideration the contribution of microglia to brain tissue homeostasis, the third and last goal of this project involved the re-differentiation of microglia-like cells (iMGs) from human blood-derived monocytes (BDMs), following a previously described protocol.

To address these goals, the expression of AD risk genes in blood-derived monocytes and monocyte-derived macrophages (MDMs) was evaluated in cells from healthy individuals exposed to different activation states (M0, M1 and M2). The expression of two risk genes in particular, *PICALM* and *BIN1,* was also evaluated in AD patients, mild cognitive impairment (MCI) patients and age-matched controls, as well in young and

elderly healthy individuals. We concluded that AD risk genes present a differential expression in the different human cell models, as well as in different activation states. *PICALM* and *BIN1* expression shows a reduction with age, which is aggravated in individuals suffering from AD or MCI. Taking into account that the two genes were shown to be increased in the M2 anti-inflammatory activation state and decreased in M1 pro-inflammatory state, it suggests that aging and dementia are associated with a shift towards an inflammatory environment.

The impact of miRNA modulation in *PICALM* and *BIN1* expression and function was also evaluated in N9 murine microglia cells and in MDMs. A decrease in the expression of *PICALM* and *BIN*, following an increase in miR-155 and miR-31 expression, respectively, was observed in N9. In addition, N9 cells presented changes in their phagocytic ability and in the release of several pro- and anti-inflammatory cytokines, following electroporation with p155, p31 and p200c.

Regarding the re-differentiation of iMGs, our results showed that, following BDM differentiation with IL-34 and GM-CSF, the levels of several microglia surface markers and the expression of microglia signature genes do not resemble those of brain-derived microglia cells.

Overall, the changes observed in AD risk genes, in particular *PICALM* and *BIN1*, show a contribution of these genes to AD pathology. Moreover, we believe that our studies on miRNA modulation provided insights into the epigenetic mechanisms involved in the regulation of Aβ clearance, and may pave the way towards the development of new miRNA-based AD therapies. However, it is important to note that the lack of a good cell model of human microglia is currently a major obstacle to research in the field of neuroinflammation, whose resolution will be crucial for a better understanding of the contribution of the innate immune system to AD and other neurodegenerative and neurodevelopmental disorders.

Key words: Late-onset Alzheimer's disease (LOAD); neuroinflammation; risk genes; *PICALM*; *BIN1*; miRNA modulation; phagocytosis.

Resumo

A doença de Alzheimer (DA) é a forma mais comum de demência e o seu diagnóstico clínico é apenas possível após a morte. Até recentemente, esta doença era caracterizada por duas principais características patológicas: a deposição extraneuronal do péptido β-amilóide (Aβ) e a presença de agregados intraneuronais da tau hiperfosforilada. Atualmente, a neuroinflamação é também considerada uma característica importante da doença, uma vez que dados experimentais, genéticos e epidemiológicos têm revelado um papel crucial para a ativação do sistema imunitário inato durante o início e a progressão da doença. A recente identificação de novos genes de risco da DA, através de estudos de associação genética de larga escala, com um papel importante nas respostas do sistema imunitário, forneceu evidências adicionais sobre a contribuição das disfunções em células do sistema imune para o agravamento da perda neuronal e do dano tecidular. Até à data, as estratégias terapêuticas usadas para combater ou atrasar a progressão da doença são limitadas e sem sucesso, em parte devido ao diagnóstico tardio e ao aparecimento de sintomas clínicos apenas num estádio avançado da doença. É também importante salientar que, atualmente, alguns miRNAs foram encontrados desregulados na DA, tanto localmente como sistemicamente, o que evidencia a possibilidade de pelo menos parte dos casos de DA estarem ligados a desregulações de miRNAs.

Neste contexto, os objetivos principais deste trabalho incluíram a clarificação da contribuição dos novos genes de risco da DA nas vias moleculares subjacentes à patogénese da doença, através da avaliação da expressão destes genes sob diferentes variáveis experimentais, que incluíram: a idade, o estado de ativação das células imunes e o estado da doença. Para além disso, um dos objetivos passou também pela compreensão da importância e potencial terapêutico das estratégias que envolvem a modulação de miRNAs, dirigidas a fagócitos mononucleares, nos mecanismos de limpeza associados à doença. Tendo em consideração a contribuição da microglia para a homeostasia do tecido cerebral, o terceiro e último objetivo deste projeto envolveu a re-diferenciação de monócitos derivados do sangue humano em células semelhantes à microglia, seguindo um protocolo já descrito.

Para concretizar estes objetivos, a expressão dos genes de risco em monócitos (derivados do sangue) e macrófagos (derivados de monócitos) foi avaliada em células de indivíduos saudáveis expostas a diferentes estímulos de ativação (M0, M1 e M2). A

expressão de dois genes em particular, *PICALM* e *BIN1*, foi também avaliada em pacientes com DA, pacientes com um défice cognitivo ligeiro e em controlos saudáveis da mesma idade, assim como em indivíduos jovens e idosos saudáveis. Concluímos que os genes de risco da DA apresentam uma expressão diferencial nos diferentes modelos celulares humanos usados, assim como em diferentes estados de ativação. A expressão do *PICALM* e *BIN1* mostrou uma diminuição com a idade, que é agravada em indivíduos com DA ou com um défice cognitivo ligeiro. Tendo em conta que a expressão destes dois genes aumenta no estado de ativação anti-inflamatório M2 e diminuí no estado pro-inflamatório M1, os resultados observados sugerem que o envelhecimento e a demência estão associados a uma transição para um ambiente pró-inflamatório.

A influência da modulação dos miRNAs na expressão e função do *PICALM* e do *BIN1* foi também avaliada em células da microglia de ratinho (linha celular N9) e em macrófagos humanos (derivados de monócitos). Observámos uma diminuição na expressão do *PICALM* e do *BIN1* nas células N9, no seguimento de um aumento da expressão do miR-155 e do miR-31, respetivamente. Para além disso, as células N9 apresentaram alterações na sua capacidade fagocítica e na libertação de algumas citoquinas pro- e anti-inflamatórias, após electroporação com os plasmídeos p155, p31 e p200c.

Em relação à re-diferenciação dos monócitos em células semelhantes a microglia, os nossos resultados mostraram que, após exposição a IL-34 e GM-CSF, os níveis de alguns marcadores de superfície da microglia e a expressão de genes únicos da microglia nas células diferenciadas não se assemelham aos da microglia derivada do cérebro.

No geral, as alterações observadas em genes de risco da DA, em particular no *PICALM* e no *BIN1*, mostram uma contribuição destes genes para a patologia da DA. Além disso, nós acreditamos que os nossos estudos, dedicados à modulação de miRNAs, forneceram conhecimento sobre mecanismos epigenéticos envolvidos na regulação da limpeza do peptídeo Aβ, o que pode abrir caminho para o desenvolvimento de novas terapias para a DA baseadas em miRNAs. Contudo, é importante notar que a falta de um bom modelo celular de microglia humana é atualmente um dos maiores obstáculos para a investigação no campo da neuroinflamação, cuja resolução será crucial para um melhor entendimento da contribuição do sistema imunitário na DA e em outras doenças neurodegenerativas e do desenvolvimento.

Palavras-chave: Doença de Alzheimer de início tardio; neuroinflamação; genes de risco; *PICALM*; *BIN1*; modulação de miRNAs; fagocitose.

Chapter 1

Introduction

Part of this chapter is included in the following publication:

Viegas, A. T., Guedes, J., Oliveira, A. R., Cardoso, A. M., Cardoso, A. L. miRNAs in Dementia. Current Pharmaceutical Design (2016) (in press).

1.1. Alzheimer disease – general remarks

Dementia is a syndrome mainly associated with aging, caused by several brain disorders. It is described by a decline in mental ability, including impairments in memory, learning, language, attention, visual-spatial recognition and problem solving skills, severe enough to interfere with the ability to carry out the simplest tasks (reviewed in [1]). Accordingly to World Health Organization (WHO), 47.5 million people live with dementia worldwide and, as a consequence of the prolonged life expectancy, is expected that this number will triple by 2050. Due to these impressive numbers and to its huge economic impact on society (about 604 billion US$ in 2010), dementia is now considered a public health priority[2].

Alzheimer's disease (AD) is the most common form of dementia, accounting for 60 to 80% of all dementia cases [www.alz.org]. This complex, multifactorial and progressive neurodegenerative disorder is typically characterized by gradual neuronal loss, impairment of other cognitive functions and inability to perform activities of daily life [WHO], a feature that impacts not only the patients but also their families.

Although Alzheimer's disease is described to have a higher incidence in elderly people, it may also affect individuals at a younger age. This variation in age of onset led the disease classification into early (<60 years age) and late (≥60 years age) onset forms. Early onset Alzheimer's disease (EOAD), which includes familial AD (FAD), is responsible for less than 5% of all AD cases and is mostly associated with patterns of inheritance with age-dependent penetrance. Thus, EOAD is believed to be a consequence of autosomal dominant mutations, some of which have already been identified. This is the case of mutations in the amyloid precursor protein (APP), presenilin-1 (*PSEN1*, gene encoding PS-1) and presenilin-2 (*PSEN2*, gene encoding PS-2) genes[3,4]. APP mutations accounts for around 14% of EOAD cases, while mutations in PS1 and PS2 corresponds to approximately 85% of all familial cases. On the other hand, late-onset Alzheimer's disease (LOAD) is much more common, corresponding to 95% of all AD cases. Due to its multifactorial nature LOAD is believed to be far more complex than EOAD. The involvement of multiple genes (gene-gene or even gene-environment interactions) and, in particular, the combination of multiple risk alleles, are proposed to increase the risk of developing the disease[5].

Until 2009, APOE ε4 genotype was considered the only and most relevant genetic risk factor for LOAD. However, recent genome-wide association studies, performed by Alzheimer Disease Genetics Consortium (ADGC), pointed other possible risk alleles, whose identification and characterization may play an important role in the design of new diagnosis and prognosis strategies for AD.

At the moment, diagnosis and treatment for AD are very limited and patients and their families have a long road until the definitive diagnosis is established. The clinical diagnosis comprises cognitive, physical and neurological tests, along with complementary tests, such as magnetic resonance imaging (MRI), positron emission tomography (PET) scanning and biomarker analysis in the cerebral spinal fluid (CSF) for quantification of the Aβ-amyloid peptide and hyperphosphorylated tau (p-tau)[6]. Unfortunately, only *post-mortem* examination provides a definitive diagnosis, through the identification of the hallmarks of the disease. Taking these difficulties into consideration, it is easy to understand the extreme importance of finding strategies to clearly identify the disease at its early stages and to fight it. Up to now, several tests already allow the distinction of individuals with an intermediate state between normal aging and dementia, known as mild cognitive impairment (MCI)[7]. MCI patients present memory impairments greater than that expected for their age, but continue to perform normal activities of the daily routine and, as a result, are not considered demented. Nevertheless, every year, about 12% of MCI cases progress to AD and, therefore, the follow-up of these patients presents great clinical importance[8].

Presently, therapeutic strategies used to target AD are still limited and mostly unsuccessful. To date, only cholinesterase inhibitors and N-methyl-D-aspartate receptor (NMDA) antagonists, which have been used to restrict cognitive impairment and decrease excitotoxicity, are approved by the USA Food and Drug Administration for the treatment of AD. Unfortunately, these drugs act in a later stage of the disease, in which neuronal death already occurred in a great extent and, therefore, they only diminish the symptoms of the disease.

Three main therapeutic strategies are currently under investigation, including: 1) reduction of Aβ production, 2) facilitation of Aβ clearance and 3) prevention of Aβ aggregation (reviewed in[9]). In the last decade, clinical trials with anti-inflammatory drugs have also been performed, although with unsuccessfully results (reviewed in[10]). Currently, several clinical trials using active and passive vaccination, which consists of humanized antibodies to recognize toxic soluble Aβ oligomers, are being conducted in asymptomatic

patients with risk of developing AD, in order to certify if immunotherapy could be used as a therapeutic approach to prevent or at least delay the progression of the disease (reviewed in[10,11]).

1.2. Hallmarks of Alzheimer's disease

The exact molecular mechanisms underlying Alzheimer's disease remain unclear. So far, AD has been mainly characterized by two pathological hallmarks, which are often accompanied by neuronal damage and death: extraneuronal deposits of β-amyloid peptide, which contribute to the formation of senile plaques[12], and intraneuronal aggregates of hyperphosphorylated tau, also known as neurofibrillary tangles (NFTs) (reviewed in[13]). Nevertheless, in the past decades, epidemiological evidences suggest that neuroinflammation is an important contributor to AD[14-16]. Moreover, it was seen that long-term use of non-steroidal anti-inflammatory drugs (NSAIDs) reduces the risk of developing AD[17]. Moreover, several lifestyle factors, such as obesity, reduced activity and systemic infection, in addition to some environmental factors, which are known to increase the risk of developing AD, have been associated with the promotion of an inflammatory environment, due to an increase in the concentration of inflammatory mediators in the periphery[18-21]. For these reasons, neuroinflammation might be considered the third hallmark of AD. Furthermore, several authors also suggest that neuroinflammation can act as a link between early deposition of β-amyloid peptide and tau hyperphosphorylation (reviewed in[22]). In the section below, the three hallmarks of AD, as well as the relationship between them, are described in more detail.

1.2.1. Extraneuronal senile plaques

Amyloid-β deposition, which results from the cleavage of APP, occurs at an early stage of Alzheimer's disease and is the main event responsible for the formation of extraneuronal senile plaques.

APP is a type I transmembrane protein delivered to the plasma membrane after maturation in the endoplasmic reticulum (ER) and Golgi apparatus. Upon arrival at the cell surface, APP is internalized in clathrin-coated vesicles, due to the activity of proteins such as PICALM, BIN1 and CD2AP, and to the presence of the YENP motif, near the carboxyl terminus of APP[13,23,24]. After endocytosis, part of APP is recycled to the cell surface, while

significant amounts are degraded in lysosomes[25]. The recycled APP, once in the plasma membrane, might be cleaved by the plasma membrane-bound α-secretases, including those of the ADAM (a disintegrin and metalloproteinase) protease family, being ADAM10 the prevalent α-secretase in the brain (reviewed in[13,23]). This α-secretase-dependent pathway is designated as the non-amyloidogenic pathway, and is the more predominant pathway for APP metabolism. On the other hand, depending on the interactions established between APP and sorting receptors, such as SORL1, APP may be redirected to the retromer compartment or to the late endosome[26,27]. In the late endosomal compartment, APP is in close contact with β-secretase (also known as BACE1), which is able to process APP through an alternative pathway, identified as the amyloidogenic pathway. The cleavage performed by BACE1 originates an N-terminal fragment (sAPPβ) and a membrane-bound C-terminal fragment (CTFβ), instead of sAPPα and CTFα produced in the non-amyloidogenic pathway. In both cases, C-terminal fragments are subjected to a secondary proteolysis by the presenilin-containing γ-secretase complex, which comprises four proteins: presenilin 1 (PS1) or presenilin 2 (PS2), nicastrin, aph-1 and pen-2[28-32]. The cleavage by the γ-secretase complex leads to the formation of amyloid precursor protein intracellular domains (AICD), which are released into the intracellular compartment, and p3 (soluble) or Aβ peptides (insoluble) with different lengths (from 38 to 42 amino acids) (in α-secretase or BACE1 pathway, respectively), which are released into the extracellular compartment (Figure 1).

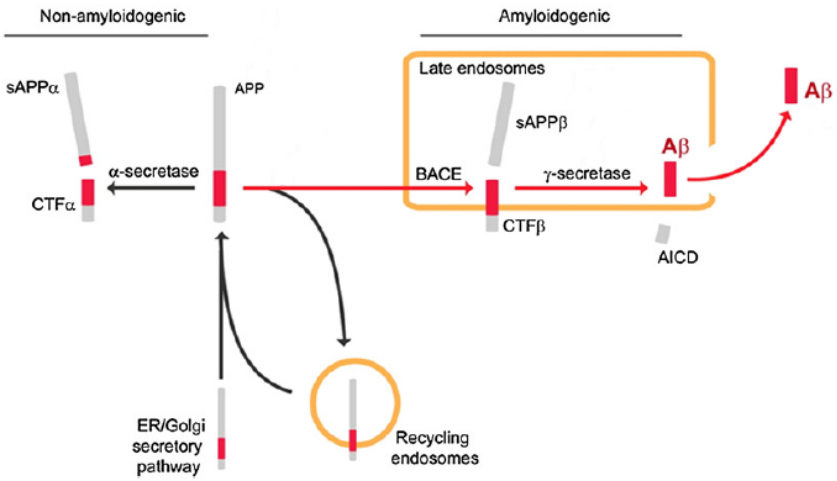

Figure 1 – APP processing pathways that are either non-amyloidogenic (cleavage by α-secretase and recycling endosome pathways) or amyloidogenic (cleavage by β-secretase). After endocytosis, APP is recycled to the cell surface, where the non-amyloidogenic pathway is prevalent, being APP cleaved by α-, following γ-secretase. Once APP is redirected to the late endosome, the contact with β-secretase, following γ-secretase leads to the cleavage of APP into the Aβ insoluble peptide. Adapted from Bohm *et al*. 2015[13].

The different lengths of the Aβ peptides are a result of three different cleavage sites by the presenilin complex (γ, ε, ζ site cleavages), being the cleavage at the γ-cleavage site, involved in the formation of $A\beta_{1-40}$ and $A\beta_{1-42,}$ the most abundant forms in the brain. The excessive production of Aβ peptides is responsible for neuronal damage and death, since these peptides are known to aggregate into neurotoxic oligomers and fibrils, which, in turn, adhere to each other contributing to the formation of insoluble amyloid plaques (reviewed in[13]).

1.2.2.Intraneuronal neurofibrillary tangles

Neurofibrillary tangles could also have a role in the progression of the disease and is thought that their formation occurs by multiple steps initiated with the detachment of the tau protein from microtubules.

Tau protein is a phosphoprotein, encoded by the *MAPT* (microtubule-associated protein tau) gene, which is predominantly abundant in the axons of neurons. In the adult brain, there are six major isoforms of tau, which are obtained by alternative splicing of the *MAPT* gene. Tau protein is involved in the stabilization of microtubules and in the maintenance of structural activity, which is, under physiological conditions, ensured by a continuous dynamic equilibrium (reviewed in[33]). This equilibrium is regulated by phosphorylation of tau, which is determined by kinases and phosphatases. Glycogen synthase kinase 3β (GSK-3β), cyclin-dependent kinase 5 (Cdk5), p38-MAPK and JNK are several kinases involved in the phosphorylation of tau, while PP1, PP2A, PP2B and PP2C are phosphatases to counterbalance the action of kinases. PP2A is considered the major tau phosphatase, accounting for 70% of tau phosphatase activity[34-37]. Under pathophysiologic conditions this equilibrium is compromised and, as a consequence, the levels of free tau increase, resulting in alterations in the conformation of tau, which in turn leads to its aggregation and fibrillization, making it insoluble and cytotoxic (Figure 2). In addition to the cytotoxic activity of hiperphosphorilated tau, it is important to consider that, once the machinery responsible for the stabilization of microtubules is impaired, microtubule-dependent cellular functions will become compromised, including axonal transport and the neurotransmission (reviewed in[33]) (Figure 2).

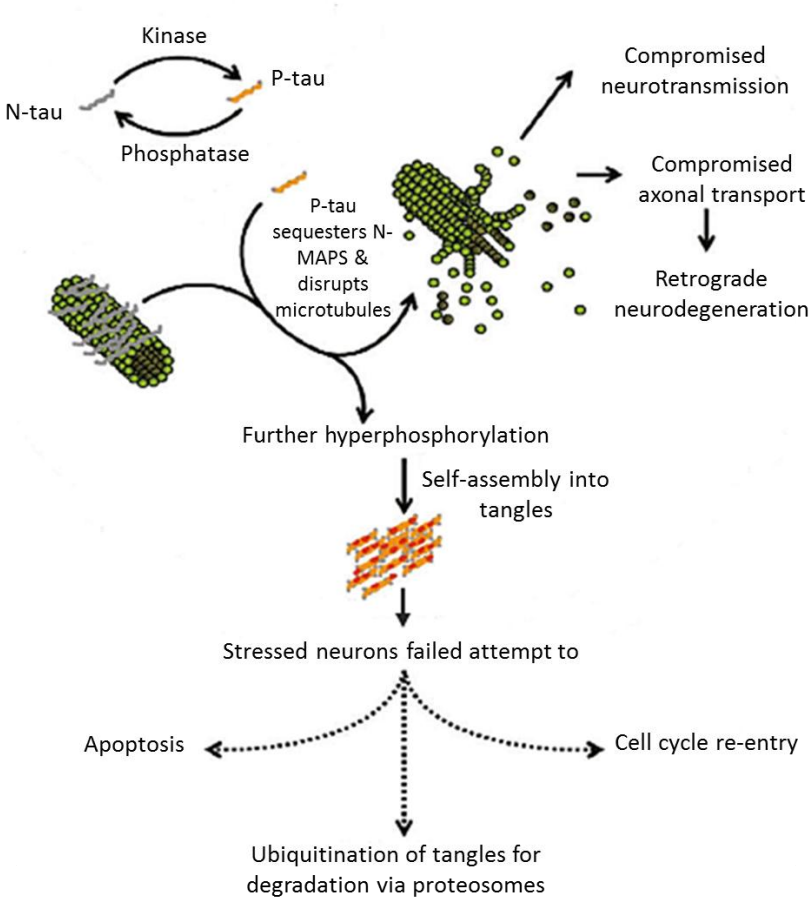

Figure 2 – Mechanism of tau-induced neurodegeneration. Hyperphosphorylated tau disrupts microtubules, impairing axonal transport. Aposptosis, ubiquitination of tangles and cell cycle re-entry might be consequences of hyperphosphorylated tau. Adapted from Beharry *et al*. 2014[38].

1.2.3. Neuroinflammation and the role of microglia and peripheral-blood mononuclear cells

In the last few years, neuroinflammation, which relies on the activation of microglial cells in the central nervous system (CNS), emerged as an important contributor to AD pathology, occupying a place similar to senile plaques and NFTs in the pathophysiology of the disease (reviewed in[10]). In the last decades, epidemiologic studies with non-steroidal anti-inflammatory drugs, such as ibuprofen and indomethacin, reported that these drugs have a protective effect when used during long periods of time, reducing the risk of developing AD [15,16,39]. However, the mechanism of action of these drugs is unknown and there are some controversy about their efficiency, since clinical trials with these anti-inflammatory drugs presented unsuccessful results. On the other hand, studies revealed that the amyloidogenic hypothesis could not completely explain sporadic AD cases, since the production of Aβ was found to be similar in AD patients and in some controls[40]. Therefore, it has been suggested that the accumulation of Aβ can be attributed to the lack of clearance mechanisms, such as those mediated by immune cells in the brain, which implicates microglia deregulation as a direct contributor to AD onset and progression[40].

Microglia, are the innate immune cells of the brain, representing around 10% of the central nervous system population. In 1993, microglia was suggested, for the first time, to derive from primitive myeloid cells from the yolk sac, but it was only later, in 1996, that the hematopoietic origin of these cells were established[41,42]. More recently, in 2010, it was shown that microglia do not derive from definitive circulating hematopoietic precursors, as suggested by Rio Hortega[43] but, instead, derive from primitive embryonic precursors, which migrate from the yolk sac to the brain between embryonic day 8 and 9, before the formation of the blood-brain barrier (BBB) [43,44]. The yolk sac precursors of microglia were identified in 2013, by Kierdorf and colleagues, as early E8 primitive c-kit$^+$ erythromyeloid yolk sac precursors (EMP), which develop into CD45$^+$ c-kit-CX3CR1$^+$ cells[45]. In the same year, blood monocytes and other bone-marrow progenitors were shown not contribute to the adult microglia numbers in the CNS, in a healthy environment[46]. Instead, local microglia cells were shown to be able to divide and maintain the microglia pool throughout life.

Microglial cells have important functions in the brain, including maintenance of tissue homeostasis, neuronal integrity, network functioning in the brain and immune defense in case of injury (reviewed in[22]). Depending on their surrounding environment,

microglia can acquire different morphologies, allowing them to establish different kinds of immune responses. For instance, under physiological conditions, resident microglia are in a "surveillance" state, presenting a ramified form with their branches constantly moving to test the surrounding microenvironment[47]. On the other hand, in response to any disturbance of nervous system homeostasis, microglia are activated and their shape changes to an amoeboid form, more adapted to chemotaxis and cell movement to the site of injury (reviewed in [48]). The interaction of microglia with neurons, as well with other glial cells, through secreted mediators, the activation or inhibition of transcription factors and, most importantly, the regulation of surface and nuclear receptors are several of the mechanisms identified as being responsible for the activation of microglia (reviewed in[49]). This process occurs mainly through the activation of pattern recognition receptors (PRRs), like Toll-like receptors (TLRs) and co-receptors, which are expressed on the surface of microglia, and peroxisome proliferator activated receptors (PPARs), which are nuclear receptors. Depending on the signal strength, tissue site and environmental conditions, microglia will respond differently, which allows the classification of these cells into a range of phenotypes with two well described extreme phenotypes: the alternative (also known as M2) phenotype and the classical (also designated as M1) phenotype. M2 activation comprises different subtypes and is induced by IL-4, IL-13, IL-10, glucocorticoid hormones and TGF-β[50-52] (reviewed in[53]). It usually induces secretion of neurotrophic factors, proteases and is known to increase phagocytosis. This type of response leads to the clearance of tissue debris and resolution of the inflammatory process. Thus, the activation of this phenotype is often considered an initial defensive response, designed more to repair tissue damage than to attack pathogens. Nevertheless, if the damage persists, cells can switch from the M2 to a M1 state, which contributes for the release of pro-inflammatory chemokines and cytokines, such as IL-1β, IL-12, IL-23, TNF-α and nitric oxide (NO), reactive oxygen species (ROS) and proteolytic enzymes. This classical inflammatory response aims to destroy any invading agent or local pathogen but, when left unresolved, can result in chronic neuroinflammation (Figure 3).

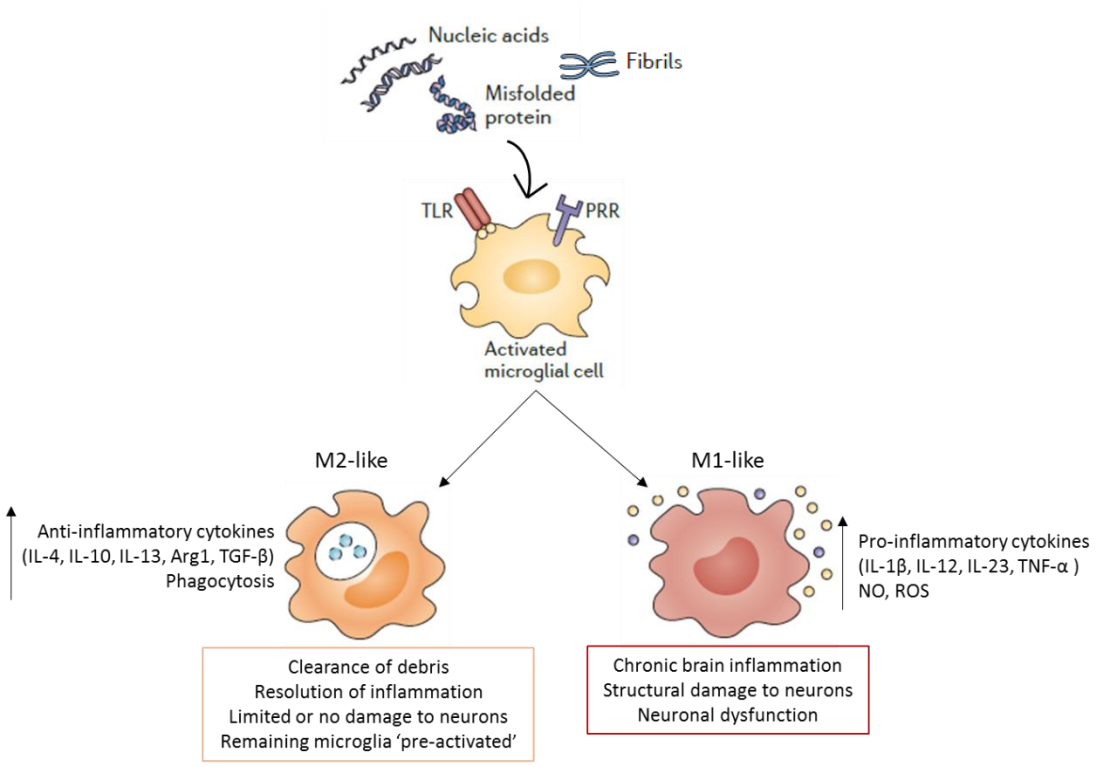

Figure 3 – Activation of microglia and functions of the different activated states. After microglia activation through pattern recognition receptors (PRRs), such as Toll-like receptor, microglia change to an amoeboid form and may respond by enhancing the removal of the stimulant or by secreting inflammatory mediators. Adapted from Heneka *et al*. 2014[22].

Many AD risk factors have been associated with neuroinflammation, including aging, several lifestyle factors, such as reduced physical activity and obesity. In addition, other metabolic changes, such as insulin resistance and diabetes, have also been associated with the release of inflammatory mediators, contributing for a chronic inflammatory response (reviewed in[10,54]). It is important to note that these metabolic factors are often found in parallel with Alzheimer's disease. For instance, Lee and colleagues saw that APP is up-regulated in adipocytes in obesity, correlating with the resistance to insulin and with an increase in the pro-inflammatory components in adipocytes. However, further studies are needed to acknowledge if increased expression of APP in adipocytes contribute to an increase in circulating Aβ peptides[55]. Moreover, in APP/PS1 mouse models, an age-dependent shift from the alternative to the classical phenotype was observed in activated microglia. At the same time, it has been established that accumulation of soluble Aβ oligomers also increases with age[56]. Thus, this activation switch could, in part, be induced by the accumulation of Aβ, which would be recognized by the receptors in microglia, leading first to M2 activation and, later, due to the persistence of the stimulus, to M1

activation, where an increase in the release of pro-inflammatory cytokines, NO and ROS, would occur, contributing to axonal and synaptic damage, inhibition of mitochondrial respiration and induction of neuronal apoptosis.

It has been observed that activated microglia develop a different gene expression pattern that could sustain a chronic type of neuroinflammation in AD. In addition, the increase in cytokine release was reported to influence the integrity of the BBB (reviewed in[54]). Once this barrier is compromised, it is easier for myeloid cells from the periphery to infiltrate the AD brain and migrate to the places where plaque formation is occurring, aiming to counterbalance the deficiencies of microglia function and helping in the clearance of Aβ[57]. In 2007, El Khoury suggested that the recruitment of brain mononuclear phagocytes is dependent on the chemokine receptor CCR2, which bind the chemokine CCL2. The authors showed that Ccr2-deficient APP mice have impaired microglia accumulation, leading to a decrease in Aβ clearance[58]. Similar conclusions were obtained in the study of Guedes and colleagues, which employed blood-derived monocytes. These authors presented evidences that protein levels of CCR2 are decreased in BDMs of AD and MCI patients, thus compromising the ability of these cells to migrate to the brain and clear the deposits of Aβ[59]. Therefore, the hypothesis proposed by Michaud, after studies in mouse models, which suggests that upon deficiencies in microglia-mediated Aβ phagocytosis, blood monocytes infiltrate the brain microenvironment and differentiate into efficient phagocytes, providing an alternative pathway for Aβ clearance, must be considered with caution. It is possible that, in humans, both microglia and blood-derived cells present disease-related deficiencies that hinder their ability to effectively remove Aβ plaques.

Microglia interaction with Aβ remains controversial. On one hand, microglia has the ability to phagocyte Aβ peptides, preventing their deposition. On the other hand, the continuous activation of microglia by Aβ leads to an increase in pro-inflammatory mediators, which may be responsible for the switch from M2 state to M1 state and, as a consequence, for the increase in neuronal damage, contributing to disease progression.

Although controversial, the study of chronic neuroinflammation in the context of dementia is becoming more and more important, mainly because 1) the amyloid cascade is not able to explain all AD cases and 2) this feature is observed at relatively early stages of disease. One strategy to identify if inflammatory processes are pathologically activated in a dementia setting is by measuring the increase in the expression and release of pro-inflammatory cytokines in the brain and cerebrospinal fluid. In addition, positron emission tomography allows the study of neuroinflammation *in vivo*, by measuring the levels of

[11C](R)PK11195 ligand [1-(2-chlorophenyl)-N-methyl-N-(1-methylpropyl)-3-isoquinoline carboxamide], a marker of neuroinflammatory events, including microglia activation. Through this technique it has been possible to observe an increase in [11C](R)PK11195 levels in mild and even early stages of AD, which suggests that microglia activation is an early event of Alzheimer's disease, that can take place even before disease onset[60,61]. These observations also suggest that monitoring neuroinflammation can be an important tool for early diagnosis of the disease, allowing early interventions that will probably have a more effective outcome.

1.2.4. The link between β-amyloid deposition, neurofibrillary tangles and neuroinflammation

The timeline of molecular events that define AD is still not well established and remains a subject of debate. Several authors believe that β-amyloid deposition precedes the formation of neurofibrillary tangles. For instance, in 2001, Gotz *et al.* saw that injection of $A\beta_{42}$ fibrils in the brain of a mutant tau transgenic mice model, P301L, increases the formation of NFTs[62]. Additionally, recent work reported that crossing Aβ species with mice presenting tau pathology aggravates tauopathy[63]. Thus, Aβ accumulation appears to contribute for tau hyperphosphorylation, but how this happens remains unclear. A currently accepted hypothesis suggests that the accumulation of Aβ peptides promotes tau hyperphosphorylation via activation of GSK-3β, due to an impairment in the insulin signaling cascade[64]. In addition, as already mentioned, insulin resistance is associated with an increase in inflammatory mediators, contributing to neuroinflammation. According to these observations, insulin signaling can play a role in all major hallmarks of AD.

There are also several studies pointing to a relationship between local microglia-driven neuroinflammation and NFT formation. In 2005, Kitazawa showed that after lipopolysaccharide (LPS) exposure, which is used as a common inducer of CNS inflammation, tau pathology increases, through CDK5 activation[65]. Moreover, it has been shown that early immunosuppression leads to reduced levels of tau pathology[66]. The receptor of the chemokine CX3CL1, CX3CR1, which is highly expressed in microglia, seems to reduce the phosphorylation of tau, since its knockdown in mice increases tau pathology. The CX3CL1-CX3CR1 axis downregulates microglial activity and reduces its toxic effects[66]. Therefore, these findings support the idea that neuroinflammation functions as an important link between Aβ deposition and NFTs since, in addition to LPS, β-amyloid

aggregates are also able to activate a M1 immune response, leading to an excessive production and release of pro-inflammatory cytokines, such as IL-1β. These cytokines will then bind to their receptors, activating several proteins, such as CDK5 and p38-MAPK and enhancing the phosphorylation and aggregation of tau (reviewed in[22]). It is also important to note that besides fibrillar Aβ deposits, intraneuronal Aβ, soluble Aβ or Aβ oligomers may also be responsible for tau pathology.

Taking into consideration the way Aβ aggregates, hyperphosphorylated tau and neuroinflammation that interact with each other, the lack of success of AD clinical trials using anti-inflammatory drugs may be because treatment starts late, at a stage in which Aβ and inflammation-driven tau pathology and neuronal death had already occurred in a great extent. Hence, targeting these three hallmarks at early stages might be the answer to fight the progression of the disease.

1.3. Novel Alzheimer's disease risk genes

Until 2009, *APOE* ε4 genotype was considered the most relevant genetic risk factor of LOAD. However, this genotype only accounts for 10-20% of LOAD risk, eliciting the possibility for the existence of other risk factors[67,68]. In fact, more recently, GWAS were performed in large cohorts of patients and controls and a correlation between common or rare variants of several genes and an increased/decreased of LOAD risk was established. These variants result from the presence of single nucleotide polymorphisms (SNPs) in or near the coding regions of genes mainly involved in three pathways: endocytosis, immunity and lipid metabolism. In this regard, GWAS studies have identified common variants of *ABCA7*, *BIN1*, *CASS4*, *CD33*, *CD2AP*, *CELF1*, *CLU*, *CR1*, *DSG2*, *EPHA1*, *FERMT2*, *HLADRB5-DBR1*, *INPP5D*, *MEF2C*, *NME8*, *PICALM*, *PTK2B*, *SLC24A4-RIN3*, *SORL1*, *ZCWPW1*, *FRMD4A* and *MS4A* family members, as well as rare variants of *TREM2* and *PLD3*, as conferring protection or increasing the risk of developing LOAD. The identification of these variants revealed a new perspective on the molecular pathways underlying AD disease pathogenesis (reviewed in[69,70]), since most of these genes are expressed in non-neuronal cells and some of them are known to play major roles in immune cells, such as microglia.

The potential mechanisms linking risk genes to AD pathogenesis are presented in Table 1.

Table 1 - Potential mechanisms linking genome-wide association studies to AD pathogenesis.

	Lipoprotein metabolism	**Lipid transport**	**Neuroplasticity**	**Inflammation**	**Aβ-aggregation**	**Aβ-clearance**	**Tau processing**	**Synapse formation/transmission**	**Intracellular trafficking**	**APP processing**	**ROS balance**
APOE	√		√	√	√	√					
ABCA7		√				√					
BIN1						√	√		√	√	
CASS4				√							
CD33				√							
CD2AP						√		√	√	√	
CELF1							√				
CLU		√			√	√					
CR1				√		√					
DSG2										√	
EPHA1							√				
FERMT2							√				
HLA-DRB5-DBR1				√							
INPP5D				√							
MS4A				√		√					
MEF2C											√
NME8											√
PICALM						√		√		√	
PTK2B			√								
SORL1	√								√	√	
SLC24A4											
ZCWPW1											
FRMD4A							√			√	
TREM2						√					
PLD3										√	

Reviewed in Karch *et al*. 2015[69] and Rosenthal *et al*. 2014[70].

The most well studied of all the recently disclosed AD risk genes is *TREM2*, a member of the innate immune receptor TREM family, which is highly expressed in resting microglial cells[71,72]. A strong association, similar in strength to that described for heterozygous APOE4 genotype, has been established between a rare variant of *TREM2*, the *rs75932628* (p.R47H), and AD[73,74]. However, the mechanisms by which *TREM2* missense mutations influence TREM2 function are still unclear. In 2014, Kleinberger and colleagues showed that several described *TREM2* missense mutations, including the R47H, decrease TREM2 shedding by protease ADAM10 and impair phagocytosis[75]. The authors also observed that a decrease in soluble TREM2 (sTREM2) is present in the CSF of patients with AD, further suggesting that reduced TREM2 function may contribute to increase AD risk. Interestingly, the levels of sTREM2 may serve a role in AD diagnosis and staging, since, contrarily to what is observed in full blown AD, an increase in sTREM2 can be observed in the plasma[76] and CSF[77] of MCI patients.

The overexpression of *TREM2* has been related with microglia ability to eliminate dead or dying neurons, with an increase in microglia phagocytic activity and with a decrease in the production of pro-inflammatory cytokines[78]. On the other hand, in the presence of inflammatory stimulus, such as LPS/interferon-γ, the expression of *TREM2* is downregulated[79], which has led to the conclusion that TREM2 is related with an anti-inflammatory phenotype. Although TREM2 is considered a phagocytosis receptor, the ligand of this receptor is yet to be identified. It has been suggested that TREM2 can mediate Aβ phagocytosis by directly binding Aβ, but this hypothesis is still far from being validated. Two very recent studies implicated TREM2 in the regulation of Aβ levels *in vivo*, although with contradictory results. On one hand, TREM2 deficiency increased Aβ accumulation in 5XFAD mice due to lack of microglia clustering around senile plaques[80]. On the other hand, in another study, TREM2 was shown to be upregulated in $Ly6C^{+}CD45^{high}$ cells located around plaques, and its absence was correlated with the amelioration of amyloid and tau pathologies[81]. Interestingly, in their work, Wang and colleagues also suggested that some lipids are capable of associating with fibrillar Aβ in lipid membranes and could be recognized by TREM2[80], acting as ligands to this receptor and triggering Aβ phagocytosis.

In what concerns humans, TREM2 protein levels were found to be downregulated in the CA1 region of the hippocampus of AD patients, with respect to age-matched controls[79]. In addition, Guedes and colleagues studied TREM2 mRNA expression in BDMs and MDMs of AD, MCI patients and controls, and observed that the expression of TREM2 was upregulated in BDMs and MDMs from MCI patients. This observation was in agreement

with the higher rate of Aβ uptake observed in macrophages from these patients. However, in AD patients, TREM2 expression was downregulated in BDMs and MDMs and the internalization of Aβ seemed to be compromised[59]. Based on these results, it stands to reason that the deregulation of TREM2 expression may interfere with the ability of the brain to clean toxic cellular debris, such as Aβ peptides, resulting in Aβ accumulation and self-aggregation into insoluble plaques.

Despite being the most well studied, *TREM2* is not the only immune-related AD risk gene under current discussion. For instance, CD33 (also known as Siglec-3) was already studied in microglial cells and circulating monocytes. CD33 is a transmembrane protein mainly expressed in immune cells, including mature monocytes, macrophages and microglia and in hematopoietic cells[82,83]. CD33 functions as a lectin, with immunoreceptor tyrosine-based inhibitory motifs that are involved in the inhibition of cellular activity, including immune response (reviewed in[84]). In 2013, Griciuc and Bradshaw reported that CD33 activity in microglia and monocytes might impact Alzheimer's disease, since the expression of CD33 risk allele *rs3865444*^{C} was increased in AD patients. This increased expression was correlated with the accumulation of activated, but less functional microglia cells, which, in turn, were implicated in a reduction of Aβ42 internalization and, consequently, in an increase in plaque burden[82,83].

Hence, it can be concluded that the identification of common or/and rare gene variants may provide new insights into AD pathogenesis. However, the functional contribution of these genes to the mechanisms of disease is, for the most part, still unknown, as well as their potential for further therapeutic development in the context of this disease. For this reason, in this study we chose to play a special attention to two new risk genes and their encoded proteins, PICALM and BIN1, which will be described in more detail in the next sections.

1.3.1.PICALM: an overview

PICALM (Phosphatidyl Inositol Clathrin Assembly Lymphoid Myeloid) encodes the CALM protein, which is ubiquitously expressed but is most prominent in neurons. This protein, which is involved in clathrin-mediated endocytosis, has two major domains: the AP180 N-terminal homolog (ANTH) domain and the clathrin-binding domain at its N-terminal region and C-terminus, respectively[85]. The last domain was seen to bind to clathrin and also to the AP2 adaptor complex, which emphasizes the role of *PICALM* on the

formation of clathrin-coated pits and, consequently, in the initial step of clathrin-mediated endocytosis[86]. On the other hand, the ANTH domain has been shown to interact with R-SNARE (Soluble NSF Attachment Receptors) proteins, such as VAMP2, VAMP3 and VAMP8, which regulate cargo docking during vesicle fusion processes[87].

PICALM is one of the risk genes presenting SNPs that have been associated with a reduction of AD risk. Two examples of these SNPs are the minor allele of *rs10792832* near *PICALM*[88] and *rs3851179*[89].

Depending on the cell type studied, *PICALM* can have different, and even contradictory roles. In 2013, Ando and colleagues saw that PICALM is highly expressed in microglial cells of LOAD brains compared to controls, which was suggested to be a result of microglia activation. In addition, the authors also reported that, in AD brains, full-length PICALM (75 kDa) was decreased, while two lower molecular weight species (50 and 25 kDa) were increased, as a consequence of proteolytic cleavage by calpains and/or caspase-3. However, whether PICALM cleavage is a result of deregulated microglia activity or due to chronic activation of microglia is not yet known. A fact is that cleaved PICALM, observed in AD brains, has been associated with synaptic and vesicle sorting defects, as a consequence of endocytic dysfunctions[90].

Studies in *PICALM* $^{+/-}$ and wild-type mice brains, as well in Neuro2a and HeLa cells transfected with small interfering RNAs (siRNAs) against CALM, showed that loss of the CALM protein is correlated with a decrease in Aβ42 at the level of γ-secretase cleavage. It was seen that γ-secretase is recognized as endocytic cargo by PICALM and is internalized by clathrin-mediated endocytosis in a PICALM-dependent manner. Thus, the authors showed that when PICALM is depleted, γ-secretase accumulates more at the cell surface and less in the late endosome and, as a consequence, the production of Aβ42 decreases. However, a change in Aβ total levels was not detected[91]. Xiao *et al*., using N2a-APP695 cells (neuroblastoma N2a cells overexpressing APP695) and brain tissues of APP/PS1 mice, also proposed a role for PICALM in APP endocytosis. Following PICALM knock-down, changes were observed in APP internalization and processing, leading not only to a decrease in Aβ42 but also in Aβ40 levels, which correlates with a reduction in amyloid plaque load[92].

Aside from the role of PICALM on Aβ production, evidences for its involvement in β-amyloid clearance through the autophagic pathway have been growing. In 2013, Tian and colleagues showed that the adaptor protein 2 (AP2) binds to LC3-II (which is targeted to elongate preautophagosomal structures, remaining on mature autophagosomes until

degradation by fusion with lysosomes), functioning as an intermediate to connect APP-CTF and LC3, thus contributing for the fusion of vesicles containing APP-CTF with LC3-containing autophagosomes. Silencing AP2 in N2a cells, stably expressing APP at full length, led to an increase in the levels of APP-CTF and Aβ40. Based on these results, the existence of a complex involving LC3, AP2 and PICALM has been proposed. The goal of this complex would be to remove APP-CTF from the cell surface, through the fusion of autophagosomes and endosomes, leading to the degradation of APP-CTF and, consequently, to the reduction of Aβ levels (Figure 4)[86]. Although the exact role of PICALM on autophagy is not well elucidated, studies by Moreau in HeLa and HEK293 cells suggested that PICALM affects autophagosome formation in its initial steps, during the maturation and enlargement of phagophore precursors. However, the authors not only reported changes in autophagosome formation, but also in its degradation, since the knockdown of PICALM deregulates VAMP8, which is known to regulate autophagosome-lysosome fusion. Hence, PICALM deficiency seems to have a dual effect on autophagy. Additionally, the modulation of PICALM has also an impact in the clearance of tau levels by autophagy and PICALM overexpression is associated with tau accumulation[93]. In addition to autophagy, other mechanisms involving PICALM have been proposed. Recently, Zhao and colleagues presented a mechanism of Aβ clearance through blood-brain barrier transcytosis (Figure 5)[94], in primary brain endothelium cells and *PICALM*-deficient *APP*$^{sw/0}$ mice. In this study, the authors showed a decrease in Aβ clearance across the BBB when *PICALM* levels were reduced, which consequently led to an increase in Aβ pathogenesis. This increase was rescued by delivery of an adenovirus expressing the *PICALM* gene. Moreover, the authors saw that *rs3851179* SNP is associated with a decrease risk of AD, since cells carrying these protective allele showed higher PICALM levels and, consequently, enhanced Aβ clearance[94].

Importantly, besides it direct link with APP processing and Aβ clearance, PICALM is also required for cellular cholesterol homeostasis, since alterations in PICALM levels, can lead to cholesterol homeostasis perturbation[95]. Accordingly, and taking into consideration the role of cholesterol in AD, the ability of PICALM to modulate cholesterol homeostasis points to an additional mechanism by which PICALM may contributes to AD.

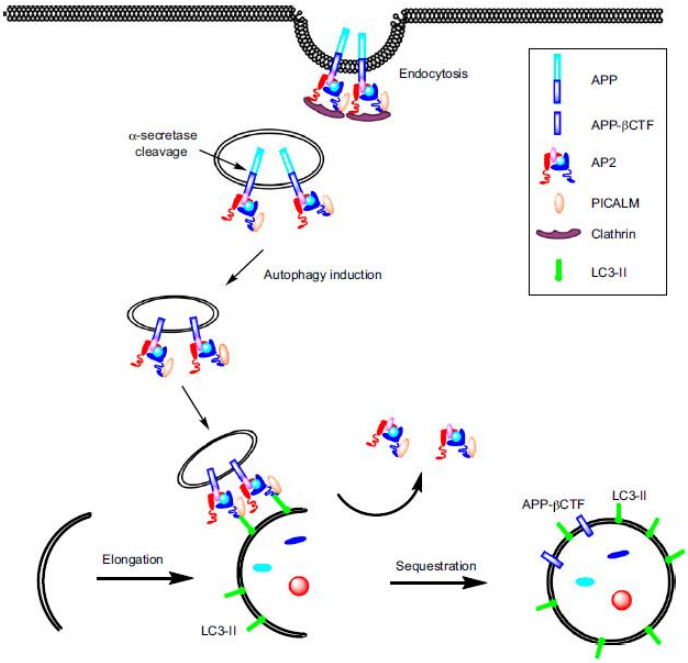

Figure 4 – Representative diagram of AP2 and PICALM targeting APP-CTF to autophagosomes for degradation. The adaptador complex AP2/PICALM recognizes and binds to the APP- βCTF of APP. Upon induction of autophagy, AP2 and PICALM shuttle βCTF to autophagosomes through binding of LC3 with the LC3-interacting region motif of AP2. Following sequestration of βCTF by autophagosomes, AP-2 and PICALM are released for recycling. From Tian *et al.* 2013[86].

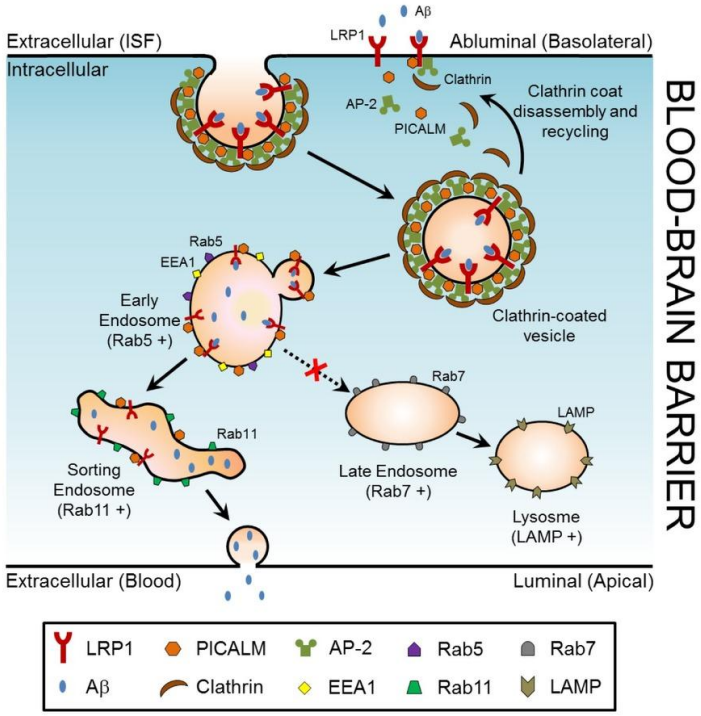

Figure 5 – Representative diagram of PICALM/clathrin–dependent internalization of the Aβ–LRP1 complex, leading to Aβ endothelial transcytosis and clearance across the BBB. From Zhao *et al.* 2015[94].

1.3.2. BIN1: an overview

Bridging Integrator 1 (BIN1), also designated as amphiphysin 2 (AmphII), is a member of the amphiphysin family of proteins. Originally, BIN1 was identified as a protein mainly expressed in muscle tissue, which was required for T-tubule formation[96] and, therefore, was associated with myopathies. Indeed, misregulated alternative splicing of *BIN1* was seen to perturb calcium homeostasis, interfering with excitation and contraction processes, leading to muscle weakness[97] and to heart failure, due to t-tubule deregulation[98]. However, nowadays, it is known that BIN1 is ubiquitously expressed and presents different cellular functions. BIN1 has been involved in the curvature of the membrane, regulation of actin filaments and endocytosis (reviewed in[99]). Like PICALM, BIN1 has two domains: the N-terminal Bin-Amphiphysin-Rvs (BAR) domain, which has been implicated in the regulation of membrane curvature and tubulation, and a SH3 (Src homology 3) C-terminal domain, mainly related with the recruitment of dynamin, which is a GTPase necessary for scission of the endosome from the plasma membrane (reviewed in[100]).

BIN1 is another one of the recently identified AD risk genes, and according to the Alzgene database (http://www.alzgene.org/) is the most important genetic susceptibility locus in LOAD after APOE. However, up to now, little is known about its expression and involvement in AD. Similarly to what has been described for *PICALM*, there are different thoughts concerning the expression and the role of *BIN1* in this disease, which is only natural, if we take into consideration the high number of interaction domains and isoforms described for the BIN1 protein (reviewed in[101]). As mentioned above, BIN1 appears to play a role in endocytosis and BIN1 CNS specific isoforms contain a clathrin and AP2 adaptor complex binding domain (CLAP), which is associated with clathrin-mediated endocytosis. This points to a role of BIN1 in the traffic of membrane proteins associated with AD and has led to research concerning BIN1 involvement in amyloid precursor protein metabolism and β-amyloid production. Additionally, BIN1 expression has also been associated with tau pathology by several authors.

In 2013, Elizabeth Glennon showed that BIN1 protein levels were decreased in temporal cortex samples collected from sporadic AD patients. Nevertheless, no effect was observed in APP expression, in the production of sAPPα or sAPPβ and in the levels of Aβ peptides following BIN1 knockdown by siRNAs in SH-SY5Y cells (a neuroblastoma cell line)[102]. In contrast, Chapuis *et al*. reported that the levels of BIN1 mRNA were increased in AD brains. Moreover, they saw that increased levels of *Amph*, the BIN1 *Drosophila*

ortholog, are associated with tau pathology, but not with amyloid load. Thus, the authors suggested that BIN1 may modulate microtubule stability and tau phosphorylation/aggregation in the earlier stages of the disease[103]. Although not much is known concerning the molecular and cellular mechanisms involving BIN1[104], last year Sottejeau found that BIN1 interacts with the proline-rich domain of tau through its SH3 domain. This interaction can have a direct impact in the early stages of AD. More recently, Miyagawa and colleagues suggested BIN1 could act as a regulator of BACE1 levels and Aβ production[105]. When knocking down *BIN1* in neuronal and non-neuronal cells, the authors observed an increase in BACE1 levels, as well as an increase in BACE1 activity, leading to an increase in Aβ production. In their work, the authors suggest a role for BIN1 in the intracellular trafficking of BACE1 from the early endosomes to the lysosomal pathway, or even to the cell surface, since in BIN1 depleted cells the trafficking of BACE1 was compromised and, as a consequence, an increase in Aβ production was observed.

In contrast to PICALM, there are no studies linking BIN1 to Aβ clearance. However, different studies from Gold and colleagues[106,107] in RAW-TT10 cells (a mouse macrophage cell line) and in murine resident peritoneal macrophages, showed that AmphII is associated with early phagosomes and cells expressing mutant amphiphysin present impairments in phagocytosis at the stage of membrane extension around the particles, since AmphII mutants fail to bind dynamin and, as a consequence, the membrane extension does not occur[106]. Later, Gold reported that *Chlamydia pneumonia*, which is an intracellular pathogen responsible for respiratory tract infections, is not effectively killed by macrophages. The authors state that this is due to the ability of bacteria to retain amphiphysin II, disrupting the maturation of macrophage phagosomes[107]. Therefore, these last studies point towards a possible involvement of BIN1 in Aβ clearance through phagocytosis.

Taking a closer look to the studies concerning PICALM and BIN1 it is clear that both proteins are involved in AD through different mechanisms and pathways. It is, therefore, crucial to clarify their true contribution to AD onset and progression and to further investigate their therapeutic potential as targets in the context of AD and other dementias.

1.4. MiRNAs

MicroRNAs (miRNAs) are abundant, endogenous and small non-coding RNAs responsible for the post-transcriptional regulation of gene expression. In the last two decades miRNAs have been shown to play important roles in development and homeostasis-related processes, including cell proliferation, migration, differentiation and death, and also in a vast number of human pathologies, including cancer, diabetes, neurodegenerative disorders, cardiovascular diseases and immune conditions.

Despite the fact that only 2588 mature miRNA sequences have been identified so far in the human genome (registered at miRBase [http://www.mirbase.org]), miRNAs are considered major regulators of gene expression, since a single miRNA might regulate multiple mRNAs, being able to modulate more than 60% of the human transcriptome[108]. Thus, miRNA biogenesis requires very strict regulation, in order to prevent the development of human diseases.

1.4.1. MiRNAs biogenesis and function

MiRNAs are ≈ 20 to 25 nucleotides long oligonucleotides that arise from intragenic or intergenic chromosomal DNA regions (Figure 6). They are transcribed by RNA polymerase II (RNA Pol II), into long RNA precursor molecules known as primary miRNAs (pri-miRNAs)[109], which go through several stages of processing, including cleavage by the microprocessor complex of Drosha and DGCR8, originating double stranded hairpin structures (pre-miRNAs)[110] that are exported to the cytoplasm by exportin-5. Alternatively, a less known mechanism of miRNA biogenesis has been described, in which miRNAs originate from intronic sequences called mirtrons, through splicing, in a pathway that is independent of Drosha (reviewed in[111]). In both cases, once in the cytoplasm, pre-miRNAs are processed by the endoribonuclease Dicer[112], which removes their hairpin structure and originates miRNA duplexes of ≈ 20–25 nucleotides in length. These duplexes, which are very similar to siRNAs, can interact with trinucleotide repeat-containing gene 6 protein (TNRC6) and with Argonaute (AGO) family members, two essential constituents of the miRISC. Once the miRISC complex is formed, the double stranded miRNA loses one of its strands and the remaining one (guide strand) guides this enzymatic complex to mRNA transcripts that present sequence motifs fully or partly complementary to each miRNA (reviewed in[113]). After biogenesis, miRNAs are able to

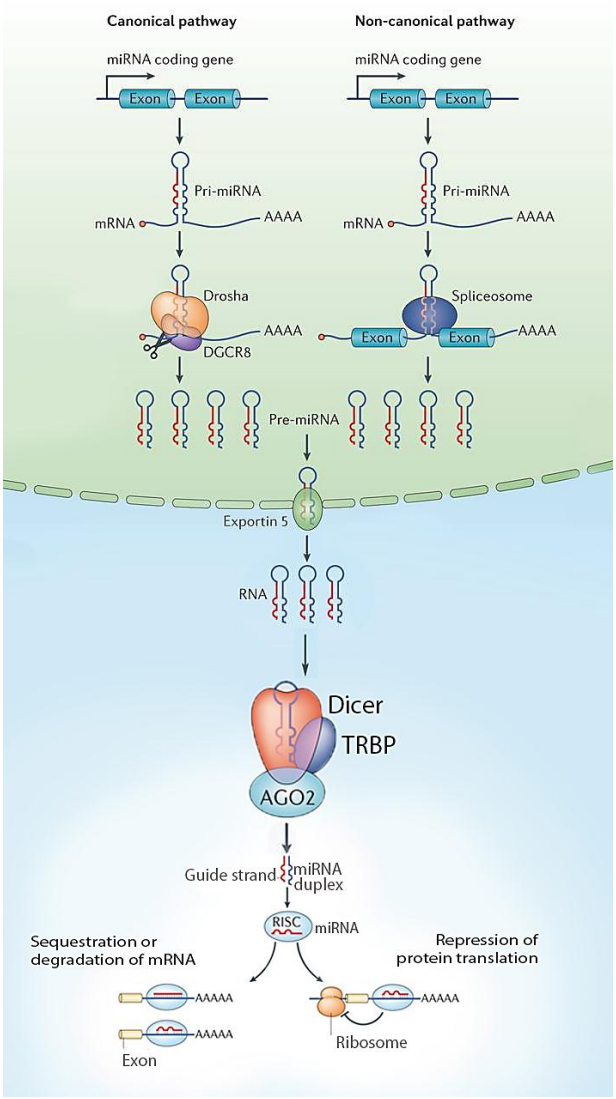

exercise their functions through binding to the 3'- untranslated region (UTR) of their target mRNAs. As a consequence of this binding, the ribosome machinery becomes temporarily or permanently unable to complete mRNA translation, which leads to changes in protein turnover. Additionally, in contrast to siRNA:mRNA interactions, only 30 to 35% complementarity between a miRNA and its target is necessary to allow transcription repression. Noteworthy, most of the time, the key to this process resides in the 6 nucleotides localized between positions 2 and 7 of the miRNA, the so called "seed sequence". The presence of sites in the target mRNA that are complementary to the seed sequence of a certain miRNA and have an additional base pair in position 8 of the

Figure 6 – Canonical and non-canonical pathways of miRNA biogenesis. In the canonical biogenesis pathway, miRNAs are transcribed by the RNA Polymerase II (Pol II) to originate primiRNAs, which are processed by the RNase III Drosha and its cofactor DGCR8 to form pre-miRNAs. The pre-miRNA is then exported to the cytoplasm by exportin 5. In the non-canonical pathway, pre-miRNAs arise in a Drosha- and DGCR-8-independent manner deriving from intronic regions of protein-coding genes that are processed by splicing. Pre-miRNAs undergo maturation in the cytoplasm by the action of Dicer and TRBP, followed by loading onto argonaute (AGO) proteins to form an effector complex called RNA-induced silencing complex (RISC), which will bind to mRNAs repressing their translation or inducing degradation. Adapted from Rottiers *et al.* 2012[114] and Li *et al.* 2014[115].

miRNA (canonical sites) tends to induce permanent mRNA degradation and to present high evolutionary conservation[116]. Nevertheless, there are other types of binding sites that induce more modest changes in gene expression, such as the marginal sites, which only present a six-nucleotide complementarity within the seed region, and the non-canonical sites, which

do not conform with the localization and type of motif binding described in the initial paradigms[117].

Hence, due to their conserved binding sites across species, their relative low number and their ability to bind more than one mRNA, it has been established that miRNAs exert crucial biological functions. The extreme consequences observed following knockout and silencing of different proteins involved in miRNA biogenesis, including Dicer and miRISC components, seems to strengthen this hypothesis[118]. However, it remains difficult to understand how these small molecules can orchestrate extremely complex events, such as the differentiation of immune lineages or the development of neuronal circuits. In this context, and in addition to translation repression and mRNA degradation, recent studies have suggested that miRNAs may be involved in other epigenetic mechanisms, including the direct regulation of nuclear transcription, through blocking of transcription factor binding sites, the triggering of enhancer regions[119] and the targeting or recruitment of chromatin remodeling machinery[120].

1.4.2. MiRNAs in Alzheimer's disease

1.4.2.1. MiRNA deregulation in the brain parenchyma

Many miRNAs are expressed in the brain and some are proposed to function in neuronal activities, such as spine development, neuronal differentiation, memory and synaptic plasticity[121]. Consequently, alterations in miRNA expression in the brain parenchyma may contribute to neurodegenerative diseases.

Currently, high-throughput functional screenings are lacking in the context of neurodegenerative disorders, but in the last few years several interesting reports have been published concerning changes in miRNA levels and their targets in different forms of dementia, including AD[122]. Different studies, employing *post-mortem* brain samples from AD patients, such as the work of Hébert and colleagues[123], have revealed changes in the miRNA profile of sporadic AD patients, giving a great contribute to the understanding of the potential role of miRNAs in the pathogenic mechanisms of AD. Hébert and coworkers identified different miRNAs that were downregulated in AD brains, compared to aged-matched controls, some of which were predicted to target APP (let-7, miR-101, -15a, and -106b) or BACE1 (miR-15a, -29b1, -9 , and -19b). In this study, BACE1 expression was also evaluated and a subgroup of sporadic AD patients were shown to display increased

levels of immature and mature BACE1 protein, compared to the control group. However, BACE1 mRNA levels remained basically unchanged in AD samples, suggesting that increased BACE1 expression was due to alterations in posttranscriptional regulatory mechanisms, implying the potential regulation of BACE1 expression by miRNAs. Using the luciferase assay, the authors showed that miR-29a and miR-29b1 bind to BACE1 in HeLa cells. Furthermore, mutations in the seed region of BACE1 3'UTR led to abrogated repression of luciferase expression by miR-29a. Moreover, a decrease in miR-29a/b1 expression was identified in the subgroup of AD with higher BACE1 levels, with respect to the control group and to a non-AD demented group. Additionally, upon treatment with miR-29a/b1 or anti-miR-29a/b1 mimics, the authors showed that BACE1 activity decreased and increased, respectively. Thus, these results indicate that miR-29a/b1 cluster may be a crucial suppressor of BACE1 protein expression and that the deregulation of both these miRNAs might contribute to increased BACE1/β-secretase expression in sporadic AD[123].

A study from Boissonneault and colleagues also addressed the possible miRNA-mediated regulation of BACE1 expression. According to these authors, an inverse correlation between BACE1 protein and miR-298 and miR-328 could be observed in a mouse model of AD and biochemical validation confirmed that these two miRNAs are able to target the 3'UTR of BACE1[124].

In a different study, Hébert and colleagues also found that miR-106b was significantly decreased in sporadic AD samples compared to aged-matched controls[125]. Therefore, the possibility of miR-106b regulating APP expression *in vitro* and at the endogenous level was evaluated and the binding of miR-106b to the 3'UTR of APP was validated by the luciferase assay. In addition, the transient transfection of miR-106b led to a decrease in APP protein expression in the mouse brain. These data suggest that miR-106b may regulate APP and that abnormal miR-106b expression may contribute to changes in APP levels in the AD brain.

In 2008, Wang and colleagues studied miRNA expression profiles during AD progression, using RNA brain samples from four patients groups: elderly non-demented with negligible AD-type pathology, non-demented with incipient AD pathology, MCI with moderate AD pathology, and AD. Microarray analysis showed that the majority of miRNA expression patterns were stable across the different clinical states and approximately 200 different miRNAs were expressed at levels below background. For instance, miR-107 was found to be significantly and consistently decreased among AD-related cases, even in patients at the earliest stages of the pathology. Unsurprisingly, considering that this miRNA

is predicted to target the 3'UTR of BACE1 in at least five different regions, the luciferase reporter assay supported that miR-107 is able to bind and regulate BACE1 translation through at least one 3'UTR microRNA response element (MRE). Thus, and as expected, data indicated that BACE1 mRNA levels and miR-107 levels were inversely correlated during the progression of AD, and that the decrease of this miRNA was associated with an acceleration of AD progression[126]. In addition, other studies supported the previous observations, since a correlation between the levels of miR-107 and the amount of senile plaques ($P<0.07$) and neurofibrillary tangles ($P<0.04$) was also established[127].

Regarding AD risk genes, until now TREM2 has been the only novel risk gene whose deregulation has been associated with faulty miRNA control. The downregulation of TREM2 has been suggested to depend on pro-inflammatory miRNAs, such as miR-34a, which is enriched in microglia and is under the control of the proinflammatory nuclear factor-κB (NF- κB)[128,129]. Using a reporter plasmid encoding the 3'UTR of TREM2 mRNA and employing the luciferase reporter assay, Zhao and co-workers observed that, in the presence of exogenous anti-miR-34a, the luciferase signal increased, indicating the presence of a positive miRNA:mRNA match between miR-34a and TREM2 mRNA. The authors also reported that inhibiting this miRNA reverted the effect, bringing TREM2 back to homeostatic levels[130].

Overall, the above-mentioned studies show how, in the last decade, significant advances have been achieved regarding miRNA expression profiles and miRNA deregulation in the brain parenchyma during the course of AD pathology. However, the possibility that miRNA levels can be subject to artifact changes, resulting from brain processing *post-mortem*[131] is an important limitation present in these studies, which has to be taken into consideration during data interpretation. Nevertheless, this issue does not exclude the relevance of further high-throughput functional analysis, designed to obtain more reliable results, since this type of studies is crucial not only to understand how miRNAs are involved in the pathological mechanisms of AD, but also to identify new biomarkers and therapeutic targets.

1.4.2.2. MiRNAs in the local and peripheral immune system

MiRNAs have long been studied in the context of immunity. As mentioned before, the innate immune system constitutes our first line of defense against most impending threats and is an integral part of the overall immune organization, comprising cells and mechanisms which primarily protect the host against infections by external organisms. This system also plays an important role in the presence of deregulated internal signals, since its activation usually allows the organism to deal with these endogenous triggers, preventing the development of pathological states. However, the exact contribution of immune cells to neurodegenerative diseases, including AD, is still a matter of great debate, owing to their neurotoxic or neuroprotective role in AD. Nevertheless, it is now accepted that neuroinflammation is an important component of this disorder and, as such, a prime target towards the development of novel therapeutic strategies.

MiRNAs are invaluable regulators of inflammatory pathways and are known to control both the differentiation and activation of immune cells[132,133]. Some miRNAs in particular, such as miR-155, miR-146a, miR-145, miR-124 and miR-21, play important roles in the regulation of inflammation, either by enhancing its propagation or by limiting its development (reviewed in[134]). For instance, an increase in the M1 activation state is accompanied by an increase in miR-155 expression and a reduction in miR-124 expression. On the other hand, the maintenance of the homeostatic balance (M0) is characterized by high levels of miR-124, while an increase in miR-145 expression has been related with the M2 activation state[135]. Therefore, these miRNAs may help to identify the activation phenotypes in different disease settings and their modulation may allow to shift these phenotypes to more favorable states that potentiate tissue recovery and reduce cell damage.

In addition to microglia, monocytes and macrophages have also been tightly associated with AD progression. This is due to their similarities with microglia, in terms of ontology and function, and because peripheral monocytes have been shown to travel from the blood to the brain parenchyma in AD animal models, infiltrating the tissue and contributing to the clearance of Aβ[136]. Despite the similarities between AD mice models and the human disease, monocytes and macrophages from AD patients exhibit significant deficits in chemotaxis and phagocytosis, when compared to control subjects. These observation suggest that, in contrast to what happens in AD mice models, in human patients these cells constitute a poor defense mechanism to fight AD progression[59]. Of note is that part of these deficits can be attributed to miRNA deregulation in these cells. In fact, Guedes

et al. has observed that several immune-related miRNAs, predicted to target proteins associated with the innate immune response and chemotaxis, are significantly altered in peripheral monocytes of AD patients. These miRNAs include miR-155, miR-27b, miR-200b and miR-128[59]. Interestingly, the results reported by Guedes *et al.* concerning miR-128 confirmed the observations reported by Tiribuzi and colleagues in 2014[137], where miR-128 was found to be upregulated in monocytes and lymphocytes from AD patients, with respect to age-matched control subjects, and its expression was shown to regulate the production of lysosomal enzymes implicated in the degradation of Aβ peptides, such as cathepsin B[137]. This study showed that, similarly to what occurs in the AD brain[138], the distribution of lysosomal proteases is also altered in peripheral cells, reinforcing the idea that most cellular mechanisms responsible for myeloid function in the periphery also have an important role in the function of brain cells. In what concerns miR-155, this miRNA was previously shown to be highly upregulated in microglia cells exposed to lipopolysaccharide (LPS) and to modulate the expression of the suppressor of cytokine signaling 1 (SOCS-1)[139], an inhibitor of the JAK/STAT and NF-kB signaling pathways. In addition, miR-155 was shown to be associated with AD pathology, since it was found to be upregulated in the brain of 3xTg AD mice, correlating with the downregulation of SOCS-1 observed in these animals[76]. Hence, has become clear that this miRNA presents a pro-inflammatory activity in the AD brain that helps to propagate neuroinflammation. Regarding miR-200b, as well as miR-200c, studies in the THP-1 cell line (a macrophage-like human monocytic cell line) reported the involvement of these miRNAs in the regulation of innate immune responses, through the regulation of TLR4 signaling and consequent NF-κB activation[140]. The exogenous introduction of miR-200b and -200c resulted in a decrease of NF-κB activity and in a decrease of IL-6, CXCL9 and TNF-α after exposure to LPS[140].

In addition to the study performed by Guedes and colleagues, which concerned circulating monocytes, several miRNAs were also found to be deregulated in the serum of AD patients with respect to controls. miRNA-146a, -93, -143 and -31 were found to be decreased in the serum of AD patients[141]. Interestingly, miR-146a has also been shown to be deregulated in different mouse models of AD and in the human brain. However, contrarily to what was described in serum, this miRNA was found to be upregulated in the AD brain, instead of downregulated. The upregulation of miR-146 was shown to result in the concomitant downregulation of two miRNA-146a molecular targets: i) the interleukin-1 receptor-associated kinase 1 (IRAK1)[128], an adaptor of toll-like receptors (TLRs) that initiates diverse downstream signaling pathways, eventually leading to the induction of pro-

inflammatory transcription factors, such as the nuclear factor-κB (NF-κB) and ii) the complement factor H (CFH), an important repressor of the inflammatory response in the brain[142]. Importantly, the expression of this miRNA is upregulated *in vitro,* in human microglia cells activated with Aβ, suggesting that, at least in part, miR-146a increased expression in AD derives from the activation of microglia[143]. To best of our knowledge, studies concerning miRNA-31 in the context of AD are not known so far. However, there are other studies relating this miRNA with inflammation. miR-31 may play a role in the regulation of inflammatory mediators, such as TGF-β, which, in turn, increases miR-31 expression[144,145].

So far, all evidences suggest that the presence of miRNAs in various body fluids makes these circulating molecules promising biomarkers for AD diagnosis and prognosis. Nevertheless, to date, there are no standardized and accepted miRNA biomarkers for this disease.

Overall, it is now undeniable that neuroinflammation is, indeed, a hallmark of AD. Thus, in the future, this feature should be considered as a potential therapeutic target in the search for new treatment options for AD, including miRNA-based therapies.

1.4.2.3. MiRNAs as potential therapeutics for AD

Since miRNAs deregulation is associated with AD pathology, these small non-coding RNAs could also be used as potential therapeutic targets or therapeutic molecules in AD. There are two possible approaches to the development of miRNA-based therapeutics: i) the use of miRNA inhibitors, which block the activity of a certain miRNA, potentially increasing the levels of miRNA target proteins and ii) the increase of the amount of a specific miRNA in the cytoplasm of the target cells, through the use of miRNA mimics or expression vectors, with the ultimate goal of downregulating miRNA target proteins.

Up to now, oligonucleotide therapeutics in the context of dementia have only been accomplished in animal models and have been designed to target AD-relevant genes. These strategies seem to offer beneficial effects, although they still need to be optimized in terms of pharmacokinetics and pharmacological activity. Due to the charged nature of nucleic-acids, this optimization faces specific challenges that can be overcome through the use of viral and non-viral delivery vectors, which provide chemical and electrostatic stabilization of oligonucleotides, improve their circulation time *in vivo* and allow the specific targeting of certain cell types. In addition, for some approaches, these vectors must also allow the

crossing of the BBB, in order to efficiently deliver their cargo into the brain parenchyma, increasing their bioavailability within the CNS (reviewed in[115]).

Most miRNA-related studies in AD have been focused on the use of miRNAs to modulate the APP processing pathway, due to the importance of APP itself, as well as BACE1, in Aβ overproduction and tau pathology. For instance, a study reported the use of a lentiviral-mediated miR-101 overexpression cassette to decrease APP expression and, consequently, reduce Aβ accumulation in the mouse brain[146]. Additionally, Zhang and colleagues showed that miR-188, which targets *BACE1 in vivo*, is downregulated in AD and that the overexpression of this miRNA in the hippocampus (through stereotaxic injection of a lentivirus expressing miR-188) reduced Aβ deposition and neuroinflammation and prevented deterioration of hippocampal basal synaptic transmission, long-term potentiation, spatial learning and memory in 5XFAD mice[147].

Despite the fact that viral vehicles are the most widely employed carriers in gene therapy studies, due to their high efficiency, they are also associated with high toxicity, as well as with immune response activation. Because of this, the use of non-viral carriers, such as nanoparticles and liposomes, has been increasing steadily over the last few years (reviewed in[148]). For instance, the above mentioned study on miR-128 was performed using the transfection reagent lipofectamine2000. In this study miR-128 upregulation resulted in a decrease of Aβ phagocytosis by monocytes of healthy subjects, whereas miR-128 inhibition improved the ability of monocytes of AD patients to degrade Aβ, which is in agreement with the idea of a positive contribution of blood monocytes to Aβ degradation, both in the periphery and in the brain (following their infiltration into the brain parenchyma)[137].

Hence, miRNAs, owing to their role as regulators of gene expression, may provide relevant insights into the cellular mechanisms regulating the expression or inhibition of AD related genes, allowing us to better understand the causes and consequences of this disease at a molecular level. Therefore, the discovery of new miRNAs in the context of dementia, as well as the validation of their targets, is crucial for the development of miRNA-based biomarkers and therapies, which could change the course of the disease, either by allowing an earlier diagnosis or by ameliorating or delaying disease symptoms. However, it is important to take into account that most studies referred above have been performed *in vivo*, in animal models of AD. Therefore, the employment of miRNA-based therapeutic strategies is still in a very premature phase, and further preclinical studies will be necessary to properly address the true potential of these approaches.

Chapter 2

Objectives

2.1. Objectives

In contrast to what is known concerning EOAD, which is usually a consequence of autosomal dominant mutations in *APP*, *PSEN1* or *PSEN2* genes, LOAD causes are much further from being completely clarified, mainly due to the multiplicity and complexity of risk factors associated to this form of dementia. At present, and thanks to recent GWAS studies, new genetic risk factors have been identified for LOAD, pointing to an important role of the immune system and neuroinflammation in the development of this form of AD. In this context, the main goal of the present work was to study the new AD risk genes, focusing on two genes in particular, *BIN1* and *PICALM*, previously related with immune cell function. We approached this study from a mechanistic point of view, in order to understand how these genes are associated with LOAD and what is the influence of miRNA deregulation in the expression and function of *BIN1* and *PICALM*. We believe that this knowledge is crucial to pave the way for future miRNA-based therapies designed to modulate the expression of these genes and recover their normal function.

Towards this purpose, this work was divided into three major tasks, each associated with a specific goal:

1) The first task of this project involved the evaluation of the expression of the new AD risk genes in blood-derived monocytes and monocyte-derived macrophages. The major aim of this task was to clarify the conditions driving the expression of the different risk genes in innate immune cells, including the effects of cell type, activation state, age and disease stage of the cell donors.

2) In the second task, and taking into consideration previous studies performed in our lab showing that several immune-related miRNAs were deregulated in monocytes from AD patients, we evaluated the impact of miRNA modulation in AD risk gene expression and function. Towards this purpose, we transfected MDMs and electroporated a murine microglia cell line (N9 cells) to increase the expression of specific miRNAs. We then evaluated changes in *BIN1* and *PICALM* expression, as well as changes in several other functional parameters related with the innate immune response, including the expression of pro- and anti-inflammatory cytokines and phagocytosis.

3) Currently, there is no easily available cell model of human microglia. This constitutes a serious drawback when studying neuroinflammation, since mouse and human microglia cells show considerable differences. Therefore, in the third task of this project,

we aimed to establish a new protocol to isolate and differentiate microglia-like cells from human blood-derived monocytes, according to a recently published protocol. In order to fully characterize these cells we investigated the levels of several surface markers, as well as the expression of several microglia signature genes.

Chapter 3

Material and Methods

3.1. Patient selection

Young healthy volunteers, with an age range between 22 to 33 years old, were recruited at the Center for Neuroscience and Cell Biology of University of Coimbra.

Patient samples were recruited at Neurology Department, Coimbra University Hospital, in previous work, as described by Guedes *et al*[59]. Subjects included age-matched healthy controls (controls), MCI patients (MCI) and AD patients (AD), whose diagnostic comprised varied exams, including the standard clinical evaluation, routine laboratory tests, imaging studies (computed tomography [CT] or MRI), SPECT, *APOE* allele genotyping and *TREM2* genotyping for R47H mutation in exon 2 (associated with higher AD risk[75]) for AD and MCI patients. PET, cerebrospinal fluid analysis and genetic studies were more restricted, although considered in younger patients. A comprehensive cognitive-functional-psychological assessment battery was carried out by a team of neuropsychologists, following a standard protocol, and comprising several tests and scales: 1) Cognitive instruments as the MMSE[149], the MoCA[150], the ADAS-Cog[151] and a comprehensive neuropsychological battery validated for the Portuguese population (Battery of Lisbon for the Assessment of Dementia[152]) were used to explore memory and other cognitive domains; 2) The Clinical Dementia Rating (CDR)[153] was used for global staging and 3) The Geriatric Depression Scale (GDS-30)[154] was used to exclude major depression. All MCI patients were classified at the global CDR staging of 0.5 (no functional impairment) and were selected according to Albert's[155] and Petersen's criteria[156]. The standard criteria for the diagnosis of AD patients were the Diagnostic and Statistical Manual of Mental Disorders – fourth edition (DSM-IV-TR) and the National Institute of Neurological and Communicative Disorders and Stroke-Alzheimer's Disease and Related Disorders (NINCDS-ADRDA)[157]. The AD group included patients with mild disease (CDR = 1) or moderate to severe (CDR = 2 and 3). The control group comprised cognitively healthy adults belonging to the local community (recruited among the patients' spouses, hospital or university staff or their relatives), that were age, education, and gender matched to the patients. Controls had normal MMSE scores (> 24) and were fully autonomous in daily life activities (CDR) according to the information obtained through a general practitioner, and/or an informant. Moreover, to be eligible for this study, subjects (patients and controls) should be in a stable condition, without acute significant events or recent/undergoing changes in medication. Exclusion criteria were: 1) significant motor,

visual or auditory deficits which could influence the neuropsychological performance; 2) neurological/psychiatric conditions other than MCI or AD; 3) CT or MRI demonstration of significant vascular burden[158]; 4) diagnosis of diabetes, chronic inflammatory, neoplastic diseases or prescription of anti-inflammatory drugs; 5) major depression indicated by a GDS score of 20 or more points; 6) active smokers; 7) patients suffered from uncontrolled hypertension. Informed consent was obtained from all participants and the study was conducted in accordance with the tenets of the Declaration of Helsinki with the approval of the local ethics committee.

3.2. Sample collection and isolation of peripheral blood mononuclear cells fraction

As performed previously for AD and MCI patients and age-matched controls, a total of 40 mL of blood was collected from young healthy individuals (at least n=13), ranging from 22 to 33 years old, in sterile 10 mL EDTA-coated tubes. Afterwards, the blood was diluted with a solution of phosphate-buffered saline (PBS) and peripheral blood mononuclear cells (PBMCs) were isolated by density gradient centrifugation [800 g without brake, 20 min at room temperature (RT)] using Histopaque-1077 (Sigma, USA). The PBMCs fraction was collected and washed 2 times with PBS [600 g, 6 min at RT] for further experiences, including isolation of blood-derived monocytes and differentiation into monocyte-derived macrophages and microglia-like cells.

3.3. Blood-derived monocytes isolation from PBMCs fraction

Magnetic-activated cell sorting (MACS) was used to isolate the $CD14^+$ subpopulations, recognized as monocytes, from the PBMC fraction. Briefly, the PBMC pellet was resuspended and incubated with rotation, for 15 min at 4ºC, in 80 μL/10^7 cells of beads buffer [PBS containing 0.5% bovine serum albumin (BSA), 2 mM EDTA, pH 7.2] and 7,5 μL/10^7 cells of magnetic microbeads associated with an anti-human CD14 antibody (#130-050-201, Miltenyi Biotec, Germany). After a brief centrifugation to remove the excess of microbeads, cells were resuspended in 500 μL of beads buffer and applied into the LS MACS column (Miltenyi Biotec), placed under the magnetic field of a MidiMACS™ Separator (Miltenyi Biotec). The column was washed 3 times to remove unlabeled cells and the retained $CD14^+$ cells were further eluted with the beads buffer, upon

column removal from the magnetic field. $CD14^+$ cells were used for subsequent experiments, including RNA extraction for qRT-PCR analysis and differentiation into monocyte-derived macrophages.

The purity of $CD14^+$ monocytes was determined by flow cytometry, using a monoclonal anti-CD14-FITC antibody (Sigma, USA), and was shown to be around 99%.

3.4. Primary cultures of monocyte-derived macrophages and microglia-like cells

$CD14^+$ cells were plated in 12 MW Costar plates at a density of 8×10^5cells/well, with RPMI-1640 culture medium without fetal bovine serum (FBS) [10 mL/L Pen/Strep, 10 mM HEPES, 12 mM Sodium Bicarbonate, 2 mM L-Glutamine, 1 mM Sodium Piruvate]. After overnight incubation, the cells were supplemented with 10% FBS and 50 ng/mL of the recombinant human Macrophage Colony-Stimulating Factor (M-CSF; Peprotech) to promote differentiation into MDMs.

Microglia-like cells (iMGs) were obtained from PBMCs according to the protocol described by Ohgidani *et al*. in 2014[159]. Briefly, PBMCs were plated with RPMI-1640 culture medium without FBS, in T25 flasks and 12 MW costar plates at a density of 3×10^6cells/well. In the following day, culture supernatant and non-adherent cells were removed. The adherent cells (which correspond to monocytes) were cultured with RPMI-1640 [10% inactivated FBS, 10 mL/L Pen/Strep, 10 mM HEPES, 12 mM Sodium Bicarbonate, 2 mM L-Glutamine, 1 mM Sodium Piruvate] supplemented with 10 ng/mL of the recombinant human Granulocyte Macrophage Colony-Stimulating Factor (GM-CSF; Peprotech) and 100 ng/mL of the recombinant human Interleukin-34 (IL-34; Peprotech). This protocol was performed in parallel to MDM differentiation from PBMCs, as described above.

The cells were cultured in standard conditions (37ºC, 5% CO_2) for 7 or 14 days to promote differentiation into MDMs and 14 days to promote differentiation into iMGs, with medium and differentiation factors replaced every 3-4 days.

The iMGs profile were characterized by flow cytometry analysis, using a monoclonal anti-CD14-FITC antibody (Sigma, USA) and an anti-human/mouse TREM2 PE-conjugated monoclonal antibody (R&B Systems, USA), and by qRT-PCR, using unique microglial signature genes, including *P2ry12*, *Hexb*, *Cx3cr1* and the transcription factor PU.1.

3.5. Stimulation of M1 and M2-like activation states in monocyte-derived macrophages

The MDMs obtained from $CD14^+$ differentiation (n=4) were activated, after 7 days of differentiation, by exposure for 24h to LPS (100 ng/mL) and IFN-γ (20 ng/mL), to induce the M1 activation state, or IL-4 (20 ng/mL), to induce the M2 activation state. In the next day, cells were frozen at -80ºC until RNA extraction for qRT-PCR experiments.

3.6. Transfection of MDMs with miR-mimics

After the 7 days of MDM differentiation from PBMCs, miRIDIAN microRNA mimics of miR-154, miR-31, miR-200c and miR-497, as well as the double stranded oligonucleotide control (all acquired from Dharmacon) were used for transfection experiments. MDMs were transfected using miRNA mimics complexed with DLS liposomes, prepared as described by Trabulo et al[160]. Briefly, 1 mg of dioctadecylamidoglycylspermidine (DOGS) (Promega, Wisconsin) and 1 mg of dioleoyl phosphatidylethanolamine (DOPE) (Sigma, Germany) were dissolved in 40 µL of 90% ethanol, followed by the addition of 360 µL of sterile H_2O, leading to a total lipid concentration of 5 mg/mL (2.5 mg/mL of DOGS and 2.5 mg/mL of DOPE). The solution was homogenized by a short vortex and incubated for 30 min at room temperature to allow liposome formation. After this period, the DLS lipoplexes were prepared by mixing a certain volume of DLS solution with a certain volume of miRNA mimic, taking into consideration an optimal ratio of 95 µg of lipid per 10 ug of oligonucleotide, in order to obtain a final concentration of 50 nM of oligonucleotide/well. The lipoplex mixture (DLS+mimic) was incubated 30 min at room temperature before administration. 50 µL of lipoplexes were added to the cells in 450 µL of RMPI-1640 medium without FBS [10 mL/L Pen/Strep, 10 mM HEPES, 12 mM Sodium Bicarbonate, 2 mM L-Glutamine, 1 mM Sodium Piruvate] in 12 MW plates (Costar). Following 4h of incubation in culture conditions, the medium was replaced by fresh RPMI-1640 medium [10% inactivated FBS, 10 mL/L Pen/Strep, 10 mM HEPES, 12 mM Sodium Bicarbonate, 2 mM L-Glutamine, 1 mM Sodium Piruvate]. 24 h after transfection, cells were subjected to the AlamarBlue® assay to evaluate cell viability and conclude on the toxicity of the transfection protocol. 48 h after transfection cells were frozen at -80ºC for further mRNA extraction and qRT-PCR of target mRNA levels.

3.7. Evaluation of cell viability

Cell viability was assessed by AlamarBlue® assay 24 h post-transfection. Briefly, cells were incubated in standard conditions with RPMI-1640 culture medium containing the resazurin dye (Sigma-Aldrich) in a dilution of 1:150. After reduction of resazurin to resorufin by metabolically active cells, 150 µL of medium, collected from each well, were transferred into a 96-well plate for absorbance measurement at 570 nm (reduced form) and 600 nm (oxidized form), in a SpectraMax Plus 384 microplate reader (Molecular Devices). In the end, the percentage of cell viability was calculated with respect to non-transfected cells, according to the equation:

$$\% \text{ Cell viability} = \frac{\Delta\text{Abs transfected cells} - \Delta\text{Abs negative control}}{\Delta\text{Abs positive control} - \Delta\text{Abs negative control}} \times 100$$

$\Delta Abs = Abs_{570nm} - Abs_{600nm}$

Transfected cells – Cells transfected with the respective miRNA mimic

Negative control – Resazurin in RPMI-1640 medium, without cells

Positive control – Non-transfected cells

3.8. Microglia cell line and culturing conditions

N9 cells (a murine microglia cell line) were cultured at 37ºC in a humidified atmosphere containing 5% CO2 and maintained in RPMI-1640 medium [5% heat inactivated fetal bovine serum (FBS), 1% Penicillin/Streptomycin (Pen/Strep), 23.8 mM Sodium Bicarbonate, 30 mM glucose]. N9 microglia cells were plated in the day of each electroporation experiment, at a density of 80 000 cells/well in 12-well multi-well plates and/or at a density of 20 000 cells/well in µ-slide 8-well ibiTreat chamber slides and maintained in culture conditions for 48 h. After 48 h, the cells were used for further experiments, including: extraction of RNA, cDNA synthesis and qRT-PCR. Phagocytosis assays were also performed, employing both flow cytometry and confocal microscopy.

3.9. Plasmid preparation

Four different plasmids were used in electroporation experiments: pMIR-31, pMIR-155, pMIR-200c and pControl. The plasmids were amplified in super competent DH5α cells (previously treated with rubidium chloride) and purified using the NucleoBond® Xtra

plasmid purification kit (Macherey-Nagel, Germany), according to the manufacturer's recommendations. Briefly, after cell transformation, pre-inoculum and inoculum culture, bacterial cells were harvested by centrifugation (6000 g, 10 min). The cell pellet was resuspended and then lysed by the addition of lysis buffer. Afterwards, the cell suspension was neutralized, loaded into an affinity purification column and the plasmid DNA was washed and then eluted with elution buffer. For plasmid concentration and desalting, NucleoBond® Finalizer Large filters were used. The pDNA concentration was quantified in a Nanodrop 2000 spectrophotometer (Thermo Scientific).

3.10. Electroporation of N9 cells with pMIR-155, pMIR-200c, pMIR-31 and pControl

N9 cells were electroporated following a modified version of the protocol described by Chu *et al*[161]. First, cells were detached from culture flasks and a cell suspension of 10×10^6 cells was prepared per experimental condition. After a brief centrifugation to pellet the cells (5min, 1200 rpm), 12.5 µg of each plasmid were diluted in a final volume of 400 µL of PBS 1x and added to the cells (the volume of plasmid used was calculated using the Promega Biomath Calculator, according to the equation):

$$\text{pmol DNA} \times \frac{660pg}{pmol} \times \frac{1\mu g}{10^6 pg} \times N = \mu g\ DNA$$

N – Number of nucleotides

$\frac{660pg}{pmol}$ – Average molecular weight of a nucleotide pair

The cell suspension was placed into 0.4 cm Gene Pulser®/MicroPulser™ electroporation cuvette (Bio-Rad #1652081) and incubated for 5 min at room temperature. Immediately prior to electroporation, the contents of the cuvette were gently mixed and then subjected to electric pulses (Volts = 0.23 kV; Capacitance = 500 µF). After the exposure to electric pulses, cells were incubated for 10 min on ice and then 5 mL of growth medium was added. Subsequently, viable cells were counted with Trypan Blue and plated with RPMI-1640 medium in µ-slide 8-well ibiTreat chamber slides (ibidi) at a density of 2×10^4 cells/well, for microscopy analysis, or in 12 MW plates, at a density of 8×10^4 cells/well, for flow cytometry analysis and RNA extraction, and further cultured for 48h. Following this period, cells were analyzed by confocal microscopy and flow cytometry in order to assess p155 and pEGFP transfection efficiency, since these two plasmids presented green fluorescent tags. Electroporated cells were also employed in phagocytosis assays,

using fluorescent-labelled latex beads, and in qRT-PCR experiments, designed to evaluate miRNA-mediated modulation of target mRNA levels.

3.11. Latex beads phagocytosis assay

MDMs transfected with mimic miRNAs and electroporated N9 cells were incubated, 48h after transfection, with 4 µL and 2 µL (in 12MW plates and 8-well ibiTreat chamber slides, respectively) of carboxylate-modified red fluorescent latex beads with a mean diameter of 2 µm (L3030, Sigma-Aldrich), during 2h30min, in culture conditions. After this period, cells were washed twice with PBS and analyzed by flow cytometry and confocal microscopy to estimate the number of cells able to perform phagocytosis, as well as the mean number of latex beads ingested by each cell.

3.12. Immunocytochemistry of MDMs and N9 cells

In order to label cells for confocal analysis, following incubation with red fluorescent latex beads, immunocytochemistry labelling β-actin was performed in N9 cells in µ-slide 8-well ibiTreat chamber slides, according to established protocols. Succinctly, after two washes with PBS, cells were fixed in 4% paraformaldehyde (PFA) in PBS during 20 min at room temperature. The cells were then permeabilized for 2 min with 0.2% Triton X-100 and non-specific binding epitopes were blocked by incubating cells for 30 min with a 3% BSA solution prepared in PBS. Cells were incubated overnight at 4ºC with the primary antibody against β-actin (1:1000), prepared in PBS with 3% of BSA. Following two washing steps with PBS, cells were incubated for 2 h at room temperature with the secondary antibody anti-mouse Alexa Fluor-488 conjugate, diluted 1:200 in PBS with 3% BSA. Subsequently, cells were rinsed twice in PBS and incubated with the DNA-specific Hoescht 33342 (1 µg/mL) for 5 min in the dark. Finally, cells were again rinsed twice in PBS and then kept in PBS at 4ºC until observation in a point scanning confocal microscope Zeiss LSM 710 Meta (Zeiss, Germany).

3.13. Extraction of total RNA and cDNA synthesis

Total RNA (including small non-coding RNA) was extracted from N9 cells, BDMs, MDMs and iMGs using the miRCURY™ RNA Isolation Kit (Exiqon, Denmark), according to the manufacturer's recommendations for cultured cells. In brief, cells were

firstly lysed with the lysis buffer (containing 10 µL of β-mercaptoethanol per milliliter), then the total RNA adsorbed to a silica matrix, incubated with DNase solution (On-column DNase I digestion set, Sigma-Aldrich), washed with the recommended buffer and eluted with 35-40 µL of elution buffer.

Once extracted, total RNA was quantified in a Nanodrop 2000 spectrophotometer (Thermo Scientific). cDNA synthesis for evaluation of gene expression was performed using the NZY First-Strand cDNA Synthesis Kit (Nzytech, Portugal). Up to 1000 ng of total RNA in 12 µL of reaction volume were used for cDNA synthesis, according to the following protocol: 10 min at 25ºC, 30 min at 50ºC and 5 min at 85ºC for reverse transcriptase inactivation. In the end, samples were incubated for 20 min at 37ºC with NZY RNase H (*E. coli*) to degrade the RNA template in cDNA:RNA hybrids after first-strand cDNA synthesis. The synthetized cDNA was further diluted up to 50 times with RNase-free water and stored at -20ºC until required. For evaluation of miRNA expression, cDNA synthesis was carried out using the Universal cDNA Synthesis Kit (Exiqon). cDNA was obtained from 5 ng of total RNA in a reaction of 10 µL, according to the following protocol: 1 h at 42ºC, followed by 5 min at 95ºC for heat-inactivation of the reverse transcriptase. The resulting cDNA was diluted 40 times with RNase-free water and stored at -20ºC until required.

3.14. Quantitative real time PCR of mRNA and miRNA

Quantitative polymerase chain reaction (qRT-PCR) was accomplished in a StepOnePlus thermocycler (Applied Biosystems) using 96-well low-profile microtitre plates and employing the SsoAdvanced Universal SYBR Green Supermix (Bio-Rad), for mRNA quantification, or the miRCURY LNA™ Universal RT microRNA PCR system (Exiqon), for miRNA quantification. All primers employed for mRNA quantification were designed through the Ensembl and Primer-Blast softwares, with the exception of the reference gene hypoxanthine phosphoribosyltransferase 1 (*HPRT1*) primer, which was previously designed with Beacon Designer software and idtDNA primer design tools and the TREM2 and APOE primers, which were purchased from Invitrogen (primer sequences are listed in table 2). The primers of TNF-α, IL-1β, TGF-1β and IL-10 were purchased from Qiagen (QuantiTect Primer, Qiagen, Hilden, Germany). For each primer set, a master mix was prepared, consisting of 5 µL of SYBR Green Supermix and 1 µL of primer, to yield a final concentration of 1µM. All reactions were performed in duplicate with 6 µL of the

prepared master mix and 4 µL of template cDNA. PCR cycle conditions consisted of polymerase activation and well-factor determination for 30 seconds at 95ºC, followed by 45 amplification cycles of 5s at 95ºC (denaturation), 20s at 60ºC (annealing) and 5s at 65ºC (elongation).

For miRNA quantification, the miRCURY LNA™ Universal RT microRNA PCR system (Eqixon) was used in combination with pre-designed primers (Exiqon) for miR-155 and reference RNAs: SNORD110 and SNORD44, for *Mus musculus* samples and *Homo sapiens* samples, respectively. Each reaction, performed in duplicate, contained 4 µL of template cDNA and a master mix comprising 5 µL of SYBR GREEN and 1 µL of the primer mix (1 µM for each primer pair). Reaction conditions consisted of enzyme activation and well-factor determination at 95°C for 10 min, followed by 45 cycles of: 10s at 95°C (denaturation) and 60s at 60°C (annealing and elongation). In all qRT-PCR experiments, a melting curve protocol started immediately after amplification, consisting of 1 minute heating at 55°C followed by 0.5°C increments in temperature (80 steps of 10 seconds) until a maximum of 95ºC. Threshold value for threshold cycle determination (Ct) was set at 10000 and the baselines adjusted for each primer set. The No Template Control (NTC) and the No Reverse Transcriptase Control (NRT) were always performed for each primer set, in every qRT-PCR run. Relative miRNA and mRNA levels were determined following the Pfaffl method[162], taking into consideration the different amplification efficiencies of each primer, obtained from a standard curve of serial sample dilutions.

Table 2 – List of primer sequences used for qRT-PCR analysis and respective melting temperatures (Tm) and product sizes.

Primer	***Primer sequence (5'->3')***	***Tm (ºC)***	***Product length (bp)***
MS4A4A	FW: TGGATGGCATGGTGCTCC	59.7	112
	RV: AGAATTAACACAACCCCACC	55.5	
MS4A6E	FW: CGAAAAGGATATACCAACCA	52.7	140
	RV: CTAGGCAGAACTCCAACA	53.4	
BIN1	FW: TTCTCCCAAAGATTAGGT	49.2	99
	RV: AACTCAACTAGAGGACAC	50.3	
SORL1	FW: CTGAATATGTGTCCTTGA	48.4	110
	RV: AGAATGATACTTGTGGTTA	48.0	
CR1	FW: GACAGGTGCAGACGTAAATC	56.6	83
	RV: CCGAACTGGATGCCTTTGATC	59.3	
CLU	FW: CTCATGGGAAGAACAGAAT	51.8	103
	RV: AAGCAGCAACTCAACATA	51.7	
INPP5D	FW: GAAAAGAAACTCAGGCGAAACC	58.4	110
	RV: AAGAGGTGCGTGAAGCGGTG	63.3	
TREM2	FW: ATGATGCGGGTCTCTACCAGTG	61.9	151
	RV: GCATCCTCGAAGCTCTCAGACT	61.9	
APOE	FW: GGGTCGCTTTTGGGATTACCTG	61.5	124
	RV: CAACTCCTTCATGGTCTCGTCC	60.7	
PICALM	FW: CCATAATCAGTAACCTATCAAG	51.6	91
	RV: AGGACACAGTTCTTCTCT	51.8	
CD33	FW: TGTTCCACAGAACCCAACAA	57.5	165
	RV: TTCCTCCTGTGGGTCTTCA	57.4	
CASS4	FW: CCCTACTGCCCAAGTCTATG	57.1	98
	RV: GCGTGAGGATGGCCTGTTTTG	62.4	
HPRT	FW: TGACACTGGCAAAACAATGCA	59.5	94
	RV: GGTCCTTTTCACCAGCAAGCT	61.1	

3.15. Flow cytometry analysis

CD14 and TREM2 surface expression in BDMs, MDMs and iMGs was analyzed by flow cytometry, using a monoclonal anti-CD14-FITC antibody (Sigma, USA) and an anti-human/mouse TREM2 PE-conjugated monoclonal antibody (R&B Systems, USA), respectively, and the corresponding isotype controls. BDMs were analyzed immediately after isolation, while iMGs and MDMs were analyzed in the last day of the differentiation protocol. Briefly, the cells were washed once with PBS 10% FBS and incubated with each antibody (10 µL/5 × 10^5cells and 5 µL/5 × 10^5cells for CD14 and TREM2, respectively) diluted in 100 µL of PBS 3% BSA, in the dark with rotation, for 30 min at 4ºC. After this period, cells were washed twice with PBS and analyzed in a FACS Calibur flow cytometer (BD Biosciences, USA). Fluorescence intensity and the % of $CD14^+$ and $TREM2^+$ cells was assessed in the FL-1 and FL-2 channels, for FITC and PE-conjugated antibodies, respectively. For each experience, depending on the cell number, a total of 5000 – 20000 events was collected in the established gate.

To evaluate electroporation efficiency in N9 cells, 48h after electroporation with p155 or pEGFP, cells were washed twice with PBS and immediately analyzed in a FACS Calibur flow cytometer (BD Biosciences, USA). The fluorescence signal associated with the expression of GFP was assessed in the FL-1 channel, through the collection a total of 10000 events in the established gate.

For the phagocytosis assay, fluorescence due to ingestion of red fluorescence latex beads was also assessed in the FL-1 channel, in a FACS Calibur flow cytometer (BD Biosciences, USA), trough the collection a total of 20000 events in the established gate, with each peak assumed to equal an additional bead.

All data were analyzed using the Cell Quest software (BD Biosciences, USA).

3.16. Confocal microscopy analysis

To access electroporation efficiency following delivery of p155 and pEGFP, cells were fixed in PBS with 4% PFA during 20 min and then stained 5 min, in the dark, with DNA-specific Hoescht 33342 (1 µg/mL) and washed twice with PBS. Images were acquired in a point scanning confocal microscope Zeiss LSM 710 Meta (Zeiss, Germany), using a 63 x oil objective and the Blue (405 nm) and Green (488 nm) lasers. Image

acquisition was performed using the Zen Black software and acquisition settings were kept constant between experiments.

For phagocytosis evaluation, following β-actin labelling by immunocytoschemistry, images were acquired in a point scanning confocal microscope Zeiss LSM 710 Meta (Zeiss, Germany), using the 63 x oil objective and the Blue (405 nm), Green (488 nm) and red (568 nm) lasers. For each experiment and experimental condition, 10 representative images were taken and the total number of cells as well as the total number of cells with internalized beads was determined to establish the phagocytosis index.

3.17. Statistical analysis

All data are expressed as mean ± standard deviation (SD) and were analyzed for statistical significance using One-way ANOVA followed by Tukey's *post hoc* test, One-way ANOVA followed by Dunnet's test and Two-way ANOVA followed by Sidak's test for multiple comparisons. In the case of risk genes expression quantification in BDMs Vs. MDMs and in iMGs Vs. MDMs, the unpaired t test, assuming Gaussian data distribution, was used. Differences were considered statistically significant for P values < 0.05. Calculations were performed using the standard statistical software GraphPad Prism 6 (La Jolla, USA).

Chapter 4

Results and discussion

4.1. Expression profile of the newly identified AD risk genes

AD is a complex and devastating disease for which, currently, there is no perfect animal model. In order to overlay pathologies and allow the study of hallmark interactions, double or triple transgenic mouse models have been generated, taking advantage of the different mutations found in the familiar and early-onset AD cases. However, currently there is no mouse model that mimics the most common late onset AD and exhibits all features of human AD (cognitive and behavioral deficits, amyloid plaques, NFTs, gliosis, synapse loss, neuron loss, neuroinflammation and neurodegeneration). Therefore, care should be taken in the interpretation of the results provided by the existing animal models (reviewed in[163]) and new models of sporadic AD should be developed to overcame this handicap. In this context, studies in human primary cultures of AD patients, such as cells from the myeloid lineage, may provide significant information, particularly concerning the recently described contribution of the immune system and neuroinflammation to this disease.

Cells from the myeloid lineage have an important role during the initial host response, leading to the activation of different defense mechanisms. In Alzheimer's disease mouse models, BDMs have been shown to play a beneficial role, infiltrating the brain parenchyma and helping in the clearance of Aβ deposits[57,136]. However, the role of these cells, as well as of MDMs, which are differentiated from BDMs, in AD patients, is yet poorly explored. In this context, our group has recently shown that these cells are compromised in AD patients, presenting impairments in important immune system functions, including chemotaxis and phagocytosis[59]. To achieve a better understanding of the role played by BDMs and MDMs in AD, and taking into consideration the recent GWAS studies correlating several immune genes with AD risk, we decided to employ these human cell models to clarify the contribution of some of the newly identified risk genes in AD development.

4.1.1. Isolation and characterization of BDMs and differentiation into MDMs

BDMs were isolated from the blood of healthy young volunteers by MACS, according to the surface expression of CD14 (Figure 7). CD14 is a 55 kDa membrane-bound glycoprotein mainly expressed by monocytes and macrophages, considered by several authors as the universal marker of monocytes[164,165]. Importantly, this glycoprotein is involved in the activation of immune cells in response to exogenous and endogenous signals[164]. The yield of the isolation procedure was around 10% and the purity of BDMs, evaluated by flow cytometry, was around 99% (Figures 7B and 7C). These results, which are in agreement with previous results obtained in our group[59], point to a specific and effective isolation process, which allows the recovery of most monocytes in circulation and generates a $CD14^{high}$ homogenized cell population.

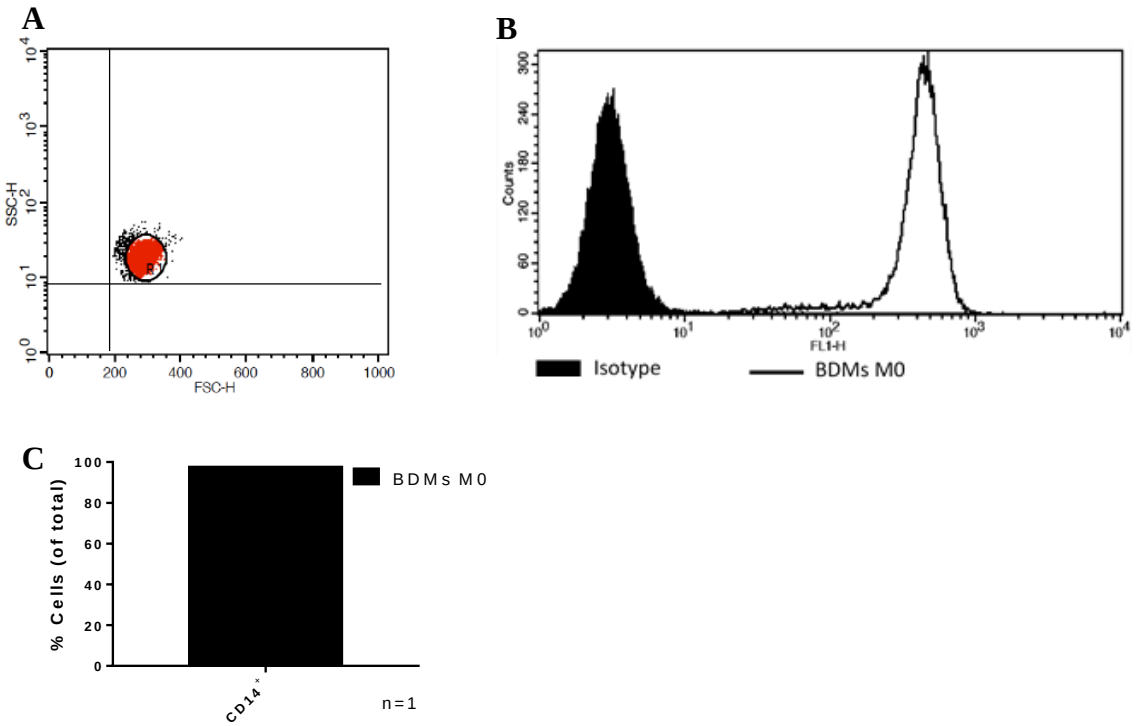

Figure 7 – Isolation of blood-derived monocytes from PBMCs by magnetic-activated cell sorting. The expression levels of the $CD14^+$ surface marker was evaluated by flow cytometry, in the FL-1 channel, after magnetic cell sorting using anti-CD14 magnetic beads. **(A)** Representative dot plot of the $CD14^+$ population. **(B)** Representative histogram of $CD14^+$ surface expression. **(C)** Percentage of sorted cells expressing $CD14^+$, following histogram analysis. The results are expressed as percentage of total cells.

Following isolation, the $CD14^+$ cell population was cultured overnight in RPMI-1640 culture medium without FBS, in order to facilitate cell adhesion, and was supplemented with 10% FBS and M-CSF (50 ng/mL) 24h later, in order to initiate the differentiation process into MDMs, since M-CSF is a glycoprotein involved in survival, proliferation and differentiation of mononuclear phagocytes, in particular of resident macrophages[166]. The differentiation process, which takes approximately 7 days[167,168], leads to profound changes in cell morphology, as can be observed in Figure 8.

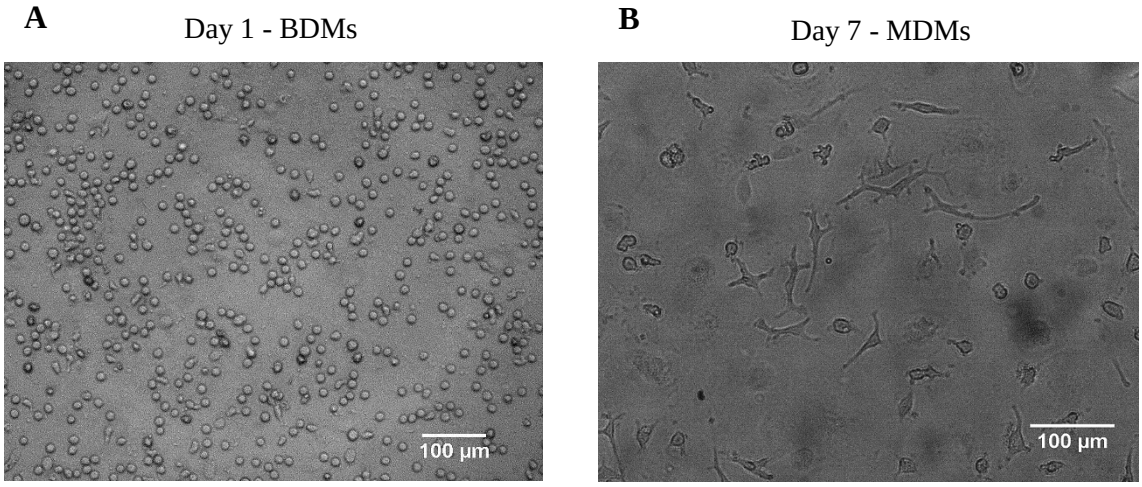

Figure 8 – Morphology of BDMs and MDMs isolated from PBMCs. Representative images showing the morphology of **(A)** BDMs 24h after isolation and plating, immediately before the addition of M-CSF (50 ng/mL) and **(B)** MDMs, obtained following 7 days of differentiation in the presence of M-CSF (50 ng/mL). The images were acquired in a light microscope equipped with the 20x objective. Results are representative of an $n = 4$.

4.1.2. Comparative analysis of AD risk gene mRNA expression in BDMs and MDMs of young healthy individuals

The identification of new genetic risk factors for AD has come to shed new light into the molecular pathways underlying AD disease pathogenesis. Some of identified risk genes are known to be highly expressed in cells of the immune system, including monocytes and macrophages, and to be involved in innate immune responses, lipid metabolism and endocytosis/cytoskeleton remodeling processes. This opens the possibility of a direct involvement of some of these genes in Aβ production and clearance pathways. Nevertheless, up to now, little is known about the functional contribution of the newly

identified AD risk genes towards disease mechanisms, as well as their therapeutic potential in the context of AD pathology.

To the best of our knowledge, the relative expression of the majority of the new AD risk genes has not been evaluated systematically in mononuclear phagocytes, including BDMs and MDMs. Therefore, in this study, we employed qRT-PCR to quantify the expression levels of 13 genes in freshly isolated BDMs and in MDMs kept in the absence of cell activators (Figure 9A). We also performed a similar quantification in MDMs following induction of the classical activation state (M1-like) and the alternative activation state (M2-like) (Figure 9B), obtained through exposure to LPS (100 ng/mL) and IFN-γ (20 ng/mL) or to IL-4 (20 ng/mL), respectively.

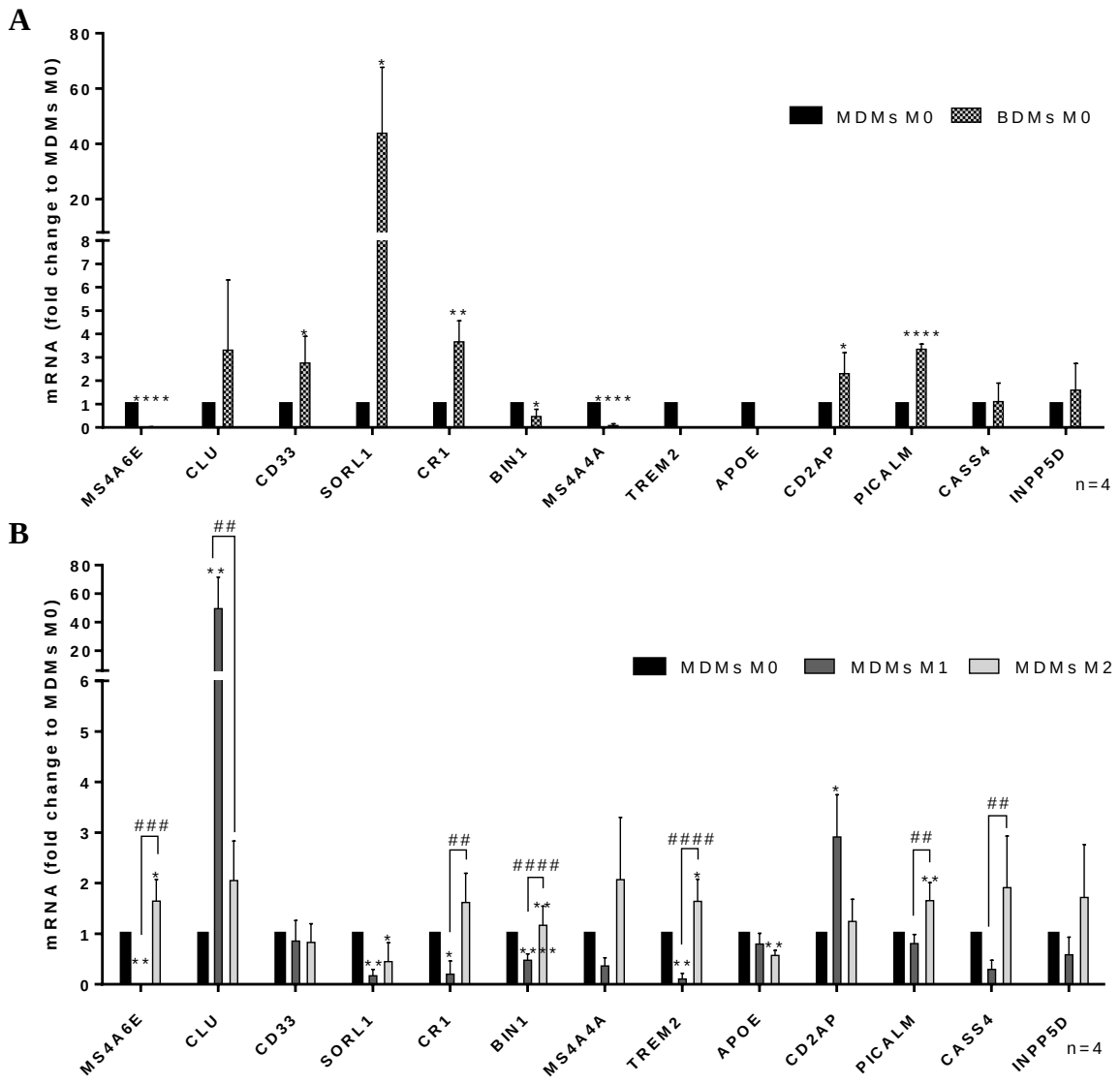

Figure 9 – Risk genes expression in BDMs and MDMs. (A) Total RNA was extracted from freshly isolated BDMs or from MDMs M0 obtained after 7 days of differentiation in the presence of M-CSF (50 ng/mL). The expression of 13 risk genes was quantified by qRT-PCR. Results are expressed as mRNA fold change with respect to MDMs M0, normalized to the reference gene *HPRT*, and are representative of an $n = 4$. Unpaired t test, following Gaussian distribution with * $p < 0.05$, ** $p < 0.01$, *** $p < 0.001$ and **** $p < 0.0001$ with respect to MDMs M0. **(B)** MDMs were further incubated with LPS (100 ng/mL) and IFN-γ (20 ng/mL) to induce the M1-like state or IL-4 (20 ng/mL) to induce the M2-like state, respectively. The same risk genes were quantified by qRT-PCR in the M0, M1 and M2 states. Results are expressed as mRNA fold change with respect to MDMs M0, normalized to the reference gene *HPRT*, and are representative of an $n = 4$; One-way ANOVA, following Tukey's *post hoc* test; * $p < 0.05$, ** $p < 0.01$, *** $p < 0.001$ and **** $p < 0.0001$ with respect to MDMs M0; ## $p < 0.01$, ### $p < 0.001$ and #### $p < 0.0001$ with respect to MDMs M1. All values are presented as mean ± SD.

As it can be observed in Figure 9A, the expression of the selected AD risk genes is different in BDMs and MDMs, although statistically significance is only achieved for 8 genes. The genes from the MS4A family (*MS4A6E* and *MS4A4A*) and *BIN1* are decreased in BDMs, while *CD33*, *SORL1*, *CR1*, *CD2AP* and *PICALM* are increased, with respect to MDMs. Importantly, when comparing the expression profile of MDMs in different activation states, significant differences can be observed when cells assume a pro-inflammatory (M1-like state) or an anti-inflammatory phenotype (M2-like state). Interestingly, for the majority of these genes, a decrease in expression has been observed in the M1-like state, accompanied by an increase in the expression of the same gene in the M2-like state, which suggests that most risk genes play an anti-inflammatory role during cell activation and immune response. This is in agreement with previous data obtained for genes like *TREM2*, *BIN1* and *PICALM*, showing that these genes play a role in endocytosis and phagocytosis[75,80,86,92,105,107], processes typically associated with the M2 phenotype. The opposite was verified only for *CLU* and *CD2AP*, which show a clear increase in expression in the M1-like state, suggesting that their expression is required during a pro-inflammatory response.

Taking into consideration that AD and other dementias have been related with changes in innate immunity and with a chronic neuroinflammatory response that promotes the M1 state, these results indicate that genes upregulated in M2, such as *MS4A6E*, *SORL1*, *CR1*, *MS4A4A*, *TREM2*, *CASS4*, *INPP5D*, *PICALM* and *BIN1*, play a protective role in AD and may be dowregulated in the context of dementia. On the other hand, genes such as *CLU*

and *CD2AP*, which present higher expression in the M1-like state, may be related with disease progression and are expected to be upregulated in AD patients.

4.1.3. Comparative analysis of *PICALM* and *BIN1* mRNA expression in MDMs of MCI patients, AD patients and age-matched controls

Taking into consideration the results presented above, we decided to evaluate the expression of several risk genes in the context of AD. For this purpose we selected 2 risk genes, *PICALM* and *BIN1*, whose expression was observed to be decreased in the M1-like state and increased in the M2-like state (Figure 9B). The choice of these two genes was also motivated by the presence, in their 3'UTR regions, of binding sites for various miRNAs already known to be deregulated in AD patients, with respect to age-matched controls[59]. This previous finding, together with their possible involvement in endocytosis and phagocytosis events, suggested that both these genes may hold interesting potential as therapeutic targets in miRNA-modulation strategies designed to improve Aβ clearance. Since Aβ phagocytosis is mostly mediated by fully differentiated mononuclear phagocytes, such as macrophages, we choose to evaluate gene expression in MDMs from AD patients, MCI patients and healthy age-matched controls (Figure 10). Table 3 presents the clinical data for each of the experimental groups.

Table 3 –Characteristics of patient and control study populations.

Variable	*Controls*	*AD*	*MCI*
Number of patients (n)	5	8	10
Gender (F/M)	2/3	6/2	2/8
Age (years)	71.2 ± 9.8	77.9 ± 8.9	71.2 ± 8.9
MMSE score	> 24	16.9 ± 6.4	27.0 ± 3.4***
MoCA score	--	14.5 ± 10.6	19.0 ± 4.8
ADAS-cog score	--	--	10.0 ± 4.4
Stage of disease (CDR) (%)			
Mild	--	75.0	--
Moderate	--	25.0	--
Severe	--	--	--
APOE genotype ε4, %	70	70	60

NOTE. Data are expressed as mean ± SD, except for gender (expressed in percentage of females–F [%] and males–M [%]), stage of disease (CDR; expressed in percentage of total), and APOE genotype ε3, ε4 (expressed in percentage of ε4 carries). For MMSE and MoCA, higher scores correspond to better performance and for the ADAS-cog, higher scores indicate greater impairment. MoCA and ADAS-cog were only performed in patients with CDR ≤ 1. One-way ANOVA was used to compare age between groups, followed by Tukey's *post hoc* test. Two-tailed t test was used to compare MMSE, MoCA, and ADAS-cog scores, and Fisher's exact test was used for APOE genotype. ***P < 0.001 with respect to AD.

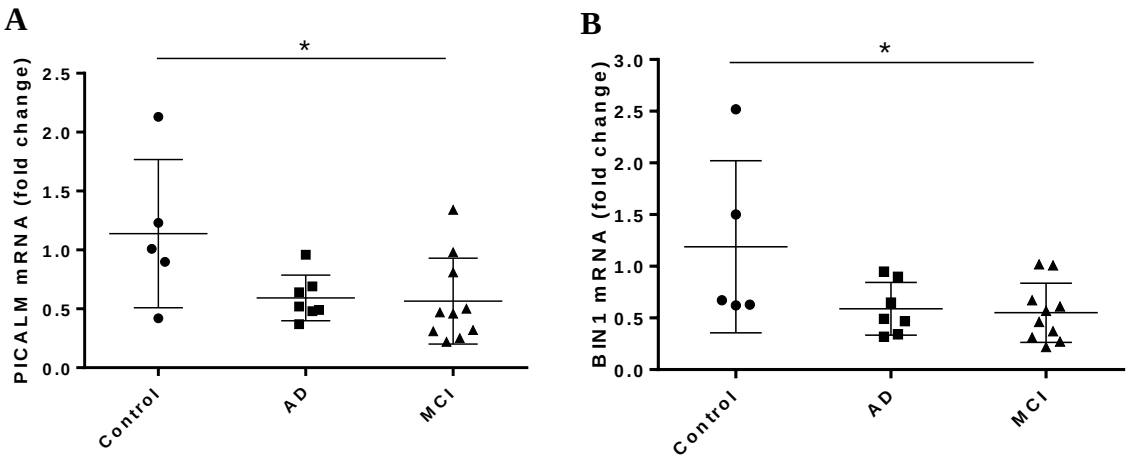

Figure 10 – Quantification of *PICALM* and *BIN1* mRNA levels in AD patients, MCI patients and age-matched controls. Following total RNA extraction from MDMs isolated and differentiated from $CD14^+$ BDMs of AD patients, MCI patients and age-matched controls, the levels of **(A)** *PICALM* and **(B)** *BIN1* mRNA were quantified by qRT-PCR. Results are expressed as mRNA fold change with respect to the mean of control subjects, normalized to the reference *HPRT*, and are representative of at least $n = 5$ per group; One-way ANOVA, following Tukey's *post hoc* test, * $p < 0.05$ with respect to control. Values are presented as mean ± SD.

As expected, we observed a decrease in the mRNA levels of both genes in MDMs of AD and MCI patients, pointing once again to a protective role of *PICALM* and *BIN1* in AD pathology. However, only MCI patients achieve significance. This may be due to the inherent variability of the control group and to the low number of control subjects in this study. Therefore, in order to further confirm the observed tendencies, the number of subjects in each experimental group, and in particular in the control group, should be increased.

To the best of our knowledge, this is the first time that a relation is established between mononuclear phagocytes, risk genes *PICALM* and *BIN1* and AD. Interestingly, the protective role observed for *PICALM* is in accordance with the studies of Tian[86], Zhao[94] and Moreau[93], that suggested the involvement of PICALM in Aβ clearance.

4.1.4. Comparative analysis of *PICALM* and *BIN1* mRNA expression in MDMs of young and elderly subjects

It is believed that genes linked to age-related diseases, such as AD, also have an important role in the aging process itself. However, up to now, only genotype studies using SNPs in the most significant risk genes were performed in the context of aging and, apart

from *APOE*, none of the other gene loci demonstrated association with this process[169]. In order to ascertain whether *PICALM* and *BIN1* risk genes are associated with aging and cellular senescence, their expression levels were assessed by qRT-PCR in MDMs of young and elderly healthy control subjects (Figure 11).

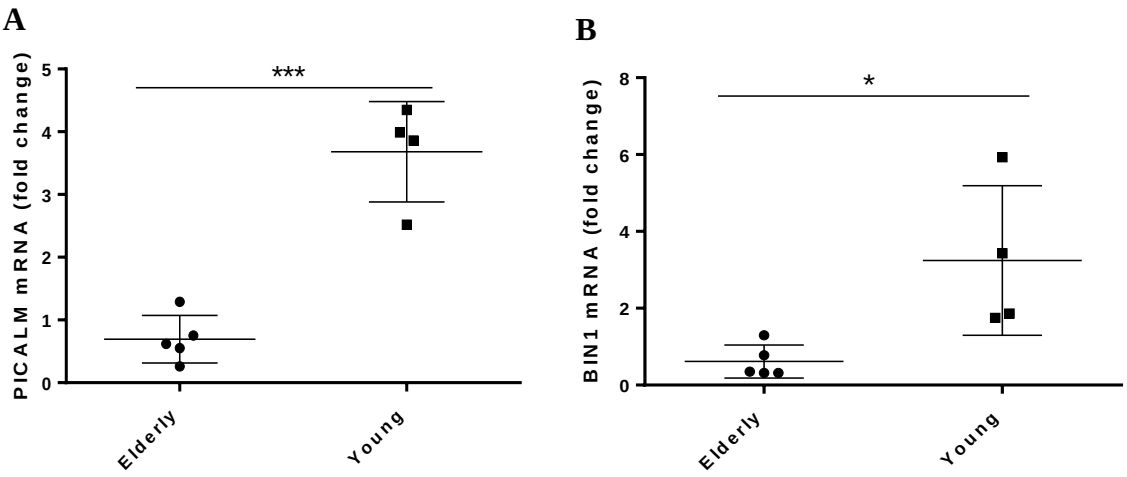

Figure 11 – Quantification of *PICALM* and *BIN1* mRNA levels in elderly and young healthy subjects. Following total RNA extraction from MDMs isolated and differentiated from $CD14^+$ BDMs of young and old healthy subjects, the levels of **(A)** *PICALM* and **(B)** *BIN1* mRNAs were quantified by qRT-PCR. Results are expressed as mRNA fold change with respect to the mean of young subjects, normalized to the reference *HPRT*, and are representative of at least $n = 4$ per group; One-way ANOVA, following Tukey's *post hoc* test, * $p < 0.05$ and *** $p < 0.001$ with respect to young subjects. Values are presented as mean ± SD.

The results in Figure 11 show a decrease in the expression of both *PICALM* and *BIN1* in older subjects with respect to younger subjects, suggesting that changes in the expression of both these genes may be a cause or consequence of the aging process.

Aging is known to be affected by genetic factors and, accordingly to GenAge database (http://genomics.senescence.info/genes/) over 250 genes possibly associated with aging have already been identified. Altered expression of mRNA levels in old mice with respect to adult mice were already observed[170]. Notably, some of the observed responses were similar to those found in human neurodegenerative disorders, including the activation of lysosomal proteases, such as cathepsin D that have been associated with APP processing to Aβ[170]. Interestingly, it has been proposed that the expression profile found in aged mice and human cells is indicative of an inflammatory response, suggesting that aging causes a systemic shift towards M1 immune responses[170,171]. This is in accordance with our results, observed in Figure 9B and also in Figure 11, that point to an anti-inflammatory function of

PICALM and *BIN1*, which is significantly impaired in old age. Moreover, and taking in consideration the results of Figure 10, it is plausible to assume that this decrease in both *BIN1* and *PICALM* expression is worsened in a dementia setting, where chronic exposure to endogenous peptides, such as Aβ, contributes to the overactivation of TLR signaling pathways and to the production of several pro-inflammatory mediators that, in turn, generate a pro-inflammatory environment that potentiates neuronal damage.

4.2. Impact of miRNA modulation in AD risk genes expression and function

miRNAs play key roles in a wide range of biological processes, including cell division and differentiation, immune cell activation and neuronal activity. In addition, it is already known that several miRNAs are deregulated in AD patients, both at the level of the brain parenchyma[122,123] and in the local and peripheral immune system[172]. In fact, recently, our group showed for the first time that specific immune-related miRNAs are deregulated in BDMs of AD and MCI patients, with respect to healthy age-matched controls[59]. In addition, using bioinformatics tools, we were able to predict that some of the new AD risk genes present at least one possible binding site for the miRNAs shown to be differentially expressed in AD patients. Taking these data into consideration, we decided to investigate, *in vitro*, the predicted interaction between these miRNAs and the new AD risk genes presented in Table 4. Through this study, we hope to clarify if the modulation of specific miRNAs can influence the levels of AD risk genes and promote beneficial functional effects in the context of AD. We believe that, if successful, our experiments could constitute an important step to develop a future miRNA-based therapy towards this type of dementia.

In this study, the modulation of miRNAs was performed in MDMs collected from healthy young subjects and also in the N9 cell line, since microglia is the most prominent immune cell type present in the brain, contributing directly to neuroinflammatory events and presenting important similarities with other mononuclear phagocytes from the periphery, such as monocytes and macrophages[43]. Although mouse and human microglia cells show considerable differences, which renders N9 cells far from being the perfect cell model, the homology of *PICALM* and *BIN1* risk genes in *Homo sapiens* and *Mus musculus* is very high (Table 5). Furthermore, these two genes, which are predominantly expressed by microglia in mice brain, share a significant number of 3'UTR binding sites in mice and in humans (Table 6 and Table 7), which makes it possible to study the functional consequences of miRNA-mediated modulation of *PICALM* and *BIN1* also in N9 cells.

Table 4 **–** Several miRNAs predicted to regulate AD risk genes in *Homo sapiens*.

miRNA / Risk gene	154	27b	200b	128	155	31	200c	497
CR1	3p	3p	5p	3p		5p		3p 5p
BIN1						5p		3p 5p
PICALM	3p 5p		3p 5p	3p	5p		3p 5p	5p
SORL1	3p	3p 5p	5p	3p	5p 3p	3p	3p 5p	3p 5p
MS4A4A		3p		3p				
CD33	3p	3p			5p			
CD2AP	3p 5p	3p	3p 5p	5p	5p 3p		3p	5p
CLU	3p 5p	3p	3p 5p	3p	5p 3p		3p	5p
TREM2						5p		
APOE								
INPP5D				3p	5p	3p		
CASS4		5p			5p			
MS4A6A	3p		5p	3p		3p 5p		
MS4A4E			5p					
MS4A6E	3p							

miR-154, -27b, -200b, -128 and -155 are immune-related miRNAs differentially expressed in AD patients. 3p and 5p refers to the precursor miRNA arm that give rise to the mature miRNA.

Four miRNA prediction algorithms were used: microT4, miRanda, miRWalk and TargetScan. The colors correspond to the number of databases where the risk gene was predicted to be regulated by each specific miRNA. Green – 4 databases; yellow – 3 databases; orange – 2 databases and red – 1 database

Table 5 – Homology between AD risk genes in *Homo sapiens* and *Mus musculus*.

Risk gene	***% Identity (protein)****	***% Identity (cDNA)****
CLU	76	81
CD33	40	46
SORL1	93	88
BIN1	**93**	**88**
MS4A4A	56	64
TREM2	57	65
APOE	71	76
CD2AP	84	85
PICALM	**98**	**94**
CASS4	56	63
INPP5D	88	85

*Data were acquired using the orthologs comparative genomics of Ensembl.

Table 6 – Several miRNAs predicted to regulate *PICALM* and *BIN1* risk genes in *Mus musculus*.

<table>
<tr><th>miRNA
Risk gene</th><th>154</th><th>27b</th><th>200b</th><th>128</th><th>155</th><th>31</th><th>200c</th><th>497</th></tr>
<tr><td rowspan="2">PICALM</td><td>3p</td><td>3p</td><td>3p</td><td rowspan="2">3p</td><td>3p</td><td rowspan="2">3p</td><td>3p</td><td>3p</td></tr>
<tr><td>5p</td><td>5p</td><td>5p</td><td>5p</td><td>5p</td><td>5p</td></tr>
<tr><td>BIN1</td><td></td><td></td><td rowspan="2">5p</td><td></td><td></td><td rowspan="2">5p</td><td></td><td>3p</td></tr>
<tr><td></td><td></td><td></td><td></td><td></td><td>5p</td></tr>
</table>

miR-154, -27b, -200b, -128 and -155 are immune-related miRNAs differentially expressed in AD patients. 3p and 5p refers to the precursor miRNA arm that give rise to the mature miRNA.

Four miRNA prediction algorithms were used: microT4, miRanda, miRWalk and TargetScan. The colors correspond to the number of databases where the risk gene was predicted to be regulated by each specific miRNA. Green – 4 databases; yellow – 3 databases; orange – 2 databases and red – 1 database.

Table 7 – Commonly miRNAs predicted to regulate *PICALM* and *BIN1* risk genes in *Homo sapiens* and *Mus musculus*.

miRNA / **Risk gene**	**154**	**27b**	**200b**	**128**	**155**	**31**	**200c**	**497**
PICALM (hsa/mmu)	√		√	√	√		√	√
BIN1 (hsa/mmu)						√		√

4.2.1. Evaluation of electroporation efficiency in N9 cells

In our first attempt to achieve miRNA modulation in N9 cells, we transfected N9 cells with miR-154, miR-31, miR-200c or miR-497 mimic oligonucleotides complexed with DLS cationic liposomes (data not shown), previously developed in our laboratory. However, this system showed very low transfection efficiency, probably due to the high division rate of N9 cells, which causes a rapid decrease in the cytoplasmic concentration of each mimic. Therefore, we decided to test an alternative transfection strategy in this cell line and miRNA delivery to N9 cells was performed by electroporation, using miRNA precursors cloned into plasmids.

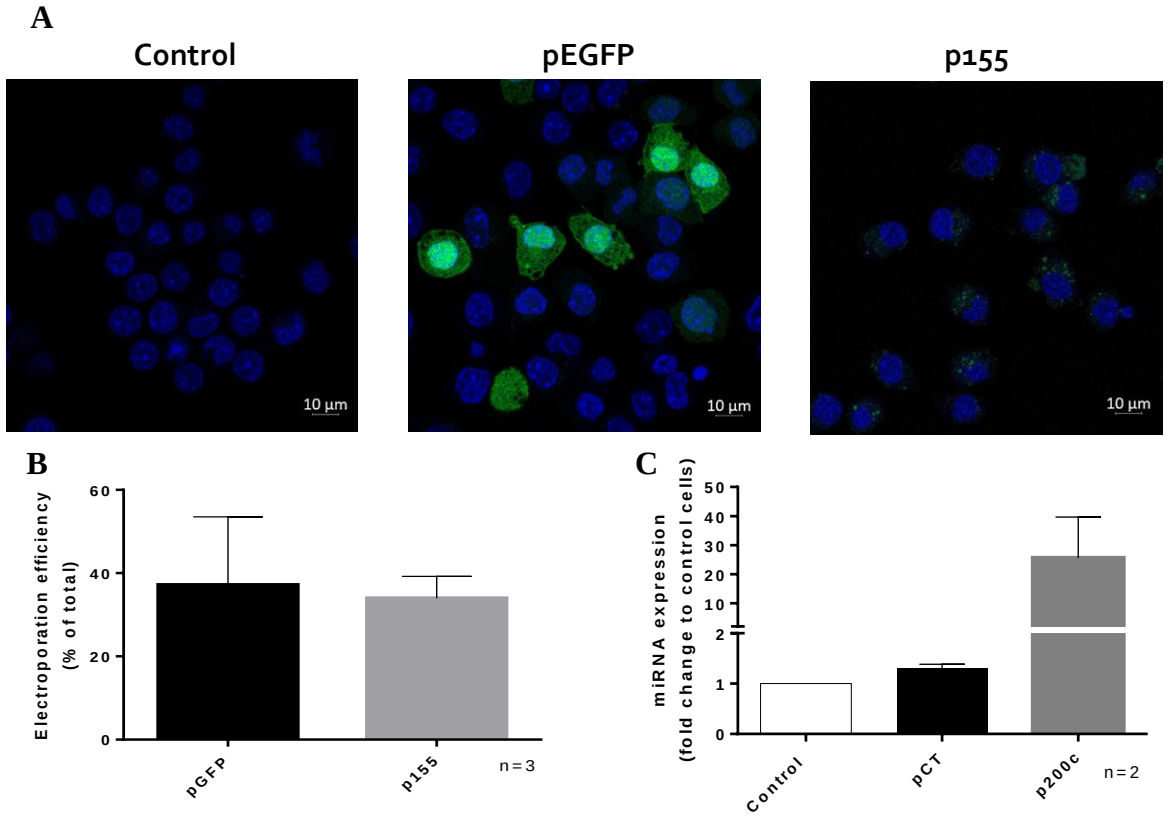

Figure 12 – Electroporation-mediated internalization of pMiRs vectors in N9 cells. After electroporation with pMiRs, cells were maintained for 48h in culture conditions. **(A)** The resulting GFP signal was evaluated by confocal analysis, following nuclei staining with DNA-specific Hoescht 33342. The panel shows representative images of control, pEGFP and p155, obtained in a Zeiss LSM 710 Meta confocal microscope equipped with the 63x oil objective. **(B)** The number of cells expressing GFP were assessed by flow cytometry in a BD Facs Calibur flow cytometer. Results are expressed as the % of cells GFP^+ and are representative of an *n = 3* **(C)** The expression levels of miR-200c were quantified by qRT-PCR following total RNA extraction. Results are expressed as miRNA fold change with respect to control cells and , normalized to the reference gene *SNORD110*, and are representative of an *n = 2*. Values are presented as mean ± SD.

Electroporation allows the delivery of oligonucleotides with direct and rapid access to their cytoplasmic or nucleic targets, thanks to the electrophoretic forces[173]. To evaluate the efficiency of miRNA delivery through this technique, pEGFP and p155, two plasmids presenting green fluorescent tags, were electroporated into N9 cells and the GFP signal obtained 48h after transfection was analyzed by confocal microscopy (Figure 12A) and flow cytometry (Figure 12B).

According to our results (Figure 12B), the efficiency of the electroporation process was around 40% for both plasmids, which can be considered a promising result, since microglial cells are usually very difficult to transfect[174]. Confocal microscopy experiments also showed the presence of green labelled cells in both experimental conditions, further confirming the efficiency of this strategy. However, as can be observed in Figure 12A, the fluorescence intensity obtained for pEGFP in confocal microscopy experiments was higher than the one obtained for p155. This may be due to the different promoters found in both plasmids: the T7 promoter for p155 and CMV promoter for pEGFP and also to the fluorescent protein itself, since p155 contains the wild-type GFP sequence, while pEGFP contains the enhanced version of GFP (EGFP) that is 35 times brighter than the wild-type, greatly increasing the sensitivity of the reporter protein[175].

Importantly, to evaluate the expression levels of the pMiRs, we performed an additional experiment in which N9 cells were electroporated with pmiR-200c and the levels of miR-200c were evaluated by qRT-PCR 48 h after transfection (Figure 12C). As can be observed in Figure 12C, an increase in the levels of miR-200c of around thirty-fold, with respect to control cells, was observed after electroporation of N9 cells with p200c. One important issue to take into consideration is that the efficiency of the electroporation process may differ between experiments, even for the same plasmid, since the time constant obtained in each round of electroporation is always different and these differences are reflected in the standard deviations obtained. Nevertheless, taken together, our results suggest that electroporation is the most efficient transfection option available for miRNA delivery to N9 cells.

4.2.2. MiRNA modulation in N9 cells and its impact on target mRNA levels

We recently showed that several immune-related miRNAs are upregulated in AD and MCI patients with respect to age-matched controls, including miR-154, miR-27b, miR-200b, miR-128 and miR-155[59]. This data, together with the fact that some of these miRNAs are predicted to bind to the 3'UTR of *PICALM* and *BIN1* mRNA, led us to hypothesize that these miRNAs may play a role in the modulation of *PICALM* and *BIN1* expression, at least in mononuclear phagocytes. To test this theory, we modulated the levels of three miRNAs: miR-155, miR-200c and miR-31 in N9 cells and evaluated, employing qRT-PCR, the impact of miRNA upregulation on target mRNA levels 48h after electroporation (Figure 13).

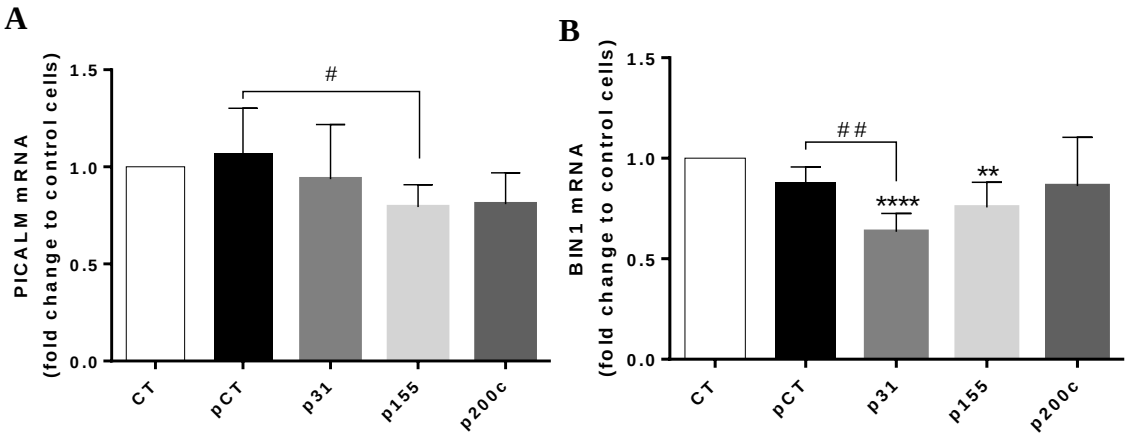

Figure 13 – Quantification of *PICALM* and *BIN1* mRNA levels in N9 cells, following electroporation with p31, p155 or p200c. N9 cells were maintained for 48h in culture conditions following electroporation with pMiRs. After this period and following total RNA extraction, the levels of **(A)** *PICALM* and **(B)** *BIN*1 mRNA were quantified by qRT-PCR. Results are expressed as mRNA fold change with respect to control cells , normalized to the reference gene *HPRT*, and are representative of at least $n = 3$; One-way ANOVA, following Dunnett's test, * $p < 0.05$, ** $p < 0.01$ and **** $p < 0.0001$ with respect to control cells; # $p < 0.05$ and ## $p < 0.01$ with respect to pCT cells. Values are presented as mean ± SD.

Since miRNAs are known to bind to the 3'UTR of their target mRNAs, it is predictable that a true mRNA:miRNA interaction will lead to a decrease in mRNA expression, since the ribosome machinery will becomes temporarily or permanently unable to complete mRNA translation. Thus, and taking into account that *PICALM* is a predicted target of miR-200c and miR-155, it was expected that the expression of this gene would

decrease upon electroporation of N9 cells with p200c and p155. Indeed, a decrease in mRNA levels of *PICALM* with respect to non-electroporated cells was observed following electroporation with p31, p155 and p200c. However, only p155 showed a significant decrease in *PICALM* expression with respect to the control plasmid. Concerning *BIN1*, which is a predicted target of miR-31, we only observed a significant decrease following electroporation with p31, once again with respect to non-electroporated cells and to pCT. Upregulation of miR-155 also resulted in a reduction of *BIN1* mRNA levels, but only with respect to the non-electroporated cells.

Our results are in full agreement with the bioinformatic predictions obtained using the microT4, miRanda, miRWalk and TargetScan algorithms. Nevertheless, it is important to take into consideration that this experiment does not completely exclude the hypothesis of an indirect effect of the miRNAs on both genes. To validate a direct interaction of each miRNA with the 3'UTR of *PICALM* and *BIN1* mRNAs, a different kind of assay should be performed, such as the luciferase validation assay or the pull-down for analysis of biotinylated miRNA mimics following cell transfection.

4.2.3. MiRNA modulation in N9 cells and its impact on phagocytosis activity

Since microglia are described as the brain-resident macrophages, it is natural to consider these cells specialized phagocytes, whose major function, under homeostatic conditions, is the cleaning of neurotransmitters, synaptic debris and also apoptotic cells. In the context of dementia-associated neurodegeneration, microglia cells have also been proposed to phagocyte misfolded proteins and protein aggregates. However, some authors have suggested that, in AD mouse models, microglia presents impairments in its phagocytic activity[59,176]. Also in this context, Guedes *et al*. studied chemotaxis and phagocytosis, at the systemic level, in AD and MCI patients and observed impairments in both these functions[59]. The authors associated these findings with the deregulation of specific miRNAs in AD patients[59]. Taking into consideration these reports, we decided to study how the modulation of miR-31, miR-155 and miR-200c influences phagocytosisin N9 cells. To accomplish this purpose, flow cytometry and confocal microscopy experiments employing fluorescently-labelled latex beads were performed (Figure 14).

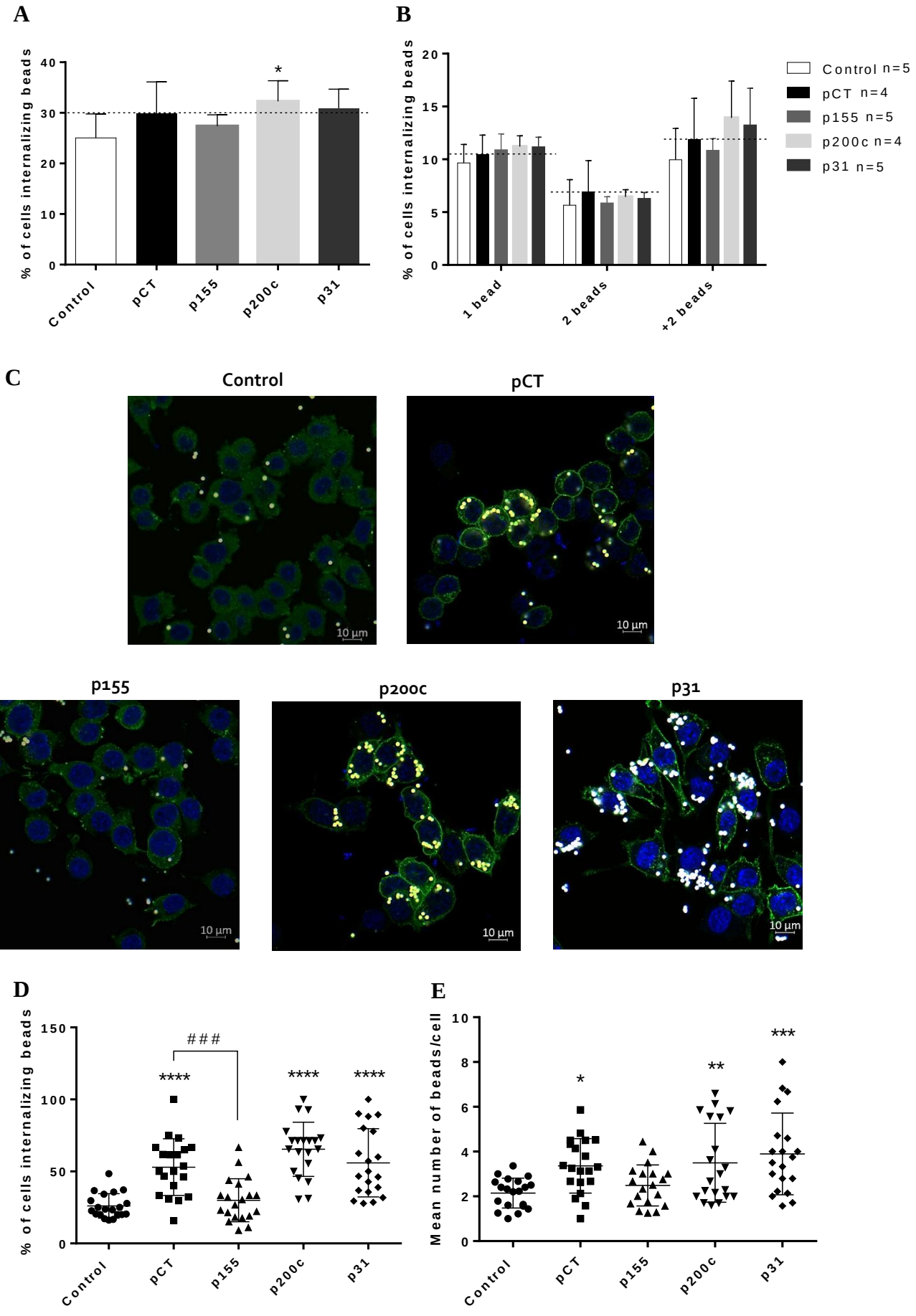
A
% of cells internalizing beads
40
30
20
10
0
*
Control
pCT
p155
p200c
p31
B
% of cells internalizing beads
20
15
10
5
0
1 bead
2 beads
+2 beads
Control n=5
pCT n=4
p155 n=5
p200c n=4
p31 n=5
C
Control
pCT
p155
p200c
p31
10 µm
D
% of cells internalizing beads
150
100
50
0
###
****
****
****
Control
pCT
p155
p200c
p31
E
Mean number of beads/cell
10
8
6
4
2
0
*
**
***
Control
pCT
p155
p200c
p31

Figure 14 – Phagocytosis of latex beads by N9 cells, following electroporation with p155, p200c or p31. N9 cells were maintained for 48h in culture conditions following electroporation with pMiRs. After this period, the cells were further incubated for 2h30min with red fluorescent latex beads and beads internalization was evaluated by **(A, B)** flow cytometry, using a BD Facs Calibur cytometer and **(C, D, E)** confocal microscopy, after fixation with PFA, immunocytochemistry labelling β-actin and staining with DNA-specific Hoescht 33342. **(A)** Percentage of cells that perform phagocytosis (at least $n = 3$). **(B)** Percentage of cells that ingested 1, 2 or more than 2 beads (at least $n = 3$). **(C)** The panel shows representative images of N9 control cells or cells electroporated with pCT, p155, p200c or p31 observed under a Zeiss LSM 710 Meta microscopy equipped with the 63x oil objective. For each experimental condition ($n = 2$), 10 images were taken and, in each image, **(D)** the percentage of cells with internalized beads and **(E)** the mean number of latex beads ingested by each cell was determined. One-way ANOVA, following Dunnett's test, * $p < 0.05$ ** $p < 0.01$ *** $p < 0.001$ and **** $p < 0.0001$ with respect to control cells and ### $p < 0.001$ with respect to pCT cells. Values are presented as mean ± SD.

These studies revealed that the modulation of the selected miRNAs leads to alterations in the phagocytic ability of N9 cells. The first striking observation that can be taken is that electroporation seems to increase the phagocytic ability of N9 cells by itself, since all electroporated plasmids, including the control plasmid show an increase in the number of internalized beads, with respect to control cells. Moreover, although only tendencies could be observed through flow cytometry analysis with respect to the plasmid control, confocal studies showed that N9 cells overexpressing miR-155 present a significant reduction in phagocytosis with respect to cells electroporated with the control plasmid. This result can be explained taking into consideration previous observations that miR-155 is essential for M1-like activation in N9 cells. The M1 phenotype is usually considered to be more pro-inflammatory, leading to the overexpression of inflammatory cytokines and to a decrease in phagocytosis activity[139]. Therefore, it is plausible that miR-155 overexpression following electroporation would lead to a decrease in the number of internalized beads. In addition, this result can also be correlated with the increased expression of miR-155 observed in BDMs of AD patients[59]. Finally, in this study we also observed changes in miR-155 expression following activation of human MDMs towards the different activation states. Similar to what was previously observed in N9 cells, miR-155 expression was also increased in the pro-inflammatory state (M1), with respect to both M0 and M2 (Figure 15). No changes were observed for miR-200c or miR-31 expression in those conditions (data not shown).

Interestingly, a slight, although not statistically significant, increase in phagocytosis was observed following overexpression of both miR-31 and miR-200c with respect to the

plasmid control (Figure 14). Taking into consideration our results concerning *PICALM* and *BIN1* expression following miRNA modulation and the role played by these proteins during endocytosis, one would expected to see a decrease in phagocytosis. However, such decrease was only observed upon overexpression of miR-155, which is not surprising if we take into account that each miRNA has multiple possible targets. Thus, upon overexpression of miR-200c and miR-31, it is possible that other genes beyond *PICALM* and *BIN1* could have become downregulated, leading to an increase in phagocytosis.

Taken together, ours results shown that miRNA modulation can interfere with the phagocytic ability of mononuclear phagocytes, which opens the way to new miRNA-based therapeutic strategies aiming at improving clearance of protein aggregates or other undesirable cellular debris.

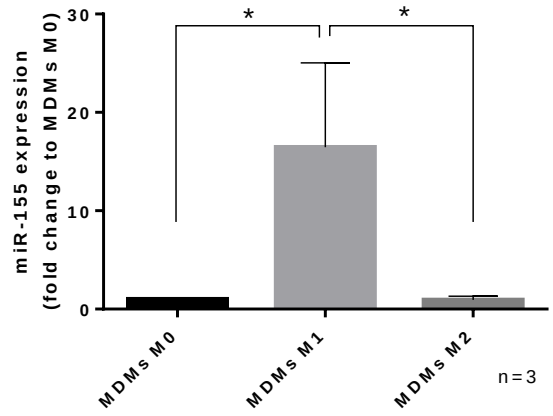

Figure 15 – miR-155 expression levels in M0, M1 and M2 MDMs. Total RNA was extracted from M0 MDMs obtained after 7 days of differentiation in the presence of M-CSF or from M1 MDMs (incubated with LPS (100 ng/mL) and IFN-γ (20 ng/mL)) or M2 MDMs (incubated with IL-4 (20 ng/mL)). The levels of miR-155 in MDMs were quantified by qRT-PCR. Results are expressed as miRNA fold change with respect to M0 MDMs and were normalized to the reference gene *SNORD44*. Results are representative of an *n = 3*; One-way ANOVA, following Tukey's *post hoc* test, * $p < 0.05$ with respect to M0 MDMs. Values are presented as mean ± SD.

4.2.4. MiRNA modulation in N9 cells and its impact on cytokines expression

In the presence of a disturbance in the nervous system, microglia is responsible for initiating the innate immune response aiming at recovering tissue homeostasis. This response will be different depending on the surrounding environment and specific signals released by local cells. As mentioned in the first chapter, there are two possible extreme activation phenotypes: the M1 state and the M2 state. The M2 state is usually activated as an initial defensive response and is characterized by the release of anti-inflammatory cytokines, such as IL-4, IL-13 and IL10 and by the production of specific proteins with a trophic and protective role, such as arginase 1 (Arg1) and TGF-β. However, it is important to clarify that in the presence of continuous damage, the M2 state tends to switch to the M1 state, leading to the release of pro-inflammatory cytokines, including IL-1β, IL-6 and TNF-α and to the production of nitric oxide and ROS (reviewed in[53]). It is already known that certain miRNAs, such as miR-155, are master regulators of microglia and macrophage activation, helping to establish a specific activation phenotype by regulating the expression of proteins involved in immune-related pathways[139]. Therefore, in this study, we decided to investigate how the modulation of miR-155, miR-200c and miR-31 could influence the basal expression of M1 and M2-related cytokines (Figure 16).

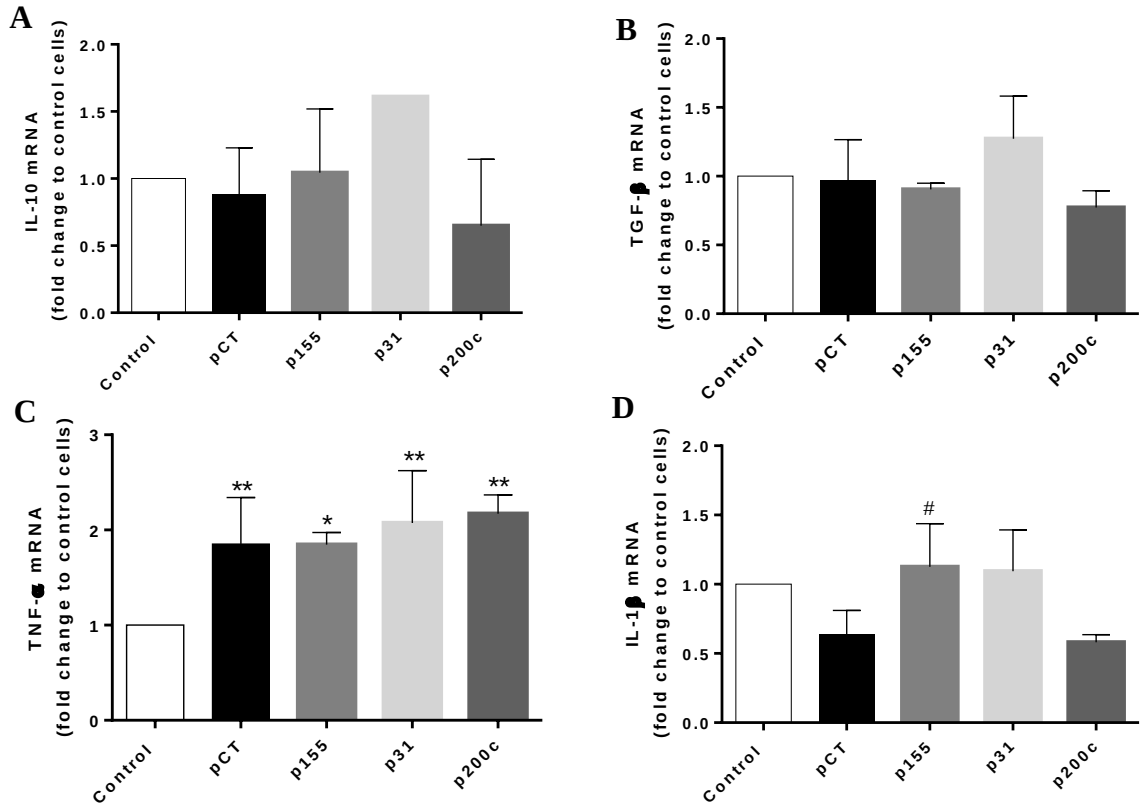

Figure 16 – Quantification of IL-10, TGF-β, TNF-α and IL-1β mRNA levels in N9 cells following electroporation with p31, p155 or p200c. N9 cells were maintained for 48h in culture conditions, after electroporation with pMiRs. Following total RNA extraction, the mRNA levels of **(A)** IL-10 **(B)** TGF-β **(C)** TNF-α and **(D)** IL-1β were quantified by qRT-PCR. Results are expressed as mRNA fold change with respect to control cells, normalized to the reference gene *HPRT*, and are representative of at least *n = 3*, except for **(A)** p31 and p155 with an *n = 1* and *n = 2*, respectively and **(C, D)** p200c with an *n = 2*; One-way ANOVA, following Dunnett's test, * $p < 0.05$ and ** $p < 0.01$ with respect to control cells, # $p < 0.05$ with respect to control plasmid. Values are presented as mean ± SD.

Taking into consideration the results presented above, concerning phagocytosis experiments (Figure 14) and the fact that phagocytosis has been more associated with the M2 state (reviewed in[177]), it would be expected to observe an increase in IL-10 and TGF-β expression following electroporation with p200c and p31. However, this increase was only observed for p31. Regarding the expression of pro-inflammatory cytokines, an increase in the expression levels of TNF-α was observed for all pMiRs, including the control plasmid, which suggests an unspecific effect due to the electroporation process *per se*. On the other hand, the expression levels of IL-1β increased after miR-155 and miR-31 overexpression and decreased after electroporation with p200c. With the exception of p31, the observed fold changes are in agreement with the decrease and increase of phagocytic ability presented in Figure 14 in the case of p155 and p200c, respectively. Interestingly, a previous work has demonstrated that transfection of THP-1 cells (a macrophage-like human monocytic cell line) with miR-200b and miR-200c mimics leads to a decrease in the expression levels of pro-inflammatory cytokines, such as TNF-α and IL-6 in response to the TLR4 agonist, LPS (an inducer of M1 state)[140].

It is, however, important to note that in contrast to what normally happens, the expression levels of these cytokines were evaluated in basal conditions, instead of in the presence of M1 and M2 phenotype inducers, which may explain the low expression values and non-significant differences observed. Thus, to better understand the involvement of each miRNA in the activation process, similar experiments should be performed in the presence of LPS or IL-4.

4.2.5. MiRNA modulation in MDMs and its impact on target mRNA levels

In addition to the work performed with the murine cell line N9, in this study we also aimed to investigate the effects mediated by specific miRNAs, previously shown to be upregulated in AD and MCI patients, in the expression of risk genes *BIN1* and *PICALM*, in human mononuclear phagocyte cells. For this purpose, and since human microglia cells are not easily available, we transfected human MDMs, obtained through differentiation of blood-derived monocytes of healthy young donors, with miRNA mimic oligonucleotides.

Since MDMs are a primary cell culture, with a low yield at the end of the differentiation process, the upregulation of miRNA levels in these cells was performed using miRNA mimics complexed with DLS cationic liposomes, instead of through electroporation, since this technique requires a high cellular yield and leads to significant cell death. The choice of the delivery vehicle for these experiments was based on previous work performed in our group[139]. Nevertheless, and in order to fully assess transfection-associated toxicity, MDM cell viability was evaluated 24h after transfection through the Alamar Blue assay (Figure 17). As can been observed in Figure 17, there was no significant toxicity associated with the transfection process in MDMs, which reinforces the idea that DLS lipoplexes are a highly biocompatible transfection system, even when working with primary human cells.

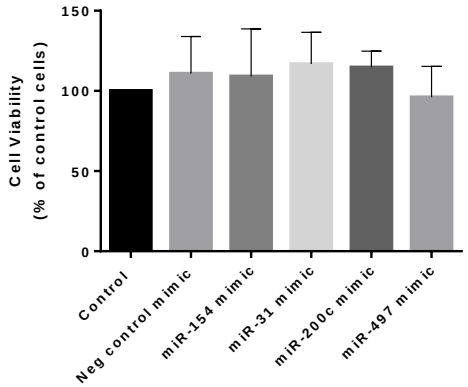

Figure 17 – Cell viability following transfection with miR-154, miR-31, miR-200c or miR-497 mimics. MDMs were incubated with miR-154/miR-31/miR-200c/miR-497 mimics or the negative control oligonucleotide (final concentration of 50 nM/well) complexed with DLS for 4h. At the end of this period the cell medium was changed and cells were further incubated for 24h with fresh medium. Cell viability was assessed by Alamar Blue assay. For this purpose, cells were incubated for approximately 1h with the Resazurin dye and the absorbance was measured at 570 nm and 600 nm. Results are expressed as the percentage of cell viability with respect to non-transfected cells (control), and are representative of at least $n = 3$; Values are presented as mean ± SD.

In what concerns the expression of *BIN1* and *PICALM*, no significant differences were observed in *PICALM* and *BIN1* mRNA levels in MDMs following transfection (Figure 18).

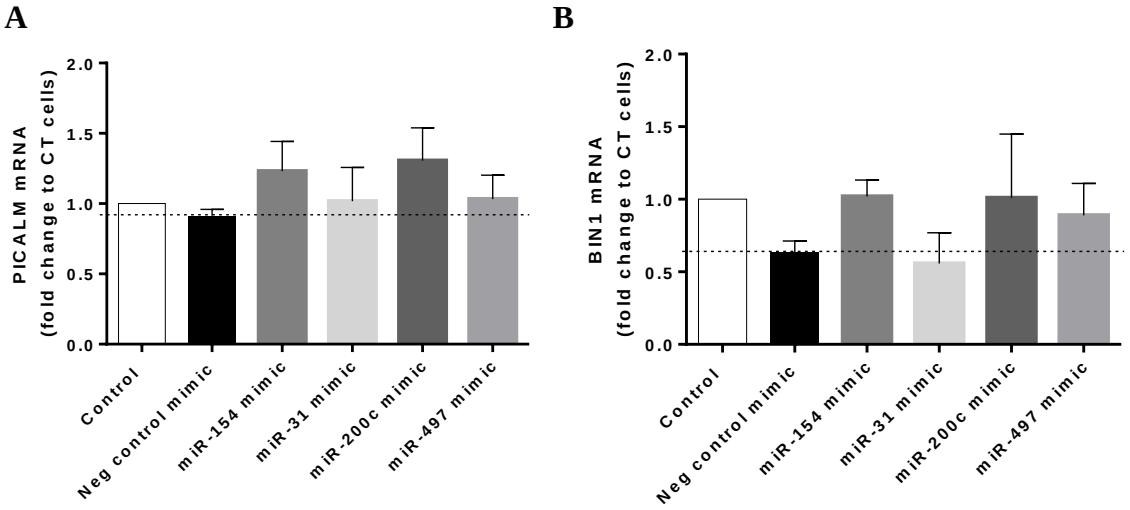

Figure 18 – Quantification of *PICALM* and *BIN1* mRNA levels in MDMs following transfection with miR-154, miR-31, miR-200c or miR-497 mimics. MDMs were incubated with miR-154/miR-31/miR-200c/miR-497 mimics or with a negative control oligonucleotide (final concentration of 50 nM/well) complexed with DLS for 4h. Following this period, the cell medium was replaced and the cells were further incubated for 48h with fresh medium. Following total RNA extraction, the expression levels of **(A)** *PICALM* and **(B)** *BIN1* mRNA were quantified by qRT-PCR. Results are expressed as mRNA fold change with respect to non-transfected cells (control cells), normalized to the reference gene *HPRT*, and are representative of at least $n = 3$, except for miR-154 and miR-200c mimic with an $n = 2$; Values are presented as mean ± SD.

Nevertheless, a non-significant reduction in *BIN1* mRNA levels was observed in the presence of miR-31 mimics. These results are in agreement with our observations in N9 cells, following electroporation with p31 (Figure 13) and suggest that miR-31 may truly bind to the 3'UTR of *BIN1* mRNA, modulating the expression of this gene at the post-transcriptional level, in both mouse and human cells.

Two other key aspects must also be mentioned in the context of this experiment. First, we observed an unexpected reduction in *BIN1* expression upon transfection with the control mimic, with respect to the control and with respect to miR-154, -200c and -497 mimics, whose delivery did not change the mRNA levels of this gene. Since this effect cannot be associated with transfection toxicity (Figure 17), this suggests an unspecific effect of the mimic sequence. Therefore, it would be important to repeat the transfection experiments in

MDMs employing a new negative control sequence, to validate the results obtained with the miR-31 mimic. Secondly, we must take into consideration that the lack of significant changes in the expression of both genes may also be due to the low transfection efficiency of the DLS system in MDMs. The inefficient delivery of miRNA mimics to the differentiated macrophages might be explained by their entrapment and quick degradation in the lysosomes, since macrophages are known to have a very high lysosomal activity, when compared to other immune cells, such as microglia and dendritic cells. The efficient escape from the lysosome is a critical step in transfection mediated by lipid-based delivery systems and failure to achieve this goal can result in low mimic availability in the cytoplasm[178]. Another relevant explanation could be the unexpected target competition, which could lead to preferential binding of the mimic to the 3'UTR of other mRNAs that present higher affinity towards the mimic sequence. This would avoid efficient modulation of *BIN1* and *PICALM* mRNA levels by the delivered mimics.

4.3. Re-differentiation of BDMs into microglia-like cells

As mentioned before, microglia play an important role in brain homeostasis, helping to maintain neuronal integrity, supporting neuronal network functioning and inducing immune defense responses when appropriate (reviewed in[22]). Since they are the most relevant immune cells of the brain and their activity, or lack thereof, has been associated with chronic neurodegeneration[179], their study has been an important topic in neuroscience research, particularly in what concerns CNS innate immune responses and their contribution to disease onset and progression.

Currently, there is no easily available primary cell model of human microglia, which restricts the study of neuroinflammation in several brain disorders. Therefore, in this study, we aimed to establish and validate a new protocol to isolate and differentiate microglia-like cells from human blood-derived monocytes, according to a recently published protocol[159]. In order to fully characterize these cells, the levels of several surface markers, as well as the expression of several microglia signature genes, were investigated and compared to those of MDMs.

4.3.1. Isolation and characterization of iMGs from PBMCs of young healthy subjects

In order to obtain iMGs, PBMCs were firstly isolated from the blood of healthy young volunteers using Histopaque-1077 density gradient centrifugation. Afterwards, the whole PBMC population was cultured overnight in RPMI-1640 culture medium without FBS, in order to facilitate cell adhesion, as mentioned in the section 4.1.1. In the following day cells were supplemented with 10% FBS and while half of the cells was supplemented with M-CSF (50 ng/mL), the other half received a mixture of GM-CSF (10 ng/mL) and IL-34 (100 ng/mL), to initiate the differentiation process into MDMs and iMGs, respectively.

M-CSF, GM-CSF and IL-34 are three cytokines involved in the differentiation of cells of the mononuclear phagocyte system. However, the activity of these molecules in the mononuclear phagocyte system is still under study. M-CSF and GM-CSF have different receptors at the cell surface (M-CSF receptor and GM-SCF receptor α, respectively), while IL-34 shares its receptor with M-CSF[180]. Nevertheless, since the structure of M-CSF and IL-34 is relatively different and the domains they bound are different, their biological activity and signal activation is not necessarily identical[181,182]. Still regarding M-CSF, this molecule is known to regulate tissue macrophage and monocyte populations without altering their "activation" state, while GM-CSF is mostly produced in inflammatory conditions, inducing the activation of monocytes and/or macrophages and also mediating monocyte differentiation into other cell types that participate in immune responses, in particular dendritic cells (reviewed in[183]).

According to Ohgidani and colleagues, after 14 days of differentiation, using IL-34 and GM-CSF, monocytes should acquire a morphology similar to that of microglial cells, with a large number of ramifications. Surprisingly, in our study, we failed to observe the small soma bodies with numerous ramifications described by the authors (Figure 19). Actually, our MDMs, differentiated by exposure to M-CSF, presented more ramifications after 14 days in culture than our iMGs, differentiated through exposure to GM-CSF and IL-34.

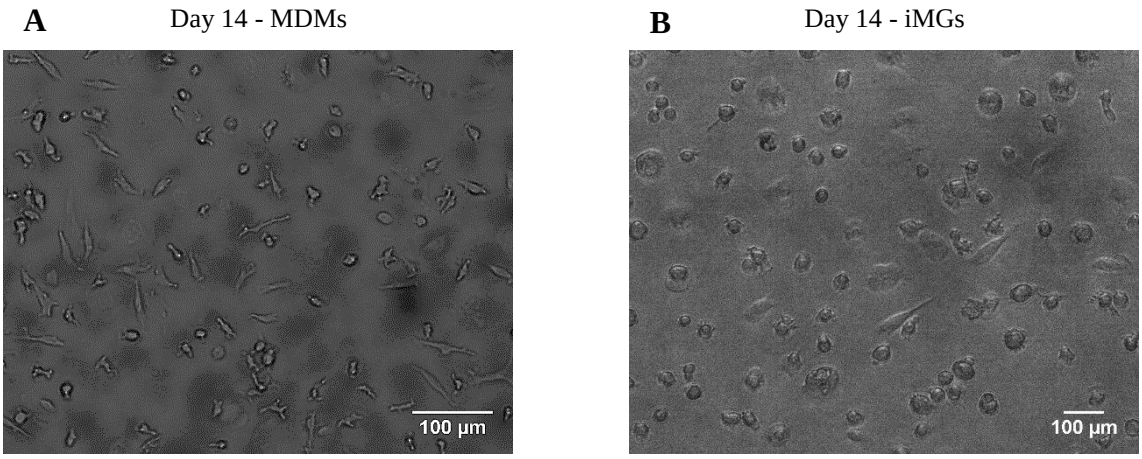

Figure 19 – Morphology of MDMs and iMGs isolated and differentiated from BDMs. Representative images showing the morphology of **(A)** MDMs, obtained following 14 days of differentiation in the presence of M-CSF (50 ng/mL) and **(B)** iMGs, obtained following 14 days of differentiation in the presence of GM-CSF (10 ng/mL) and IL-34 (100 ng/mL). The images were acquired in a light microscope equipped with the 20x objective. Results are representative of an $n = 4$.

Unfortunately, the discrimination between macrophages and microglia cells is still challenging, due to the lack of useful and specific membrane markers. Therefore, in order to characterize the obtained iMG cells, we decided to evaluate a set of markers using both flow cytometry and qRT-PCR. Similarly to Ohgidani and colleagues, we started by evaluating, employing flow cytometry, the expression of the monocyte surface marker CD14 (Figure 20E), whose surface levels should decrease upon monocyte differentiation to microglia-like cells[159,184]. In addition, the expression of the innate immune receptor TREM2 was also evaluated in our study (Figure 20F), since this receptor is known to be expressed in resting microglial cells[71,72].

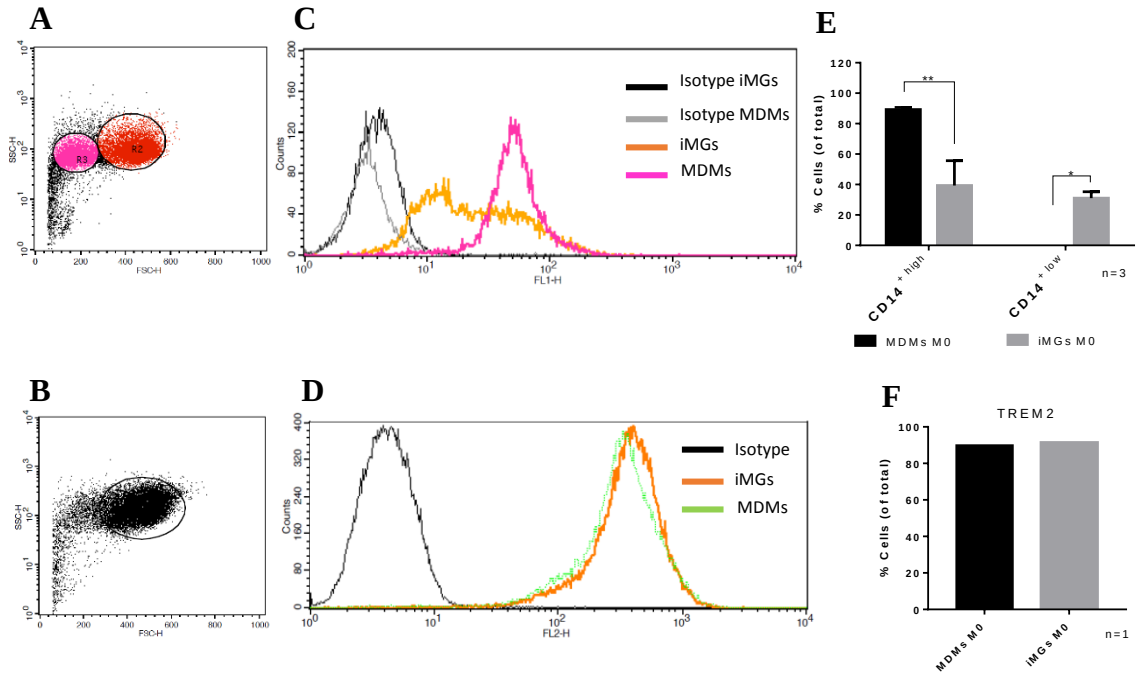

Figure 20 – Characterization of iMGs isolated from PBMCs. The expression levels of $CD14^+$ and TREM2 surface markers was evaluated in MDMs and iMGs by flow cytometry, in the FL-1 and FL-2 channel, respectively. **(A, B)** Representative dot plot of MDMs and iMGs, respectively. **(C, D)** Representative histogram of **(C)** $CD14^+$ and **(D)** TREM2 surface expression. **(E, F)** Percentage of sorted cells expressing **(E)** $CD14^+$ and **(F)** TREM2, following histogram analysis. Results are expressed as percentage of total cells and as mean ± SD. Two-way ANOVA, following Sidak's test; * $p < 0.05$ and ** $p < 0.01$, with respect to MDMs M0.

The obtained results show that MDMs present a heterogeneous profile (Figure 20A), since we could observe cells with different sizes and complexity. On the contrary, iMGs show a more homogeneous profile (Figure 20B). Our results also unveiled the existence of two types of iMGs cells in what concerns CD14 expression: the cells that express high levels of $CD14^+$ ($CD14^{+\ high}$) and cells expressing low levels of $CD14^+$ ($CD14^{+\ low}$) (Figure 20C). As described by some authors, the expression of $CD14^+$ is lower in microglia cells, which is in agreement with our results that show a decrease in the percentage of iMGs cells expressing high levels of CD14, with respect to MDMs. This decrease in the $CD14^{+\ high}$ population occurs in parallel with the appearance of a $CD14^{+\ low}$ population only in iMGs (Figure 20E).

Concerning the innate immune receptor TREM2, no changes were observed in iMGs and MDMs. This result, together with the lack of a ramified morphology led us to question the validity of the protocol described by Ohgidani.

Recently, Hickman and colleagues used direct RNA sequencing (DRS), fluorescent dual *in situ* hybridization, quantitative PCR and proteomic analysis to characterize and

compare the transcriptome and proteome of mouse microglia and peritoneal macrophages[71]. This study found 70% of similarity between microglia and macrophage transcripts. The study also provided a unique molecular signature that defines microglia cells and distinguishes them from other types of tissue-resident macrophages, based on the expression of *P2ry12, P2ry13, Tmem119, Gpr34, Siglech, Trem2, Cx3cr1* and *HexB*, several genes found to be exclusively present in microglia[71]. In addition, employing gene profiling analysis and quantitative mass spectrometry analysis, Butovsky confirmed the expression of several unique microglial genes and showed that *P2ry12, Gpr34, Merkt, C1qa, Pros1* and *Gas6* were uniquely or highly expressed in human microglia and not in mouse microglia. Importantly, this second study compared the expression of the identified genes in microglia and in other cells of the CNS, including neurons, astrocytes and oligodendrocytes. The authors found that genes such as *Fcrls, Olfm13, Tmem119, P2ry12, Hexb* and *Tgfbr1* were only expressed in microglia, reinforcing their designation as unique microglial genes[185].

In order to further conclude on the effectiveness of the re-differentiation protocol proposed by Ohgidani, we decided to evaluate the expression of several of the new microglia signature genes in iMGs and MDMs. We employed qRT-PCR to quantify the levels of *Cx3cr1, P2ry12, HexB* and *Spi I* (Figure 21). *Spi I* is encoded by PU.1, which was identified as the most significant transcription factor of microglia[185].

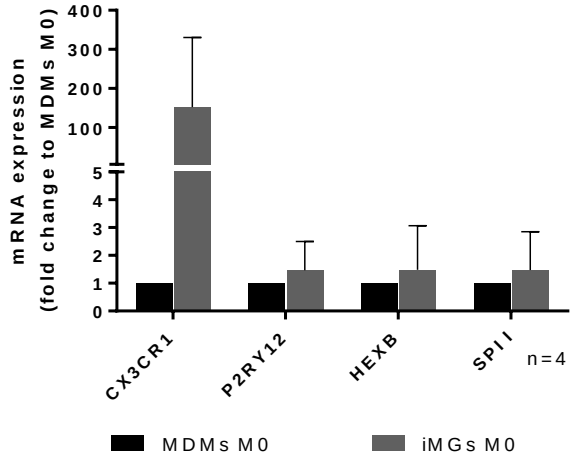

Figure 21 – Quantification of microglia signature genes in iMGs and MDMs. Total RNA was extracted from MDMs and iMGs obtained after 14 days of differentiation in the presence of M-CSF (50 ng/mL) or GM-CSF (10 ng/mL) and IL-34 (100 ng/mL), respectively. The expression of *Cx3cr1*, *P2ry12*, *HexB* and *Spi I* was quantified by qRT-PCR. Results are expressed as mRNA fold change with respect to MDMs M0, normalized to the reference gene *HPRT*, and are representative of an $n = 4$. All values are presented as mean ± SD.

The results presented in Figure 21 show that the expression of the selected genes is slightly increased in iMGs with respect to MDMs, although without statistically significance, due to the variations obtained in each independent experiment. In addition, the differences observed between iMGs and MDMs are not identical to the ones observed by Hickman and Butovsky[71,185], which were much more pronounced. Actually, in his work, Butovsky already suggested that recruited monocytes do not acquire the microglia signature. Thus, taking into consideration that microglia do not derive from definitive circulating hematopoietic precursors, but from primitive embryonic precursors from the yolk sac[43,44] and considering recent studies showing that blood monocytes and other bone-marrow progenitors do not contribute to the adult microglia pool in the CNS[46], we do not find it surprising that the obtained iMG cells do not resemble microglia cells. For that reason, we believe that the protocol established by Ohgidani is not sufficient to generate a cellular model that can mimic human microglia in culture, despite the fact that these cells were shown to present low expression of CD14, an increase in the expression of CX3CR1 and phagocytic ability[159]. We also believe that the expression of microglia signature genes is crucial to elucidate the cell type obtained after isolation and differentiation and should be taken in consideration in future protocols designed to obtain human microglia cells.

Chapter 5

Conclusions and future directions

5.1. Conclusions

The study of chronic neuroinflammation is gaining increased importance in AD, since this feature can be observed at relatively early stages of the disease. Recently, new AD risk genes were identified through GWAS studies and some of these genes were found to play a role in immune system responses, providing additional evidence that neuroinflammatory and neuroimmune events should be explored in the context of the design of new diagnosis and therapeutic strategies for AD. This is also true for miRNAs, since several members of the miRNA family have been shown to play an important role in AD pathophysiology, both locally and peripherally.

Our results showed that the newly identified AD risk genes present differential expression in the two opposite activation states of MDMs, pointing to a protective role of genes upregulated in the M2-like state (*MS4A6E*, *SORL1*, *CR1*, *MS4A4A*, *TREM2*, *CASS4*, *INPP5D*, *PICALM* and *BIN1*) and a possible involvement in disease progression of genes upregulated in the M1-like state (*CLU* and *CD2AP*). The observed decrease in *PICALM* and *BIN1* mRNA levels in AD and MCI patients, with respect to healthy age-matched individuals, reinforces the protective role of these two genes in healthy condition, pointing once more to their involvement in Aβ clearance mechanisms. Importantly, a decrease in the expression of these genes was also observed in elderly healthy individuals, though worsened in a dementia setting, indicating that age, by itself, influences immune cell function.

In this work, we also showed that the modulation of miRNAs in N9 cells, in particular miR-155 and miR-31, induced a decrease in the expression of the target genes *PICALM* and *BIN1*, respectively. Despite the lack of statistical significance, a similar result was observed in MDMs for miR-31 and *BIN1*. These results, which are in agreement with bioinformatics predictions, suggest that these miRNAs regulate risk gene expression, in both mouse and human cells. Additionally, we observed that an increase of miR-155 leads to a decrease in phagocytosis, while an increase in miR-31 and -200c leads to the contrary effect, establishing that miRNA modulation interferes with the phagocytic ability of mononuclear cells. Taken together, our results support the involvement of *PICALM* and *BIN1* in AD pathophysiology and strengthen the hypothesis that miRNA dysfunction, as previously reported by our group in AD and MCI patients, may be directly related with the

dysfunction of Aβ clearance mechanisms observed in these patients, further suggesting that miRNA modulation strategies may be worth exploring in the context of AD therapeutics.

Apart from these results, we performed experiments to evaluate the possibility of using re-differentiated human monocytes, prepared according to a previously described protocol, as an *in vitro* model of microglia-like cells. After evaluating the levels of several surface markers, as well as the expression of several microglia signature genes, we concluded that cells obtained through this protocol do not mimic human microglia cells, which is not surprising taking in consideration that microglia cells and circulating monocytes do not share a direct precursor. Given the growing importance of microglia cells in the regulation of brain homeostasis and neuronal development, these results stress once again the urgent need to establish new protocols to obtain human microglia-like cells that efficiently mimic, from a molecular point of view, microglia in their native environment.

5.2. Future directions

The results presented in this study revealed new intervenients in AD pathophysiology and opened new avenues in the design of AD therapeutics. However, further studies should be performed in order to clarify the major functions of *PICALM* and *BIN1* AD risk genes in cells of the immune system and to inform on the possibility of using miRNA modulation strategies to revert *PICALM* and *BIN1* loss in the context of aging and dementia. For example, the direct interaction of each miRNA with the 3'UTR of *PICALM* and *BIN1* mRNAs should be validated by the luciferase validation assay or through the miRNA-biotin pull down assay. Furthermore, and in order to overcome the low transfection efficiency of microglia and macrophage cells, virus-mediated overexpression of the selected miRNAs should be performed in N9 cells and in human macrophage cells, with the intention of generating a more stable cell lines for the validation of the obtained miRNA modulation and phagocytosis results.

In addition, and taking into consideration the autophagic studies performed by some authors, it would be interesting study how the modulation of miRNAs influences the role of BIN1 and PICALM proteins in endocytosis and autophagy. Importantly, *PICALM* and *BIN1* should be silenced using a more specific strategy, such as siRNA-mediated RNA interference, in order to clarify if these genes have indeed a direct role in Aβ clearance mechanisms, such as phagocytosis and autophagy.

References

List of bibliographic references

1 Robinson, L., Tang, E. & Taylor, J. P. Dementia: timely diagnosis and early intervention. *Bmj* **350**, h3029, doi:10.1136/bmj.h3029 (2015).

2 Prince M, A. E., Guerchet M, Prina M. World Alzheimer Report 2014. Dementia and Risk Reduction: an analysis of protective and modifiable factors. *Alzheimer's Disease International* (2014).

3 Goate, A. *et al.* Segregation of a missense mutation in the amyloid precursor protein gene with familial Alzheimer's disease. *Nature* **349**, 704-706, doi:10.1038/349704a0 (1991).

4 Scheuner, D. *et al.* Secreted amyloid beta-protein similar to that in the senile plaques of Alzheimer's disease is increased in vivo by the presenilin 1 and 2 and APP mutations linked to familial Alzheimer's disease. *Nature medicine* **2**, 864-870 (1996).

5 Gatz, M. *et al.* Role of genes and environments for explaining Alzheimer disease. *Archives of general psychiatry* **63**, 168-174, doi:10.1001/archpsyc.63.2.168 (2006).

6 Alzheimer's, A. 2014 Alzheimer's disease facts and figures. *Alzheimer's & dementia : the journal of the Alzheimer's Association* **10**, e47-92 (2014).

7 Petersen, R. C. *et al.* Mild cognitive impairment: clinical characterization and outcome. *Archives of neurology* **56**, 303-308 (1999).

8 Petersen, R. C. Clinical practice. Mild cognitive impairment. *The New England journal of medicine* **364**, 2227-2234, doi:10.1056/NEJMcp0910237 (2011).

9 Karran, E., Mercken, M. & De Strooper, B. The amyloid cascade hypothesis for Alzheimer's disease: an appraisal for the development of therapeutics. *Nature reviews. Drug discovery* **10**, 698-712, doi:10.1038/nrd3505 (2011).

10 Heneka, M. T., Golenbock, D. T. & Latz, E. Innate immunity in Alzheimer's disease. *Nature immunology* **16**, 229-236, doi:10.1038/ni.3102 (2015).

11 Lambracht-Washington, D. & Rosenberg, R. N. Advances in the development of vaccines for Alzheimer's disease. *Discovery medicine* **15**, 319-326 (2013).

12 Terry, R. D. & Katzman, R. Senile dementia of the Alzheimer type. *Annals of neurology* **14**, 497-506, doi:10.1002/ana.410140502 (1983).

13 Bohm, C. *et al.* Current and future implications of basic and translational research on amyloid-beta peptide production and removal pathways. *Molecular and cellular neurosciences* **66**, 3-11, doi:10.1016/j.mcn.2015.02.016 (2015).

14 Breitner, J. C. The role of anti-inflammatory drugs in the prevention and treatment of Alzheimer's disease. *Annual review of medicine* **47**, 401-411, doi:10.1146/annurev.med.47.1.401 (1996).

15 Sastre, M. *et al.* Nonsteroidal anti-inflammatory drugs and peroxisome proliferator-activated receptor-gamma agonists modulate immunostimulated processing of amyloid precursor protein through regulation of beta-secretase. *The Journal of neuroscience : the official journal of the Society for Neuroscience* **23**, 9796-9804 (2003).

16 Weggen, S. *et al.* A subset of NSAIDs lower amyloidogenic Abeta42 independently of cyclooxygenase activity. *Nature* **414**, 212-216, doi:10.1038/35102591 (2001).

17 in t' Veld, B. A. *et al.* Nonsteroidal antiinflammatory drugs and the risk of Alzheimer's disease. *The New England journal of medicine* **345**, 1515-1521, doi:10.1056/NEJMoa010178 (2001).

18 Holmes, C. *et al.* Systemic inflammation and disease progression in Alzheimer disease. *Neurology* **73**, 768-774, doi:10.1212/WNL.0b013e3181b6bb95 (2009).

19 Iwashyna, T. J., Ely, E. W., Smith, D. M. & Langa, K. M. Long-term cognitive impairment and functional disability among survivors of severe sepsis. *Jama* **304**, 1787-1794, doi:10.1001/jama.2010.1553 (2010).

20 Whitmer, R. A., Gunderson, E. P., Quesenberry, C. P., Jr., Zhou, J. & Yaffe, K. Body mass index in midlife and risk of Alzheimer disease and vascular dementia. *Current Alzheimer research* **4**, 103-109 (2007).

21 Larson, E. B. *et al.* Exercise is associated with reduced risk for incident dementia among persons 65 years of age and older. *Annals of internal medicine* **144**, 73-81 (2006).

22 Heneka, M. T., Kummer, M. P. & Latz, E. Innate immune activation in neurodegenerative disease. *Nature reviews. Immunology* **14**, 463-477, doi:10.1038/nri3705 (2014).

23 Haass, C., Kaether, C., Thinakaran, G. & Sisodia, S. Trafficking and proteolytic processing of APP. *Cold Spring Harbor perspectives in medicine* **2**, a006270, doi:10.1101/cshperspect.a006270 (2012).

24 Ruth G. Perez, S. S., Jay D. Hayes, Beth Ostaszewskii, Weiming Xiai, & Dennis J. Selkoei, X. C., Gorazd B. Stokin, and Edward H. Koo. Mutagenesis Identifies New Signals for b-Amyloid Precursor Protein Endocytosis, Turnover, and the Generation of Secreted Fragments, Including Ab42. *The Journal of Biological Chemistry* **274**, 18851-18856 (1999).

25 Haass, C., Koo, E. H., Mellon, A., Hung, A. Y. & Selkoe, D. J. Targeting of cell-surface beta-amyloid precursor protein to lysosomes: alternative processing into amyloid-bearing fragments. *Nature* **357**, 500-503, doi:10.1038/357500a0 (1992).

26 Rogaeva, E. *et al.* The neuronal sortilin-related receptor SORL1 is genetically associated with Alzheimer disease. *Nature genetics* **39**, 168-177, doi:10.1038/ng1943 (2007).

27 Bhalla, A. *et al.* The location and trafficking routes of the neuronal retromer and its role in amyloid precursor protein transport. *Neurobiology of disease* **47**, 126-134, doi:10.1016/j.nbd.2012.03.030 (2012).

28 Sherrington, R. *et al.* Cloning of a gene bearing missense mutations in early-onset familial Alzheimer's disease. *Nature* **375**, 754-760, doi:10.1038/375754a0 (1995).

29 Rogaev, E. I. *et al.* Familial Alzheimer's disease in kindreds with missense mutations in a gene on chromosome 1 related to the Alzheimer's disease type 3 gene. *Nature* **376**, 775-778, doi:10.1038/376775a0 (1995).

30 Finckh, U. *et al.* High prevalence of pathogenic mutations in patients with early-onset dementia detected by sequence analyses of four different genes. *American journal of human genetics* **66**, 110-117, doi:10.1086/302702 (2000).

31 Yu, G. *et al.* Nicastrin modulates presenilin-mediated notch/glp-1 signal transduction and betaAPP processing. *Nature* **407**, 48-54, doi:10.1038/35024009 (2000).

32 Francis, R. *et al.* aph-1 and pen-2 are required for Notch pathway signaling, gamma-secretase cleavage of betaAPP, and presenilin protein accumulation. *Developmental cell* **3**, 85-97 (2002).

33 Ballatore, C., Lee, V. M. & Trojanowski, J. Q. Tau-mediated neurodegeneration in Alzheimer's disease and related disorders. *Nature reviews. Neuroscience* **8**, 663-672, doi:10.1038/nrn2194 (2007).

34 Hamdane, M. *et al.* Mitotic-like tau phosphorylation by p25-Cdk5 kinase complex. *J Biol Chem* **278**, 34026-34034, doi:10.1074/jbc.M302872200 (2003).

35 Estelle Sontag, Viyada Nunbhakdi-Craig, Lee., G., Bloom, G. S. & Mumby, M. C. Regulation of the Phosphorylation State and Microtubule-Binding Activity of Tau by Protein Phosphatase 2A. *Neuron* **17**, 1201-1207, doi:10.1016/S0896-6273(00)80250-0 (1996).

36 Qian, W. *et al.* PP2A regulates tau phosphorylation directly and also indirectly via activating GSK-3beta. *Journal of Alzheimer's disease : JAD* **19**, 1221-1229, doi:10.3233/JAD-2010-1317 (2010).

37 Atzori, C. *et al.* Activation of the JNK/p38 pathway occurs in diseases characterized by tau protein pathology and is related to tau phosphorylation but not to apoptosis. *Journal of neuropathology and experimental neurology* **60**, 1190-1197 (2001).

38 Beharry, C. *et al.* Tau-induced neurodegeneration: mechanisms and targets. *Neuroscience bulletin* **30**, 346-358, doi:10.1007/s12264-013-1414-z (2014).

39 Rogers, J. *et al.* Clinical trial of indomethacin in Alzheimer's disease. *Neurology* **43**, 1609-1611 (1993).

40 Mawuenyega, K. G. *et al.* Decreased clearance of CNS beta-amyloid in Alzheimer's disease. *Science* **330**, 1774, doi:10.1126/science.1197623 (2010).

41 Cuadros, M. A., Martin, C., Coltey, P., Almendros, A. & Navascues, J. First appearance, distribution, and origin of macrophages in the early development of the avian central nervous system. *The Journal of comparative neurology* **330**, 113-129, doi:10.1002/cne.903300110 (1993).

42 McKercher, S. R. *et al.* Targeted disruption of the PU.1 gene results in multiple hematopoietic abnormalities. *The EMBO journal* **15**, 5647-5658 (1996).

43 Ginhoux, F. *et al.* Fate mapping analysis reveals that adult microglia derive from primitive macrophages. *Science* **330**, 841-845, doi:10.1126/science.1194637 (2010).

44 Alliot, F., Godin, I. & Pessac, B. Microglia derive from progenitors, originating from the yolk sac, and which proliferate in the brain. *Brain research. Developmental brain research* **117**, 145-152 (1999).

45 Kierdorf, K. *et al.* Microglia emerge from erythromyeloid precursors via Pu.1- and Irf8-dependent pathways. *Nature neuroscience* **16**, 273-280, doi:10.1038/nn.3318 (2013).

46 Hashimoto, D. *et al.* Tissue-resident macrophages self-maintain locally throughout adult life with minimal contribution from circulating monocytes. *Immunity* **38**, 792-804, doi:10.1016/j.immuni.2013.04.004 (2013).

47 Nimmerjahn, A., Kirchhoff, F. & Helmchen, F. Resting microglial cells are highly dynamic surveillants of brain parenchyma in vivo. *Science* **308**, 1314-1318, doi:10.1126/science.1110647 (2005).

48 Hanisch, U. K. & Kettenmann, H. Microglia: active sensor and versatile effector cells in the normal and pathologic brain. *Nature neuroscience* **10**, 1387-1394, doi:10.1038/nn1997 (2007).

49 Saijo, K., Crotti, A. & Glass, C. K. Regulation of microglia activation and deactivation by nuclear receptors. *Glia* **61**, 104-111, doi:10.1002/glia.22423 (2013).

50 Maher, F. O., Nolan, Y. & Lynch, M. A. Downregulation of IL-4-induced signalling in hippocampus contributes to deficits in LTP in the aged rat. *Neurobiology of aging* **26**, 717-728, doi:10.1016/j.neurobiolaging.2004.07.002 (2005).

51 Lyons, A. *et al.* CD200 ligand receptor interaction modulates microglial activation in vivo and in vitro: a role for IL-4. *The Journal of neuroscience : the official journal of the Society for Neuroscience* **27**, 8309-8313, doi:10.1523/JNEUROSCI.1781-07.2007 (2007).

52 Nolan, Y. *et al.* Role of interleukin-4 in regulation of age-related inflammatory changes in the hippocampus. *J Biol Chem* **280**, 9354-9362, doi:10.1074/jbc.M412170200 (2005).

53 Varnum, M. M. & Ikezu, T. The classification of microglial activation phenotypes on neurodegeneration and regeneration in Alzheimer's disease brain. *Archivum immunologiae et therapiae experimentalis* **60**, 251-266, doi:10.1007/s00005-012-0181-2 (2012).

54 Calsolaro, V. & Edison, P. Neuroinflammation in Alzheimer's disease: Current evidence and future directions. *Alzheimer's & dementia : the journal of the Alzheimer's Association*, doi:10.1016/j.jalz.2016.02.010 (2016).

55 Lee, Y. H. *et al.* Amyloid precursor protein expression is upregulated in adipocytes in obesity. *Obesity* **16**, 1493-1500, doi:10.1038/oby.2008.267 (2008).

56 Jimenez, S. *et al.* Inflammatory response in the hippocampus of PS1M146L/APP751SL mouse model of Alzheimer's disease: age-dependent switch in the microglial phenotype from alternative to classic. *The Journal of neuroscience : the official journal of the Society for Neuroscience* **28**, 11650-11661, doi:10.1523/JNEUROSCI.3024-08.2008 (2008).

57 Michaud, J. P., Bellavance, M. A., Prefontaine, P. & Rivest, S. Real-time in vivo imaging reveals the ability of monocytes to clear vascular amyloid beta. *Cell reports* **5**, 646-653, doi:10.1016/j.celrep.2013.10.010 (2013).

58 El Khoury, J. *et al.* Ccr2 deficiency impairs microglial accumulation and accelerates progression of Alzheimer-like disease. *Nature medicine* **13**, 432-438, doi:10.1038/nm1555 (2007).

59 Guedes, J. R. *et al.* MicroRNA deregulation and chemotaxis and phagocytosis impairment in Alzheimer's disease. *Alzheimer's & Dementia: Diagnosis, Assessment & Disease Monitoring* **3**, 7-17, doi:10.1016/j.dadm.2015.11.004 (2016).

60 Cagnin, A. *et al.* In-vivo measurement of activated microglia in dementia. *The Lancet* **358**, 461-467, doi:10.1016/s0140-6736(01)05625-2 (2001).

61 Edison, P. *et al.* Microglia, amyloid, and cognition in Alzheimer's disease: An [11C](R)PK11195-PET and [11C]PIB-PET study. *Neurobiology of disease* **32**, 412-419, doi:10.1016/j.nbd.2008.08.001 (2008).

62 Gotz, J., Chen, F., van Dorpe, J. & Nitsch, R. M. Formation of neurofibrillary tangles in P301l tau transgenic mice induced by Abeta 42 fibrils. *Science* **293**, 1491-1495, doi:10.1126/science.1062097 (2001).

63 Stancu, I. C. *et al.* Tauopathy contributes to synaptic and cognitive deficits in a murine model for Alzheimer's disease. *FASEB journal : official publication of the Federation of American Societies for Experimental Biology* **28**, 2620-2631, doi:10.1096/fj.13-246702 (2014).

64 Tokutake, T. *et al.* Hyperphosphorylation of Tau induced by naturally secreted amyloid-beta at nanomolar concentrations is modulated by insulin-dependent Akt-GSK3beta signaling pathway. *J Biol Chem* **287**, 35222-35233, doi:10.1074/jbc.M112.348300 (2012).

65 Kitazawa, M., Oddo, S., Yamasaki, T. R., Green, K. N. & LaFerla, F. M. Lipopolysaccharide-induced inflammation exacerbates tau pathology by a cyclin-dependent kinase 5-mediated pathway in a transgenic model of Alzheimer's disease. *The Journal of neuroscience : the official journal of the Society for Neuroscience* **25**, 8843-8853, doi:10.1523/JNEUROSCI.2868-05.2005 (2005).

66 Bhaskar, K. *et al.* Regulation of tau pathology by the microglial fractalkine receptor. *Neuron* **68**, 19-31, doi:10.1016/j.neuron.2010.08.023 (2010).

67 Corder, E. H. *et al.* Gene dose of apolipoprotein E type 4 allele and the risk of Alzheimer's disease in late onset families. *Science* **261**, 921-923 (1993).

68 Strittmatter, W. J. *et al.* Apolipoprotein E: high-avidity binding to beta-amyloid and increased frequency of type 4 allele in late-onset familial Alzheimer disease. *Proceedings of the National Academy of Sciences of the United States of America* **90**, 1977-1981 (1993).

69 Karch, C. M. & Goate, A. M. Alzheimer's disease risk genes and mechanisms of disease pathogenesis. *Biological psychiatry* **77**, 43-51, doi:10.1016/j.biopsych.2014.05.006 (2015).

70 Rosenthal, S. L. & Kamboh, M. I. Late-Onset Alzheimer's Disease Genes and the Potentially Implicated Pathways. *Current genetic medicine reports* **2**, 85-101, doi:10.1007/s40142-014-0034-x (2014).

71 Hickman, S. E. *et al.* The microglial sensome revealed by direct RNA sequencing. *Nature neuroscience* **16**, 1896-1905, doi:10.1038/nn.3554 (2013).

72 Sessa, G. *et al.* Distribution and signaling of TREM2/DAP12, the receptor system mutated in human polycystic lipomembraneous osteodysplasia with sclerosing leukoencephalopathy dementia. *The European journal of neuroscience* **20**, 2617-2628, doi:10.1111/j.1460-9568.2004.03729.x (2004).

73 Guerreiro, R. *et al.* TREM2 variants in Alzheimer's disease. *The New England journal of medicine* **368**, 117-127, doi:10.1056/NEJMoa1211851 (2013).

74 Jonsson, T. *et al.* Variant of TREM2 associated with the risk of Alzheimer's disease. *The New England journal of medicine* **368**, 107-116, doi:10.1056/NEJMoa1211103 (2013).

75 Kleinberger, G. *et al.* TREM2 mutations implicated in neurodegeneration impair cell surface transport and phagocytosis. *Science translational medicine* **6**, 243ra286, doi:10.1126/scitranslmed.3009093 (2014).

76 Guedes, J. R. *et al.* Early miR-155 upregulation contributes to neuroinflammation in Alzheimer's disease triple transgenic mouse model. *Human molecular genetics* **23**, 6286-6301, doi:10.1093/hmg/ddu348 (2014).

77 Suarez-Calvet, M. *et al.* sTREM2 cerebrospinal fluid levels are a potential biomarker for microglia activity in early-stage Alzheimer's disease and associate with neuronal injury markers. *EMBO molecular medicine* **8**, 466-476, doi:10.15252/emmm.201506123 (2016).

78 Takahashi, K., Rochford, C. D. & Neumann, H. Clearance of apoptotic neurons without inflammation by microglial triggering receptor expressed on myeloid cells-2. *The Journal of experimental medicine* **201**, 647-657, doi:10.1084/jem.20041611 (2005).

79 Schmid, C. D. *et al.* Heterogeneous expression of the triggering receptor expressed on myeloid cells-2 on adult murine microglia. *Journal of neurochemistry* **83**, 1309-1320 (2002).

80 Wang, Y. *et al.* TREM2 lipid sensing sustains the microglial response in an Alzheimer's disease model. *Cell* **160**, 1061-1071, doi:10.1016/j.cell.2015.01.049 (2015).

81 Jay, T. R. *et al.* TREM2 deficiency eliminates TREM2+ inflammatory macrophages and ameliorates pathology in Alzheimer's disease mouse models. *The Journal of experimental medicine* **212**, 287-295, doi:10.1084/jem.20142322 (2015).

82 Bradshaw, E. M. *et al.* CD33 Alzheimer's disease locus: altered monocyte function and amyloid biology. *Nature neuroscience* **16**, 848-850, doi:10.1038/nn.3435 (2013).

83 Griciuc, A. *et al.* Alzheimer's disease risk gene CD33 inhibits microglial uptake of amyloid beta. *Neuron* **78**, 631-643, doi:10.1016/j.neuron.2013.04.014 (2013).

84 Crocker, P. R., McMillan, S. J. & Richards, H. E. CD33-related siglecs as potential modulators of inflammatory responses. *Annals of the New York Academy of Sciences* **1253**, 102-111, doi:10.1111/j.1749-6632.2011.06449.x (2012).

85 Tebar, F., Bohlander, S. K. & Sorkin, A. Clathrin assembly lymphoid myeloid leukemia (CALM) protein: localization in endocytic-coated pits, interactions with clathrin, and the impact of overexpression on clathrin-mediated traffic. *Molecular biology of the cell* **10**, 2687-2702 (1999).

86 Tian, Y., Chang, J. C., Fan, E. Y., Flajolet, M. & Greengard, P. Adaptor complex AP2/PICALM, through interaction with LC3, targets Alzheimer's APP-CTF for terminal degradation via autophagy. *Proceedings of the National Academy of Sciences of the United States of America* **110**, 17071-17076, doi:10.1073/pnas.1315110110 (2013).

87 Miller, S. E. *et al.* The molecular basis for the endocytosis of small R-SNAREs by the clathrin adaptor CALM. *Cell* **147**, 1118-1131, doi:10.1016/j.cell.2011.10.038 (2011).

88 Lambert, J. C. *et al.* Meta-analysis of 74,046 individuals identifies 11 new susceptibility loci for Alzheimer's disease. *Nature genetics* **45**, 1452-1458, doi:10.1038/ng.2802 (2013).

89 Harold, D. *et al.* Genome-wide association study identifies variants at CLU and PICALM associated with Alzheimer's disease. *Nature genetics* **41**, 1088-1093, doi:10.1038/ng.440 (2009).

90 Ando, K. *et al.* Clathrin adaptor CALM/PICALM is associated with neurofibrillary tangles and is cleaved in Alzheimer's brains. *Acta neuropathologica* **125**, 861-878, doi:10.1007/s00401-013-1111-z (2013).

91 Kanatsu, K. *et al.* Decreased CALM expression reduces Abeta42 to total Abeta ratio through clathrin-mediated endocytosis of gamma-secretase. *Nature communications* **5**, 3386, doi:10.1038/ncomms4386 (2014).

92 Xiao, Q. *et al.* Role of phosphatidylinositol clathrin assembly lymphoid-myeloid leukemia (PICALM) in intracellular amyloid precursor protein (APP) processing and amyloid plaque pathogenesis. *J Biol Chem* **287**, 21279-21289, doi:10.1074/jbc.M111.338376 (2012).

93 Moreau, K. *et al.* PICALM modulates autophagy activity and tau accumulation. *Nature communications* **5**, 4998, doi:10.1038/ncomms5998 (2014).

94 Zhao, Z. *et al.* Central role for PICALM in amyloid-beta blood-brain barrier transcytosis and clearance. *Nature neuroscience* **18**, 978-987, doi:10.1038/nn.4025 (2015).

95 Mercer, J. L. *et al.* Modulation of PICALM Levels Perturbs Cellular Cholesterol Homeostasis. *PloS one* **10**, e0129776, doi:10.1371/journal.pone.0129776 (2015).

96 Lee, E. *et al.* Amphiphysin 2 (Bin1) and T-tubule biogenesis in muscle. *Science* **297**, 1193-1196, doi:10.1126/science.1071362 (2002).

97 Fugier, C. *et al.* Misregulated alternative splicing of BIN1 is associated with T tubule alterations and muscle weakness in myotonic dystrophy. *Nature medicine* **17**, 720-725, doi:10.1038/nm.2374 (2011).

98 Caldwell, J. L. *et al.* Dependence of cardiac transverse tubules on the BAR domain protein amphiphysin II (BIN-1). *Circulation research* **115**, 986-996, doi:10.1161/CIRCRESAHA.116.303448 (2014).

99 Dawson, J. C., Legg, J. A. & Machesky, L. M. Bar domain proteins: a role in tubulation, scission and actin assembly in clathrin-mediated endocytosis. *Trends in cell biology* **16**, 493-498, doi:10.1016/j.tcb.2006.08.004 (2006).

100 Prokic, I., Cowling, B. S. & Laporte, J. Amphiphysin 2 (BIN1) in physiology and diseases. *Journal of molecular medicine* **92**, 453-463, doi:10.1007/s00109-014-1138-1 (2014).

101 Tan, M. S., Yu, J. T. & Tan, L. Bridging integrator 1 (BIN1): form, function, and Alzheimer's disease. *Trends in molecular medicine* **19**, 594-603, doi:10.1016/j.molmed.2013.06.004 (2013).

102 Glennon, E. B. *et al.* BIN1 is decreased in sporadic but not familial Alzheimer's disease or in aging. *PloS one* **8**, e78806, doi:10.1371/journal.pone.0078806 (2013).

103 Chapuis, J. *et al.* Increased expression of BIN1 mediates Alzheimer genetic risk by modulating tau pathology. *Molecular psychiatry* **18**, 1225-1234, doi:10.1038/mp.2013.1 (2013).

104 Sottejeau, Y. *et al.* Tau phosphorylation regulates the interaction between BIN1's SH3 domain and Tau's proline-rich domain. *Acta Neuropathologica Communications* **3**, doi:10.1186/s40478-015-0237-8 (2015).

105 Miyagawa, T. *et al.* BIN1 regulates BACE1 intracellular trafficking and amyloid-beta production. *Human molecular genetics*, doi:10.1093/hmg/ddw146 (2016).

106 Gold, E. S. *et al.* Amphiphysin IIm, a novel amphiphysin II isoform, is required for macrophage phagocytosis. *Immunity* **12**, 285-292 (2000).

107 Gold, E. S. *et al.* Amphiphysin IIm is required for survival of Chlamydia pneumoniae in macrophages. *The Journal of experimental medicine* **200**, 581-586, doi:10.1084/jem.20040546 (2004).

108 Lim, L. P. *et al.* Microarray analysis shows that some microRNAs downregulate large numbers of target mRNAs. *Nature* **433**, 769-773, doi:10.1038/nature03315 (2005).

109 Lee, Y. *et al.* MicroRNA genes are transcribed by RNA polymerase II. *The EMBO journal* **23**, 4051-4060, doi:10.1038/sj.emboj.7600385 (2004).

110 Lee, Y. *et al.* The nuclear RNase III Drosha initiates microRNA processing. *Nature* **425**, 415-419, doi:10.1038/nature01957 (2003).

111 Scott, M. S. & Ono, M. From snoRNA to miRNA: Dual function regulatory non-coding RNAs. *Biochimie* **93**, 1987-1992, doi:10.1016/j.biochi.2011.05.026 (2011).

112 Lee, Y. S. *et al.* Distinct roles for Drosophila Dicer-1 and Dicer-2 in the siRNA/miRNA silencing pathways. *Cell* **117**, 69-81 (2004).

113 Krol, J., Loedige, I. & Filipowicz, W. The widespread regulation of microRNA biogenesis, function and decay. *Nature reviews. Genetics* **11**, 597-610, doi:10.1038/nrg2843 (2010).

114 Rottiers, V. & Naar, A. M. MicroRNAs in metabolism and metabolic disorders. *Nature reviews. Molecular cell biology* **13**, 239-250, doi:10.1038/nrm3313 (2012).

115 Li, Z. & Rana, T. M. Therapeutic targeting of microRNAs: current status and future challenges. *Nature reviews. Drug discovery* **13**, 622-638, doi:10.1038/nrd4359 (2014).

116 Lewis, B. P., Burge, C. B. & Bartel, D. P. Conserved seed pairing, often flanked by adenosines, indicates that thousands of human genes are microRNA targets. *Cell* **120**, 15-20, doi:10.1016/j.cell.2004.12.035 (2005).

117 Helwak, A., Kudla, G., Dudnakova, T. & Tollervey, D. Mapping the human miRNA interactome by CLASH reveals frequent noncanonical binding. *Cell* **153**, 654-665, doi:10.1016/j.cell.2013.03.043 (2013).

118 Hebert, S. S. *et al.* Genetic ablation of Dicer in adult forebrain neurons results in abnormal tau hyperphosphorylation and neurodegeneration. *Human molecular genetics* **19**, 3959-3969, doi:10.1093/hmg/ddq311 (2010).

119 Xiao, M. *et al.* MicroRNAs Activate Gene Transcription Epigenetically as an Enhancer Trigger. *RNA biology*, 0, doi:10.1080/15476286.2015.1112487 (2016).

120 Suzuki, H., Maruyama, R., Yamamoto, E. & Kai, M. Epigenetic alteration and microRNA dysregulation in cancer. *Frontiers in genetics* **4**, 258, doi:10.3389/fgene.2013.00258 (2013).

121 Ashraf, S. I., McLoon, A. L., Sclarsic, S. M. & Kunes, S. Synaptic protein synthesis associated with memory is regulated by the RISC pathway in Drosophila. *Cell* **124**, 191-205, doi:10.1016/j.cell.2005.12.017 (2006).

122 Lau, P. & de Strooper, B. Dysregulated microRNAs in neurodegenerative disorders. *Seminars in cell & developmental biology* **21**, 768-773, doi:10.1016/j.semcdb.2010.01.009 (2010).

123 Hebert, S. S. *et al.* Loss of microRNA cluster miR-29a/b-1 in sporadic Alzheimer's disease correlates with increased BACE1/beta-secretase expression. *Proceedings of the National Academy of Sciences of the United States of America* **105**, 6415-6420, doi:10.1073/pnas.0710263105 (2008).

124 Boissonneault, V., Plante, I., Rivest, S. & Provost, P. MicroRNA-298 and microRNA-328 regulate expression of mouse beta-amyloid precursor protein-converting enzyme 1. *J Biol Chem* **284**, 1971-1981, doi:10.1074/jbc.M807530200 (2009).

125 Hebert, S. S. *et al.* MicroRNA regulation of Alzheimer's Amyloid precursor protein expression. *Neurobiology of disease* **33**, 422-428, doi:10.1016/j.nbd.2008.11.009 (2009).

126 Wang, W. X. *et al.* The expression of microRNA miR-107 decreases early in Alzheimer's disease and may accelerate disease progression through regulation of beta-site amyloid precursor protein-cleaving enzyme 1. *The Journal of neuroscience : the official journal of the Society for Neuroscience* **28**, 1213-1223, doi:10.1523/JNEUROSCI.5065-07.2008 (2008).

127 Nelson, P. T. & Wang, W. X. MiR-107 is reduced in Alzheimer's disease brain neocortex: validation study. *Journal of Alzheimer's disease : JAD* **21**, 75-79, doi:10.3233/JAD-2010-091603 (2010).

128 Cui, J. G., Li, Y. Y., Zhao, Y., Bhattacharjee, S. & Lukiw, W. J. Differential regulation of interleukin-1 receptor-associated kinase-1 (IRAK-1) and IRAK-2 by microRNA-146a and NF-kappaB in stressed human astroglial cells and in Alzheimer disease. *The Journal of biological chemistry* **285**, 38951-38960, doi:10.1074/jbc.M110.178848 (2010).

129 Li, J. *et al.* Transcriptional activation of microRNA-34a by NF-kappa B in human esophageal cancer cells. *BMC molecular biology* **13**, 4, doi:10.1186/1471-2199-13-4 (2012).

130 Zhao, Y. *et al.* Regulation of TREM2 expression by an NF-small ka, CyrillicB-sensitive miRNA-34a. *Neuroreport* **24**, 318-323, doi:10.1097/WNR.0b013e32835fb6b0 (2013).

131 Sethi, P. & Lukiw, W. J. Micro-RNA abundance and stability in human brain: specific alterations in Alzheimer's disease temporal lobe neocortex. *Neuroscience letters* **459**, 100-104, doi:10.1016/j.neulet.2009.04.052 (2009).

132 Fazi, F. *et al.* A minicircuitry comprised of microRNA-223 and transcription factors NFI-A and C/EBPalpha regulates human granulopoiesis. *Cell* **123**, 819-831, doi:10.1016/j.cell.2005.09.023 (2005).

133 Rosa, A. *et al.* The interplay between the master transcription factor PU.1 and miR-424 regulates human monocyte/macrophage differentiation. *Proceedings of the National Academy of Sciences of the United States of America* **104**, 19849-19854, doi:10.1073/pnas.0706963104 (2007).

134 Cardoso, A. L., Guedes, J. R. & de Lima, M. C. Role of microRNAs in the regulation of innate immune cells under neuroinflammatory conditions. *Current opinion in pharmacology* **26**, 1-9, doi:10.1016/j.coph.2015.09.001 (2016).

135 Freilich, R. W., Woodbury, M. E. & Ikezu, T. Integrated expression profiles of mRNA and miRNA in polarized primary murine microglia. *PloS one* **8**, e79416, doi:10.1371/journal.pone.0079416 (2013).

136 Koronyo, Y. *et al.* Therapeutic effects of glatiramer acetate and grafted CD115(+) monocytes in a mouse model of Alzheimer's disease. *Brain : a journal of neurology* **138**, 2399-2422, doi:10.1093/brain/awv150 (2015).

137 Tiribuzi, R. *et al.* miR128 up-regulation correlates with impaired amyloid beta(1-42) degradation in monocytes from patients with sporadic Alzheimer's disease. *Neurobiology of aging* **35**, 345-356, doi:10.1016/j.neurobiolaging.2013.08.003 (2014).

138 Asai, M. *et al.* An alternative metabolic pathway of amyloid precursor protein C-terminal fragments via cathepsin B in a human neuroglioma model. *FASEB journal : official publication of the Federation of American Societies for Experimental Biology* **25**, 3720-3730, doi:10.1096/fj.11-182154 (2011).

139 Cardoso, A. L., Guedes, J. R., Pereira de Almeida, L. & Pedroso de Lima, M. C. miR-155 modulates microglia-mediated immune response by down-regulating SOCS-1 and promoting cytokine and nitric oxide production. *Immunology* **135**, 73-88, doi:10.1111/j.1365-2567.2011.03514.x (2012).

140 Wendlandt, E. B., Graff, J. W., Gioannini, T. L., McCaffrey, A. P. & Wilson, M. E. The role of microRNAs miR-200b and miR-200c in TLR4 signaling and NF-kappaB activation. *Innate immunity* **18**, 846-855, doi:10.1177/1753425912443903 (2012).

141 Dong, H. *et al.* Serum MicroRNA Profiles Serve as Novel Biomarkers for the Diagnosis of Alzheimer's Disease. *Disease markers* **2015**, 625659, doi:10.1155/2015/625659 (2015).

142 Lukiw, W. J., Zhao, Y. & Cui, J. G. An NF-kappaB-sensitive micro RNA-146a-mediated inflammatory circuit in Alzheimer disease and in stressed human brain cells. *J Biol Chem* **283**, 31315-31322, doi:10.1074/jbc.M805371200 (2008).

143 Li, Y. Y. *et al.* Differential expression of miRNA-146a-regulated inflammatory genes in human primary neural, astroglial and microglial cells. *Neuroscience letters* **499**, 109-113, doi:10.1016/j.neulet.2011.05.044 (2011).

144 Xu, N. *et al.* MicroRNA-31 is overexpressed in psoriasis and modulates inflammatory cytokine and chemokine production in keratinocytes via targeting serine/threonine kinase 40. *Journal of immunology* **190**, 678-688, doi:10.4049/jimmunol.1202695 (2013).

145 Hu, J. *et al.* The role of the miR-31/FIH1 pathway in TGF-beta-induced liver fibrosis. *Clinical science* **129**, 305-317, doi:10.1042/CS20140012 (2015).

146 Vilardo, E., Barbato, C., Ciotti, M., Cogoni, C. & Ruberti, F. MicroRNA-101 regulates amyloid precursor protein expression in hippocampal neurons. *J Biol Chem* **285**, 18344-18351, doi:10.1074/jbc.M110.112664 (2010).

147 Zhang, J., Hu, M., Teng, Z., Tang, Y. P. & Chen, C. Synaptic and cognitive improvements by inhibition of 2-AG metabolism are through upregulation of microRNA-188-3p in a mouse model of Alzheimer's disease. *The Journal of neuroscience : the official journal of the Society for Neuroscience* **34**, 14919-14933, doi:10.1523/JNEUROSCI.1165-14.2014 (2014).

148 Li, Y., Wang, J., Zhang, S. & Liu, Z. Neprilysin gene transfer: A promising therapeutic approach for Alzheimer's disease. *Journal of neuroscience research* **93**, 1325-1329, doi:10.1002/jnr.23564 (2015).

149 Folstein, M. F., Folstein, S. E. & McHugh, P. R. "Mini-mental state". A practical method for grading the cognitive state of patients for the clinician. *Journal of psychiatric research* **12**, 189-198 (1975).

150 Nasreddine, Z. S. *et al.* The Montreal Cognitive Assessment, MoCA: a brief screening tool for mild cognitive impairment. *Journal of the American Geriatrics Society* **53**, 695-699, doi:10.1111/j.1532-5415.2005.53221.x (2005).

151 Mohs, R. C., Rosen, W. G. & Davis, K. L. The Alzheimer's disease assessment scale: an instrument for assessing treatment efficacy. *Psychopharmacology bulletin* **19**, 448-450 (1983).

152 Guerreiro, M. Contributo da Neuropsicologia para o estudo das demências [Contribution of Neuropsychology to the study of dementia](Unpublished doctoral dissertation). University of Lisbon, Lisbon. (1998).

153 Morris, J. C. The Clinical Dementia Rating (CDR): current version and scoring rules. *Neurology* **43**, 2412-2414 (1993).

154 Yesavage, J. A. *et al.* Development and validation of a geriatric depression screening scale: a preliminary report. *Journal of psychiatric research* **17**, 37-49 (1982).

155 Albert, M. S. *et al.* The diagnosis of mild cognitive impairment due to Alzheimer's disease: recommendations from the National Institute on Aging-Alzheimer's Association workgroups on diagnostic guidelines for Alzheimer's disease. *Alzheimer's & dementia : the journal of the Alzheimer's Association* **7**, 270-279, doi:10.1016/j.jalz.2011.03.008 (2011).

156 Petersen, R. C. Mild cognitive impairment as a diagnostic entity. *Journal of internal medicine* **256**, 183-194, doi:10.1111/j.1365-2796.2004.01388.x (2004).

157 McKhann, G. M. *et al.* The diagnosis of dementia due to Alzheimer's disease: recommendations from the National Institute on Aging-Alzheimer's Association workgroups on diagnostic guidelines for Alzheimer's disease. *Alzheimer's & dementia : the journal of the Alzheimer's Association* **7**, 263-269, doi:10.1016/j.jalz.2011.03.005 (2011).

158 Roman, G. C. *et al.* Vascular dementia: diagnostic criteria for research studies. Report of the NINDS-AIREN International Workshop. *Neurology* **43**, 250-260 (1993).

159 Ohgidani, M. *et al.* Direct induction of ramified microglia-like cells from human monocytes: dynamic microglial dysfunction in Nasu-Hakola disease. *Scientific reports* **4**, 4957, doi:10.1038/srep04957 (2014).

160 Trabulo, S., Cardoso, A. L., Mano, M. & de Lima, M. C. P. Cell-Penetrating Peptides—Mechanisms of Cellular Uptake and Generation of Delivery Systems. *Pharmaceuticals* **3**, 961-993, doi:10.3390/ph3040961 (2010).

161 Chu, G., Hayakawa, H. & Berg, P. Electroporation for the efficient transfection of mammalian cells with DNA. *Nucleic acids research* **15**, 1311-1326 (1987).

162 Pfaffl, M. W. A new mathematical model for relative quantification in real-time RT-PCR. *Nucleic acids research* **29**, e45 (2001).

163 Puzzo, D., Gulisano, W., Palmeri, A. & Arancio, O. Rodent models for Alzheimer's disease drug discovery. *Expert opinion on drug discovery* **10**, 703-711, doi:10.1517/17460441.2015.1041913 (2015).

164 Pugin, J. *et al.* CD14 is a pattern recognition receptor. *Immunity* **1**, 509-516 (1994).

165 Ulevitch, R. J. & Tobias, P. S. Receptor-dependent mechanisms of cell stimulation by bacterial endotoxin. *Annual review of immunology* **13**, 437-457, doi:10.1146/annurev.iy.13.040195.002253 (1995).

166 Giulian, D. & Ingeman, J. E. Colony-stimulating factors as promoters of ameboid microglia. *The Journal of neuroscience : the official journal of the Society for Neuroscience* **8**, 4707-4717 (1988).

167 Falk, L. A. & Vogel, S. N. Comparison of bone marrow progenitors responsive to granulocyte-macrophage colony stimulating factor and macrophage colony stimulating factor-1. *Journal of leukocyte biology* **43**, 148-157 (1988).

168 Louis, C. *et al.* Specific Contributions of CSF-1 and GM-CSF to the Dynamics of the Mononuclear Phagocyte System. *Journal of immunology* **195**, 134-144, doi:10.4049/jimmunol.1500369 (2015).
169 Shi, H. *et al.* Genetic variants influencing human aging from late-onset Alzheimer's disease (LOAD) genome-wide association studies (GWAS). *Neurobiology of aging* **33**, 1849 e1845-1818, doi:10.1016/j.neurobiolaging.2012.02.014 (2012).
170 Lee, C. K., Weindruch, R. & Prolla, T. A. Gene-expression profile of the ageing brain in mice. *Nature genetics* **25**, 294-297, doi:10.1038/77046 (2000).
171 Lee, D. C. *et al.* Aging enhances classical activation but mitigates alternative activation in the central nervous system. *Neurobiology of aging* **34**, 1610-1620, doi:10.1016/j.neurobiolaging.2012.12.014 (2013).
172 Guedes, J. R. *et al.* MicroRNA deregulation and chemotaxis and phagocytosis impairment in Alzheimer's disease. *Alzheimer's & dementia* **3**, 7-17, doi:10.1016/j.dadm.2015.11.004 (2016).
173 Orio, J. *et al.* Sub-cellular temporal and spatial distribution of electrotransferred LNA/DNA oligomer. *Journal of RNAi and gene silencing : an international journal of RNA and gene targeting research* **9**, 479-485 (2013).
174 Balcaitis, S., Weinstein, J. R., Li, S., Chamberlain, J. S. & Moller, T. Lentiviral transduction of microglial cells. *Glia* **50**, 48-55, doi:10.1002/glia.20146 (2005).
175 Zhang, G., Gurtu, V. & Kain, S. R. An enhanced green fluorescent protein allows sensitive detection of gene transfer in mammalian cells. *Biochemical and biophysical research communications* **227**, 707-711, doi:10.1006/bbrc.1996.1573 (1996).
176 Krabbe, G. *et al.* Functional impairment of microglia coincides with Beta-amyloid deposition in mice with Alzheimer-like pathology. *PloS one* **8**, e60921, doi:10.1371/journal.pone.0060921 (2013).
177 Biswas, S. K. & Mantovani, A. Macrophage plasticity and interaction with lymphocyte subsets: cancer as a paradigm. *Nature immunology* **11**, 889-896, doi:10.1038/ni.1937 (2010).
178 Juliano, R., Alam, M. R., Dixit, V. & Kang, H. Mechanisms and strategies for effective delivery of antisense and siRNA oligonucleotides. *Nucleic acids research* **36**, 4158-4171, doi:10.1093/nar/gkn342 (2008).
179 Gomez-Nicola, D., Fransen, N. L., Suzzi, S. & Perry, V. H. Regulation of microglial proliferation during chronic neurodegeneration. *The Journal of neuroscience : the official journal of the Society for Neuroscience* **33**, 2481-2493, doi:10.1523/JNEUROSCI.4440-12.2013 (2013).
180 Lin, H. *et al.* Discovery of a cytokine and its receptor by functional screening of the extracellular proteome. *Science* **320**, 807-811, doi:10.1126/science.1154370 (2008).
181 Chihara, T. *et al.* IL-34 and M-CSF share the receptor Fms but are not identical in biological activity and signal activation. *Cell death and differentiation* **17**, 1917-1927, doi:10.1038/cdd.2010.60 (2010).
182 Ma, X. *et al.* Structural basis for the dual recognition of helical cytokines IL-34 and CSF-1 by CSF-1R. *Structure* **20**, 676-687, doi:10.1016/j.str.2012.02.010 (2012).
183 Ushach, I. & Zlotnik, A. Biological role of granulocyte macrophage colony-stimulating factor (GM-CSF) and macrophage colony-stimulating factor (M-CSF) on cells of the myeloid lineage. *Journal of leukocyte biology*, doi:10.1189/jlb.3RU0316-144R (2016).
184 Melief, J. *et al.* Phenotyping primary human microglia: tight regulation of LPS responsiveness. *Glia* **60**, 1506-1517, doi:10.1002/glia.22370 (2012).
185 Butovsky, O. *et al.* Identification of a unique TGF-beta-dependent molecular and functional signature in microglia. *Nature neuroscience* **17**, 131-143, doi:10.1038/nn.3599 (2014).